uOttawa

L'Université canadienne
Canada's university

FACULTÉ DES ÉTUDES SUPÉRIEURES ET POSTOCTORALES

uOttawa

L'Université canadienne
Canada's university

FACULTY OF GRADUATE AND POSDOCTORAL STUDIES

William M. Stecho
AUTEUR DE LA THÈSE / AUTHOR OF THESIS

M.Sc. (Microbiology and Immunology)
GRADE / DEGREE

Department of Biochemistry, Microbiology and Immunology
FACULTÉ, ÉCOLE, DÉPARTEMENT / FACULTY, SCHOOL, DEPARTMENT

The Effect of Adaptive Mutations in the Influenza A NS1 Protein on CPSF30 and PABP1 Binding
TITRE DE LA THÈSE / TITLE OF THESIS

Dr. Earl Brown
DIRECTEUR (DIRECTRICE) DE LA THÈSE / THESIS SUPERVISOR

CO-DIRECTEUR (CO-DIRECTRICE) DE LA THÈSE / THESIS CO-SUPERVISOR

EXAMINATEURS (EXAMINATRICES) DE LA THÈSE / THESIS EXAMINERS

Dr. Kathryn Wright

Dr. David Stodjl

Gary W. Slater
Le Doyen de la Faculté des études supérieures et postdoctorales / Dean of the Faculty of Graduate and Postdoctoral Studies

The Effect of Adaptive Mutations in the Influenza A NS1 Protein

on CPSF30 and PABP1 Binding

By

William M. Stecho

Thesis Submitted to the
Faculty of Graduate and Postdoctoral Studies
In Partial Fulfillment of the Requirements
for the Master of Science Degree in Microbiology and Immunology.

Department of Biochemistry, Microbiology, and Immunology
Faculty of Medicine
University of Ottawa

Your file Votre référence
ISBN: 978-0-494-51860-1
Our file Notre référence
ISBN: 978-0-494-51860-1

ABSTRACT

The Influenza A NS1 protein is an interferon (IFN) antagonist and a major virulence determinant. To characterize the genetic basis of NS1-mediated virulence, highly pathogenic mouse-adapted Influenza A strains were derived from human A/Hong Kong/1/68 H3N2 by experimental evolution in the mouse lung. Within these strains seven specific NS1 mutations were identified, some of which conferred greater IFN resistance and/or increased viral protein synthesis to the virus. Most of these mutations were shown to affect NS1 CPSF30 binding, which may affect post-transcriptional processing and increase host IFN induction. Some of these mutations were also shown to increase NS1 binding to host translation initiation factor PABP1, supporting a model of increased IFN resistance through direct modulation of host translation.

ACKNOWLEDGEMENTS

I would like to give special thanks to Dr. Brown, who gave me the opportunity and taught me the skills to accomplish this thesis.

I would also like to thank the members of my thesis advisory committee; Dr. Ken Dimock and Dr. Martin Pelchat for their advice

A huge thanks goes out to my "lab partners", past and present: Jay Majithia, Liya Keleta, Shaui Wang, Samra Uzicanin, Samar Dankar, Nicole Forbes, Shelly Luu, Jasminka Bozic , and Song Liu. You all made life in the lab so incredibly enjoyable. I can't imagine meeting another group as great as you guys. You all also helped me find countless missing reagents.

Thanks also to Neil McKenna and Reza Nokhbeh for their invaluable input.

Finally, I am grateful to my parents, my brothers, my fiancée, and my friends for keeping me sane throughout this experience.

I would like to dedicate this thesis to my fiancée, Am, who stood by me through thick and thin during these trying years and also to my parents who paid for the whole thing.

TABLE OF CONTENTS

FIGURE LIST

TABLE LIST

LIST OF APPEDICES

LIST OF ABBREVIATIONS

5' UTR	5' end untranslated region
A_λ	units of measured absorbance at wavelength λ
Ab	antibody
Amp	ampicillin
AP	alkaline phosphatase
BCIP	5-Bromo-4-Chloro-3'-Indolyphosphate p-Toluidine Salt
βME	β-mercaptoenthanol (2-mercaptoethanol)
BSA	bovine serum albumin
cDNA	complementary DNA
Cm	chloramphenicol
CPSF	cleavage and polyadenylation specificity factor complex
CPSF30 (CPSF4)	30 kDa subunit of the cleavage and polyadenylation specificity factor
cRNA	complementary RNA
DMSO	dimethyl sulfoxide
DNA	deoxyribonucleic acid
dNTP	deoxyribonucleotide

DPI	dots per inch
DTT	dithiothreitol
EDTA	ethylenediaminetetraacetic acid
FluAV	Influenza virus A
eIF4G1	eukaryotic translation and initiation factor 4G1
g	g-force
HA	Influenza A hemagglutinin protein
HK-wt	Influenza A/Hong Kong/1/68
HK-MA	mouse adapted progenies of Influenza A/Hong Kong/1/68
HPAI	highly pathogenic avian influenza A virus
HPLC	high performance liquid chromatography
HRP	horse radish peroxidase
IFN	interferon
IFNAR	interferon-α/β receptor
IPTG	isopropyl-b-D-thiogalactopyranoside
IRF	interferon regulatory factor
ISG	interferon stimulated gene

ISGF	interferon stimulated gene factor
ISRE	interferon stimulated response element
JAK	Janus family intracellular non-receptor tyrosine kinase
kDa	kilodaltons
M1	Influenza A matrix protein
M2	Influenza A ion channel protein
MA	mouse-adapted
MEM	minimal essential medium
mLD_{50}	median lethal dose for 50% fatality
MOI	multiplicity of infection
mRNA	messenger ribonucleic acid
NA	Influenza A neuraminidase protein
NAI	neuraminidase inhibitor
NEP (NS2)	Influenza A nuclear export protein
NF-κB	nuclear factor κB
NP	Influenza A nucleocapsid protein
NPT	Nitro-Blue Tetrazolium Chloride

NS1	Influenza A nonstructural protein 1
NS1-BP	NS1 binding protein
NS1-I	NS1 interactor
OAS	2',5'-oligoadenylate synthetase
ORF	open reading frame
PA	Influenza A polymerase acidic protein
PABII (PABPNI)	polyadenylate-binding protein II (nuclear polyadenylate-binding protein I)
PABPI	polyadenylate-binding protein I (cytoplasmic polyadenylate-binding protein I)
PB1	Influenza A polymerase basic protein 1
PB2	Influenza A polymerase basic protein 2
PBS	phosphate buffered saline
PCR	polymerase chain reaction
PEG	polyethylene glycol
Pfu	plaque forming units
PIC	protease inhibitor cocktail
PI3-k	Phosphoinositide 3 kinase

PKR	RNA-dependant protein kinase
PMSF	phenylmethyl sulfonyl fluoride
PNK	polynucleotide kinase
PPO	polyphenylene oxide
PVDF	polyvinylidene fluoride
RIG-I	Retinoic Acid Inducible Gene I
RNA	ribonucleic acid
RNP	ribonucleoprotein
Rpm	revolutions per minute
RT-PCR	reverse transcriptase PCR
SDS	sodium dodecyl sulfate
SDS-PAGE	sodium dodecyl sulfate polyacrylamide gel electrophoresis
snRNA	Small Nuclear RNA
STAT	signal transducer and activator of transcription
TBE	Tris, borate, and EDTA containing buffer
TE	Tris and EDTA containing buffer
TLCK	1-Chloro-3-tosylamido-7-amino-2-heptanone HCl
TLR3	toll-like receptor 3

TOPO	DNA Topoisomerase I
TPCK	1-Chloro-3-tosylamido-4-phenyl-2-butanone
U	units
vRNA	Viral Genomic RNA
Wt	wild type

INTRODUCTION

Influenza A is a common human pathogen and influenza epidemics occur every year as different human influenza strains evolve and circle the globe. In Canada, seasonal influenza epidemics annually infect 10 – 25% of the population, resulting in an estimated 4,000 deaths, mostly among seniors (MacDonald *et al.*, 2007). Of greater concern than the annual epidemics are the irregular influenza pandemics that accompany the introduction of a new influenza subtype into the human population from its avian reservoir. These pandemic influenza strains are able to spread rapidly and infect a greater proportion of the population due to our lack of immunity for the new subtype. An influenza pandemic will generally result in approximately 1 million deaths worldwide, with a known exception being the highly pathogenic H1N1 Spanish influenza pandemic of 1918 (Spanish flu) which resulted in an estimated 50 million deaths (Johnson & Mueller, 2002). The Spanish flu was also exceptional due to its unusual mortality pattern, in that the majority of the resultant deaths were among young and otherwise healthy adults (Simonsen *et al.*, 1998). More recently, the new highly pathogenic H5N1 avian influenza strain (HPAI) is circulating throughout Europe and Asia in domestic poultry and appears to be spread by migratory birds. HPAI has proven to be devastating to the poultry industry with mortality rates approaching 100% in domestic chickens (OiE; Isoda *et al.*, 2006; Ellis *et al.*, 2004, Chen *et al.*, 2004). Although HPAI is not yet directly transmissible between humans, to date there have been more than 380 reported cases of zoonotic human infection from birds with a 63% mortality rate (World Health Organization). The deadly virulence of HPAI and the Spanish flu seem to be attributable, in part, to their resistance to the innate immune response

combined with the inflated and aberrant innate immune response that is uniquely elicited by both of these viruses (Kobasa *et al.*, 2007; Perrone *et al.*, 2008). Given the dangerous pandemic potential of HPAI, it is essential that we develop an understanding of the molecular and genetic basis of virulence in highly pathogenic influenza strains. Such insight into influenza virulence will allow us to accurately identify and track current and future influenza strains with pandemic potential, as well as allowing us to develop more effective anti-viral therapeutics to protect ourselves from future pandemics.

The influenza A non-structural protein 1 (NS1) has been linked to the increased virulence of both HPAI and the Spanish flu (Basler *et al.*, 2001; Basler & Aguilar, 2008; Seo *et al.*, 2004; Li, Z. *et al.*, 2006; Taubenberger, 2006). Therefore, this thesis focuses on the effects that adaptive mutations found in the NS1 proteins of highly pathogenic mouse-adapted influenza strains may have on the binding affinities of NS1 to its various binding partners; specifically the 30 kDa subunit of the cleavage and polyadenylation specificity factor (CPSF30) and the cytoplasmic polyadenylate binding protein (PABP1).

1.1 Virion Structure, Genetic Organization, and Encoded Proteins

The Influenza A genus of viruses belongs to the family *Orthomyxoviridae*, which it shares with four other genera: *Influenza virus B*, *Influenza virus C*, *Thogotovirus,* and *Isavirus*. Influenza A viruses (FluAV) are further classified into subtypes based on the antigenicity of their hemagglutinin (HA) and neuraminidase (NA) envelope proteins (Wright *et al.*, 2007). There are currently 16 known HA and 9 known NA FluAV subtypes, all of which are present in the avian FluAV reservoir. However, of these subtypes, only four combinations are known

to readily infect humans (H1N1, H1N2, H2N2, and H3N2) (Kamps *et al.*, 2006). The nomenclature of the FluAV viruses consists of: the type of virus, the host of origin (excluded for human strains), the geographic location of isolation, the strain number, the year of isolation, and, in parenthesis, the subtype (Fig. 1).

FluAV is an enveloped virus. As such, the core of the virion is covered with a host-derived lipid bilayer called an envelope. The hemagglutinin and neuraminidase proteins are integral membrane proteins that protrude from this envelope (Palese & Shaw, 2007). The M2 protein is also found in the envelope, where it forms transmembrane homotetramers which run through the lipid bilayer to create pH-gated ion channels (Pinto *et al.*, 1992; Sakaguchi *et al.*, 1997; Mould *et al.*, 2000). Beneath the envelope lies a polymeric protein shell that is formed by the M1 protein. The M1 shell surrounds the viral core that is comprised of the eight ribonucleoproteins (RNPs) that make up the viral genome (Ruigrok *et al*, 2000; Ruigrok *et al.* 1989). Each RNP consists of a single segment of viral genomic RNA (vRNA) coated with nucleoprotein (NP) and associated with a RNA-dependent RNA polymerase complex. This RNA polymerase complex is a heterotrimer consisting of the viral PA, PB1, and PB2 proteins. (Compans *et al.*1972; Hsu *et al.* 1987) (Fig. 2).

The FluAV genome is segmented and consists of eight strands of negative sense single-stranded genomic RNA (vRNA). Within these 8 RNA segments are encoded the eleven known FluAV proteins (Brown *et al.*, 2000; Palese & Schulman, 1976) (Fig. 3). These eight segments all have non-coding regions at the 5′ and 3′ ends. The 5′ terminal thirteen base pairs and the 3′ terminal twelve base pairs of the non-coding regions are conserved across all eight segments. Proximal to the outer conserved non-coding regions lie a second set of

Figure 1. Nomenclature of the Influenza A Virus. The nomenclature of the influenza viruses consists of: the type of virus, the host of origin (excluded for human strains), the geographic location of isolation, the strain number, the year of isolation, and the subtype in parenthesis.

Influenza Virus Nomenclature

For viruses of human origin:

Genus/Location/Isolation #/Year (HA and NA subtype)

For example:

A/Hong Kong/1/68 (H3N2)

For viruses of non-human origin:

Genus/Species of original isolation/Location/Isolation #/Year (HA and NA subtype)

For example:

A/Goose/Guangdong/1/96 (H5N1)

Figure 2. Structure of the influenza A virion.
The white helical lines in the viral core correspond to RNPs consisting of genomic vRNA bound by nucleoprotein and the polymerase complex. The white numbers to the left of the RNP denote the genomic segment number, while the white letters to the left indicate the viral proteins encoded in the corresponding segment. The length of the RNA strand depicts the relative length of the vRNA segments. From Kaiser, J. (2006). A one-size-fits-all flu vaccine? Science 312, 380-382. Reprinted with permission from AAAS.

PB1, PB2, PA: the polymerase complex proteins
HA: hemagglutinin trimer
NA: neuraminidase tetramer
M_1: M1 matrix protein
M_2: M2 ion channel tetramer
Lipid bilayer: viral envelope

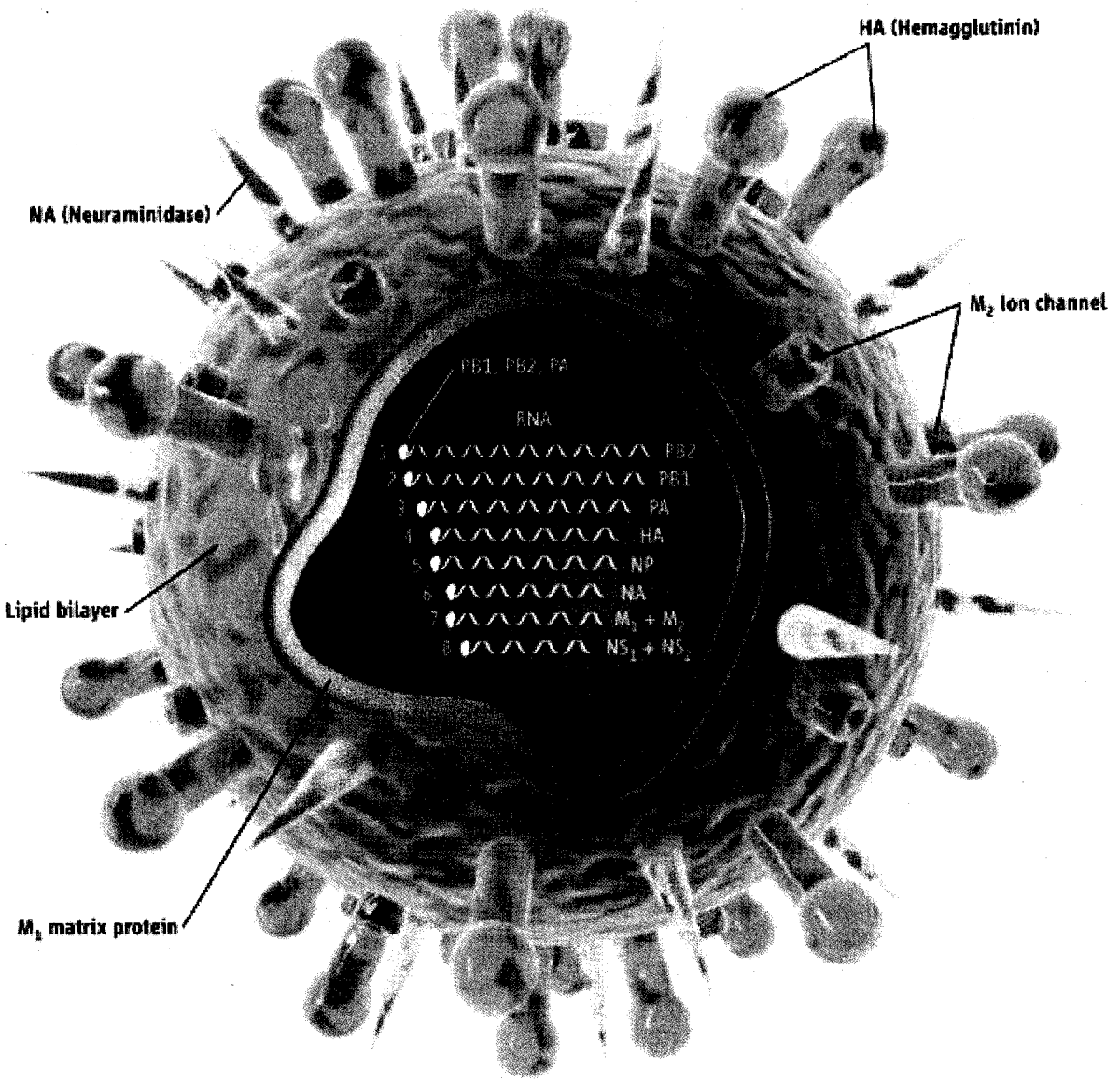

Figure 3. The influenza A genome and its encoded proteins. Viral segments are listed numerically from top to bottom. Viral genes are denoted on the encoding segment by the common acronym of the corresponding protein. The numbers to the left and right of each segment mark the segment length in nucleotides. Numbers located on top of each ORF denote the length of the encoded protein in amino acids. A short description of the function of each protein is given on the far right.

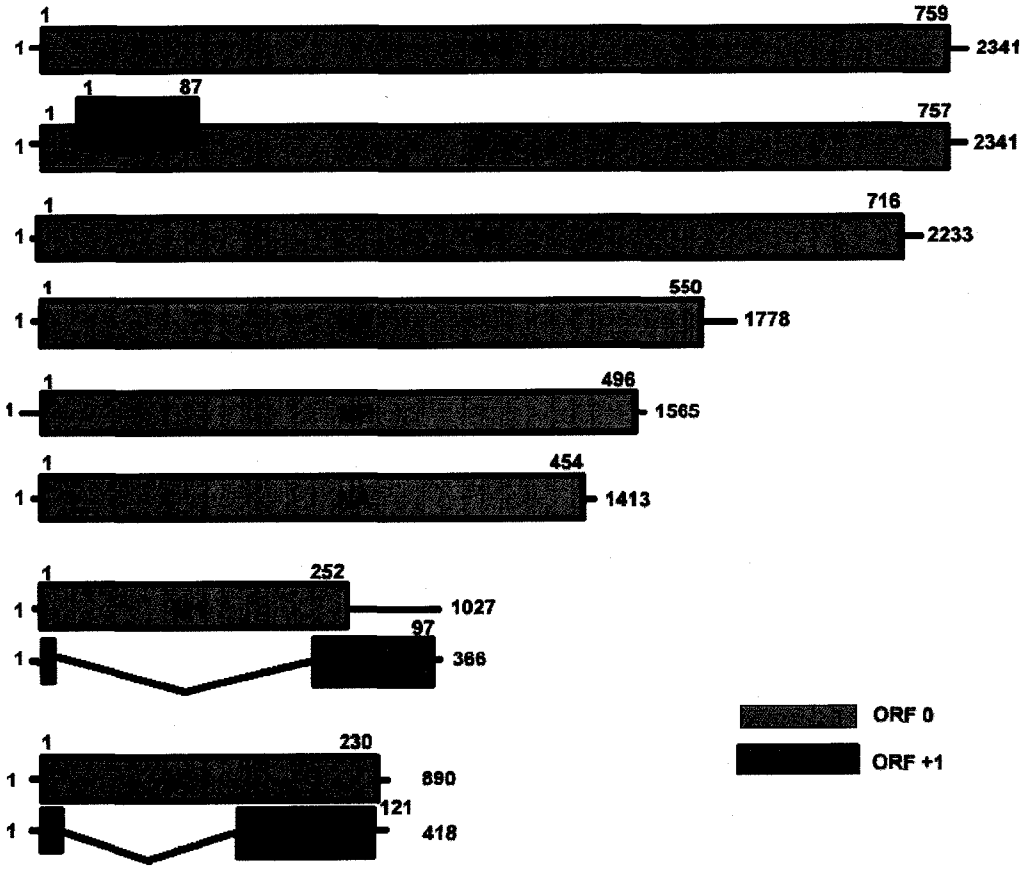

PB2: component of RNA polymerase, cap recognition

PB1- F2: pro-apoptotic activity

PB1: component of RNA polymerase, endonuclease activity, elongation

PA: component of RNA polymerase, protease

HA: surface glycoprotein, receptor binding, fusion activity, major antigen

NP: RNA binding, RNA synthesis, RNA nuclear import

NA: surface glycoprotein, neuraminidase activity

M1: matrix protein, interaction with vRNPs and surface glycoproteins, nuclear export, budding

M2: membrane protein, ion channel activity, assembly

NS1: multi-functional protein, *viral IFN antagonist*

NEP/NS2: nuclear export of vRNPs

non-coding regions that are specific and unique to each of the eight segments (Palese & Shaw, 2007).

The first three segments of the genome encode the three subunits of the polymerase complex: PB1, PB2, and PA. The PB2 subunit is able to recognize and bind the 5' m^7G caps of host mRNA transcripts (Fechter *et al.*, 2003; Shi *et al.*, 1995). PB2 holds these 5' caps in place while the PB1 subunit cleaves the host mRNA transcript from them, freeing the caps to be used as primers for viral mRNA transcription (Plotch *et al.*, 1981). The PB1 subunit also contains the ribonucleotide polymerization function which catalyzes the elongation of the viral mRNA transcripts as well as vRNA during replication (Lee *et al.*, 2003; Donis *et al.*, 2001). Finally, the PA subunit is involved in the replication of the viral genome (Area *et al.*, 2004; Deng *et al.*, 2005; Fodor *et al.*, 2002; Fodor *et al.*, 2004; Murti *et al.*, 1988). The second genomic segment also encodes the PB1-F2 protein from an alternate open reading frame (Chen *et al.* 2001). The function of the PB1-F2 protein is unclear, but it has been shown to induce apoptosis (Chanturiya *et al.*, 2004; Henklein *et al.*, 2005). The fourth genomic segment encodes the first FluAV surface antigen; hemagglutinin (HA). HA functions as a trimer and is responsible for recognizing the host cell surface receptors and attaching the virus to them. Additionally, HA mediates the fusion of the viral envelope with the cytoplasmic membrane to result in the uncoating of the viral genomic RNP (Hernandez *et al.*, 1996; Jardtzky & Lamb, 2004; Skehel & Wiley, 2000; Wiley & Skehel, 1987). The HA protein is also the major surface antigen that is targeted by the adaptive immune system (Abe *et al.*, 2004; Li *et al.*, 2005; Wagner *et al.*, 2005). The fifth segment encodes NP, which encapsulates the vRNA and is also important in regulating viral replication during infection

(Compans *et al.*, 1972; Heggeness *et al.*, 1982; Martin-Benito *et al.*, 2001; Beaton and Krug, 1986). The sixth segment encodes the second FluAV surface antigen; neuraminidase (NA). NA cleaves sialic acid and is important in viral release and also in the release of viral particles from sialic acid containing inhibitors in the mucus (Palese *et al.*, 1974; Schulman & Palese, 1977; Suzuki *et al.*, 2005). The seventh and eighth genomic segments each code for two proteins. The M1 and NS1 genes are encoded by genes that reside at the 5' ends of the seventh and eighth genomic segments respectively and require no splicing of the mRNA for translation. Meanwhile, the M2 and NS2 proteins are encoded near the 3' ends of their respective segments, partially overlapping the NS1 and M1 genes in alternate reading frames. The M2 and NS2 proteins are translated from spliced transcripts of the respective seventh and eighth genomic segments (Lamb & Choppin, 1979; Lamb & Choppin, 1981; Lamb & Lai, 1980; Lamb *et al.* 1981), which are generated using cellular splicing machinery (Lamb & Lai, 1982; Lamb & Lai, 1984). The NS2 protein, also known as the nuclear export protein (NEP), plays an integral role in exporting replicated viral genomes, in the form of RNP associated with M1, out of the nucleus by mediating RNP association with host nuclear export machinery (Neumann *et al.*, 2000; O'Neill *et al.*, 1998; Yasuda *et al.*, 1993). As mentioned above, the M1 and M2 proteins encode for the matrix and ion channel proteins respectively. The NS1 protein will be discussed in greater detail in section 1.3.

1.2 Viral Replication

Viral replication begins with the binding of the HA to the sialic acid containing surface receptors of a host cell. Once bound, the FluAV virion is endocytosed into a clathrin-

coated pit (Matlin *et al.* 1981). The decreasing pH of the late endosome (approximately pH 5.3) triggers a conformational change in the HA trimers, uncovering their fusion peptide. The fusion peptide associates with the cellular membrane, pulling the virion and the membrane into juxtaposition to mediate fusion (Stegmann, 2000). The binding of numerous HA trimers thus results in the fusion of the cellular membrane with the viral envelope, creating pores through which the contents of the virion can be released into the cytoplasm (Stegmann, 2000). Previous to fusion, the M2 ion channels allow endosomal H+ ions to permeate into the virion, wherein they dissociate the bonds between the M1 matrix and the RNPs. Free of the viral matrix, the RNPs are ushered directly to the nucleus via their nuclear localization signals which interact with the host nuclear transport machinery (O'Neill *et al.* 1995; Cros *et al.* 2005).

Transcription of viral mRNA occurs in the nucleus when a viral polymerase complex binds to both the 5' and 3' ends of a viral genomic segment via the PB1 subunit forming a vRNA loop, as well as to the 5' cap of a host pre-mRNA via the PB2 subunit (Haggen *et al.*, 1994; Krug, 1981). The pre-mRNA is subsequently cleaved by PB1 at a site 10-13 nucleotides downstream of the cap structure (Beaton and Krug, 1981; Plotch *et al.*, 1981). A guanosine residue is added to the 3' end of the capped primer which, in turn, base pairs with the penultimate 3' cytosine of the viral RNA, thereby initiating transcription (Beaton and Krug, 1981). Elongation of the viral mRNA is catalyzed by the PB1 subunit as the vRNA template is threaded through the polymerase complex (Lee *et al.*, 2003; Donis *et al.*, 2001). Once the nascent viral mRNA is finished transcribing the gene, the polymerase encounters a short stretch of five to seven continuous uracil residues on the vRNA (Li and Palese, 1994).

Simultaneously, because the 5' end of the vRNA is still bound to PB1, steric hindrance from the shrinking vRNA loop prevents the vRNA from continuing to thread through the polymerase as the 5' end of the vRNA template is reached. Due to this steric hindrance and the short uracil stretch, the polymerase develops a stutter in the vRNA template at the end of transcription. This stutter results in the addition of a poly(A) tail to the 3' end of the viral mRNA due to the reiterative transcription of the uracil stretch (Poon *et al.*, 1999; Zheng *et al.*, 1999).

The viral polymerase complex is also responsible for the replication of vRNA, as well as the positive sense complimentary RNA (cRNA) which serves as the template for vRNA synthesis. Replication of cRNA and vRNA are quite different from that of mRNA in that initiation does not require a capped primer and transcription of the full length cRNA and vRNA is not terminated early by polyadenylation. The means through which the virus coordinates the production of mRNA, cRNA, and vRNA by the polymerase complex is not yet fully understood, although it is hypothesized that the switch may be dependent on the concentration of soluble NP, in that NP may act to stabilize a structural change in the polymerase complex that permits cRNA and vRNA transcription (Beaton and Krug, 1986; Vreede *et al.*, 2004).

Once cRNA and vRNA are synthesized they are quickly encapsidated by NP. Encapsidated vRNA also associates with M1 and the polymerase complex to form new RNP-M1 complexes (Huang *et al.*, 2001). The newly formed RNP-M1 complexes are bound by NS2, which mediates their nuclear export by means of the NS2 protein's ability to interact with the host nuclear export machinery (Neumann *et al.*, 2000; O'Neill *et al.*, 1998; Yasuda

et al., 1993). Once free of the nucleus, the RNPs are directed to the virus assembly site on the apical plasma membrane where the viral envelope proteins (HA, NA, and M2) have assembled (Boulan and Pendergast, 1980). The envelope proteins are translated into the endoplasmic reticulum and later progress through the Golgi apparatus before being directed to the apical plasma membrane of the infected cell via the apical sorting signal in their trans-membrane domains (Barman *et al.*, 2001; Doms *et al.*, 1993). At the virus assembly site, the M1-bound RNPs are congregated into complete complements of the viral genome through an, as of yet, undiscovered means (Palese and Shaw, 2007). The M1 shell that is formed by the developing inner core is thought to cause the extrusion of the plasma membrane until the budding membrane fuses to enclose the viral core, resulting in the pinching off of the fully developed virus particle. The final step in viral replication is the release of the viral particle from the sialic acids which anchor the particle to the plasma membrane (Nayak *et al.*, 2004; Schmitt and Lamb, 2005). The release is mediated by NA, which cleaves sialic acids on the plasma membrane. NA also cleaves sialic acids on the viral envelope itself, thereby preventing the aggregation of viral particles (Palese *et al.*, 1974; Schulman & Palese, 1977; Suzuki *et al.*, 2005). Because the function of NA is antagonistic to the binding function of HA, a delicate balance is necessary between the proportions of these proteins that are present in the viral envelope (Wagner *et al.*, 2002) (Fig. 4).

Figure 4. The Influenza A replication cycle.
The influenza virion associates with a human host cell by binding to the sialic acid receptors on the cytoplasmic membrane. The bound virus is then endocytosed. As the pH lowers in the endosome, the HA protein mediates fusion of the viral envelope and the plasma membrane. Simultaneously, the M2 ion channel allows H+ ions into the viral core, releasing the RNPs from the M1 matrix into the cytoplasm. The RNPs are then transported into the nucleus where transcription and translation take place. The viral proteins are expressed and eventually assemble with vRNAs at the virus assembly site. Newly assembled virions then bud out from the host cell and move on to infect neighbouring cells. Reprinted with permission from Reactome, 2008.

1.3 Properties of NS1

The 26 kDa NS1 protein can vary in size from 124 to 237 amino acids depending on the FluAV strain. NS1 is functionally active as a homodimer and is proposed to assume different dimerization structures in a ligand-dependant manner. (Das *et al.*, 2008; Hale *et al.*, 2008; Lamb and Krug, 2001; Nemeroff *et al.* 1995) (Fig. 5). Each NS1 monomer consists of an N-terminal RNA-binding domain that is able to bind dsRNA, followed by a C-terminal functional domain that binds to numerous host factors (Hatada *et al.*, 1992; Qian *et al.*, 1994; Qian *et al.* 1995; Wang and Krug, 1996) (Table 1, Fig. 6). The protein is present and active in both the nucleus and the cytoplasm of the infected cell due to its dual nuclear localization signals and latent nuclear export sequence (Greenspan *et al.*, 1988; Li *et al.*, 1998). NS1 is a multifunctional protein, known properties of which include binding dsRNA, the ability to enhance viral protein translation, and the ability to antagonize and modulate the Type II interferon (IFN) pathway of the cellular immune response (Hatada *et al.* 1992; Palese & Shaw, 2007). It is the ability to antagonize the immune system that is arguably the most important function of NS1, as FluAV strains lacking the NS1 gene have been shown to productively infect mice that are unable to mount an IFN cellular immune response (Garcia-Sastre *et al.* 1998). In contrast, NS1 is critical for productive infection of normal mice, and the NS1 gene alone has been shown to inhibit IFN-β promoter activation and IFN induction (Wang *et al*, 2000; Talon *et al.* 2000; Geiss *et al.* 2002). Although virulence in FluAV is multigenetically controlled (Brown *et al.*, 2001; Brown and Bailly, 1999), the NS1 protein's ability to inhibit the IFN response is a critical virulence factor. Indeed, single base-pair substitutions in the NS1 gene have been shown to drastically alter IFN induction and

Figure 5. Crystal structures of the Influenza A NS1 protein. (A) NS1 is presented here in the homodimerized form. The individual NS1 monomers are colour-coded for clarity. The crystal structures of the NS1 RNA-binding and effector domains were solved independently of each other(Bornholdt & Prasad, 2006 and Chein *et al.*, 1997). The RNA-binding domain is the uppermost structure, while the effector domain is located below. The connecting 3' residues of the RNA-binding domains and 5' residues of the effector domains are marked with black arrows. NS1 may be able to form different homodimer structures in a ligand-dependant manner. Alternative proposed models for NS1 effector domain dimerization include: **(B)** the helix-helix homodimer (Hale *et al.*, 2008); and **(C)** the dimerization structure seen when NS1 is bound to CPSF30 (Das *et al.*, 2008). The dissociated blue bar in (B) corresponds to amino acid residues 218-224 at the C-terminus of monomer 2. The C-terminal region is hypothesized to be unstructured which is why it is difficult to image with crystallography.

A

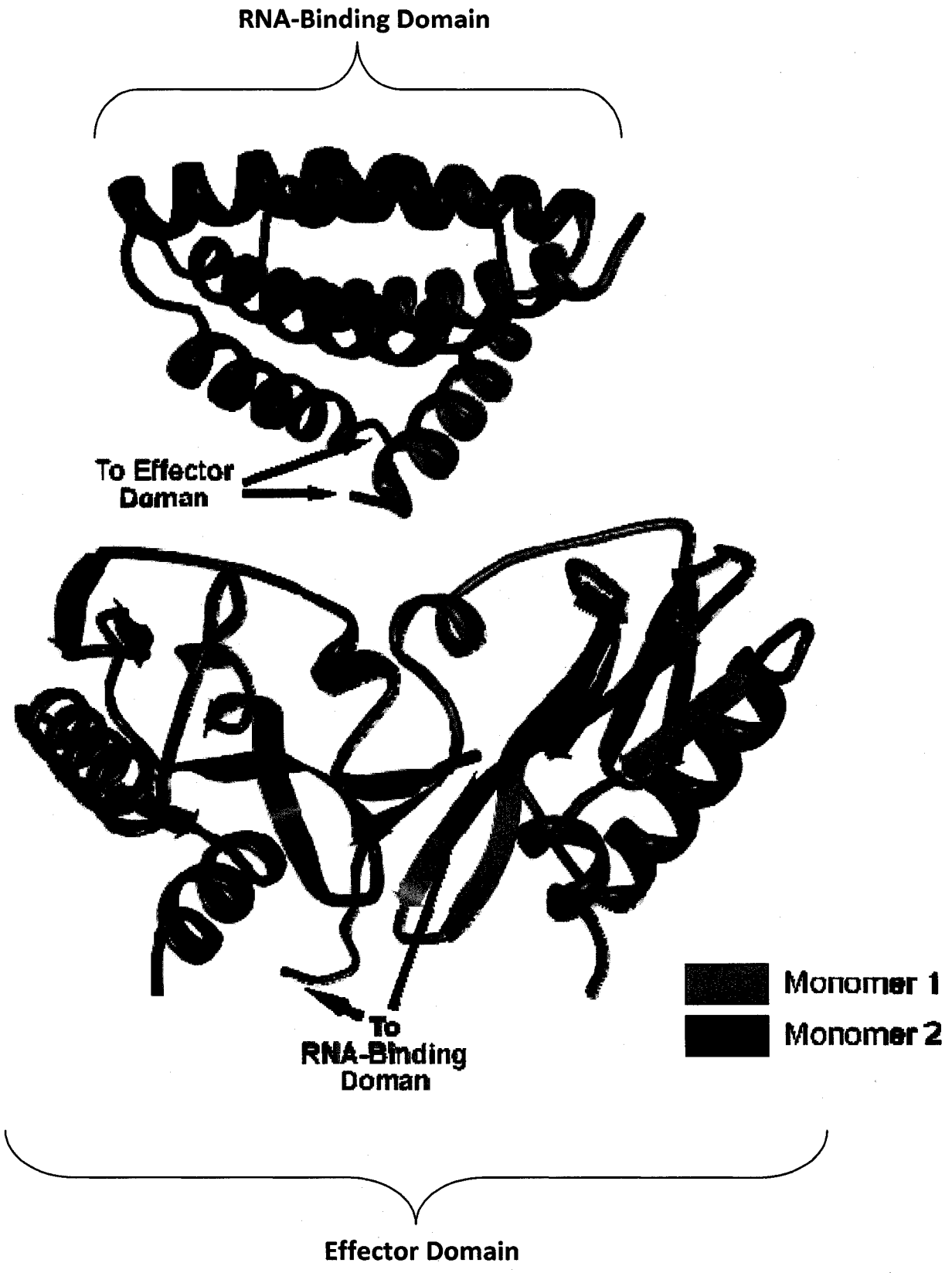

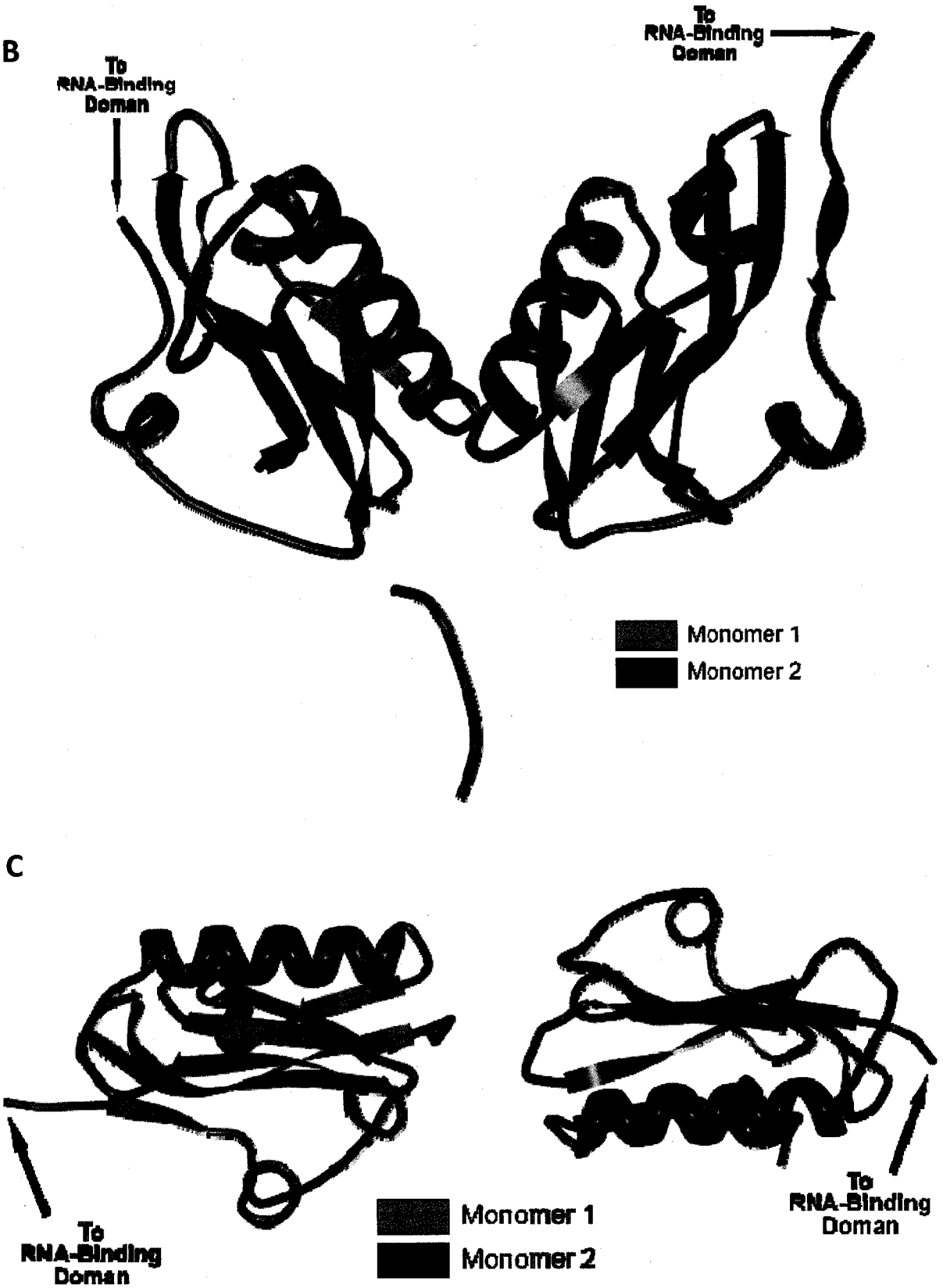

Table 1. Known NS1 binding partners. All host proteins that have been shown to interact to date are indicated below. The location of the binding domain for the corresponding protein (if mapped) is indicated by the relevant amino acid sequences on the NS1 protein. The proposed effect of NS1 interaction with the corresponding protein is also noted.

Binding Partner	Binding Domain on NS1	Proposed Effect	Reference(s)
CPSF30	144 - 186 103, 106	Inhibition of post-transcriptional poly-adenylation	Koch *et al.*, 2007 Li *et al.*, 2001 Nemeroff *et al.* 1998 Noah *et al.*, 2003 Twu *et al.* 2006 Twu *et al.* 2007
Crk/CrkL	164-7, 212-6	Increased cell growth and survival	Heikkinen *et al.* 2008
dsRNA	1-73	Masking of dsRNA from innate immune system	Hatada *et al.* 1992
eIF4G1	81-113	Preferential translation of viral mRNA over host mRNA	Aragon *et al*, 2000
hStaufen	N-terminal domain	mRNA transportation and localization to polysomes	Falcon *et al.* 1999
NS1-BP	Unknown	Unknown – localizes to regions enriched with spliceosomes	Wolff *et al.* 1998
NS1-I	Unknown	Unknown – partial homolog to a porcine steroid metabolism protein	Wolff *et al.* 1996
PABP1	1-81	Preferential translation of viral mRNA over host mRNA	Burgui *et al.* 2003
PABPNI (PABII)	223-37	Inhibition of post-transcriptional polyadenylation	Chen *et al.* 1999
PDZ Domain	233-7	Modulation of virulence through interaction with unknown host PDZ domain containing protein	Jackson *et al.* 2008 Obenauer *et al.* 2006
p85β subunit of PI3-k	89-93, 164-7, 212-6	Increased cell growth and survival	Hale *et al.* 2008 Li *et al.* 2008 Shin *et al*, 2007
PKR	123-7	Inhibition of PKR	Min let all., 2007 Tan, & Katze, 1998
Poly(A) ssRNA	1-73	Inhibition of mRNA nuclear export	Qiu & Krug, 1994
RIG-I	Unknown	Inhibition of IFN induction	Mibayashi *et al.* 2007
U6 snRNA	1-73	Inhibition of mRNA splicing	Qiu *et al.* 1995
U6atac snRNA	1-73	Inhibition of mRNA splicing – AT/AC slice specific	Wang & Krug, 1998
Viral mRNA	1-73	Preferential translation of viral mRNA over host mRNA	Park & Katze, 1995

Figure 6. Functional map of the Influenza A NS1 protein. Mapped locations for RNA, PABP1, eIF4G1, CPSF30 (marked "CPSF"), PABII, and PKR interaction are shown. SH2 and SH3 stand for Src homology 2 and 3 domains which are responsible for PI3-k and Crk/CrkL interaction. Also listed are the nuclear localization signals (NLS1 and NLS2) and the nuclear export sequence (NES). The separate RNA-binding and effector domains are marked below.

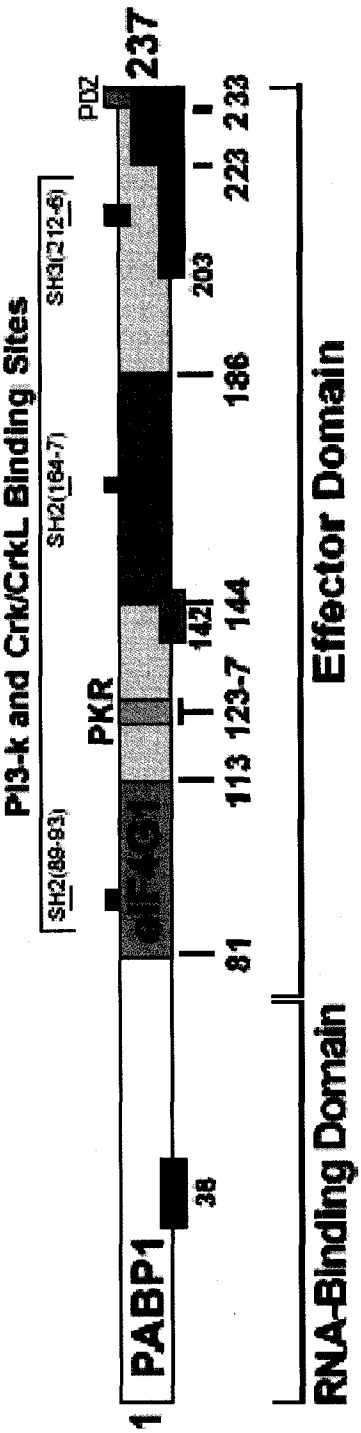

resistance, viral protein production, and/or pathogenicity on the affected viruses in a mouse model (E.G. Brown, unpublished data). The functions of NS1 will be further described in later sections as they become relevant to the discussion.

1.4 The Effect of NS1 on Viral Replication

Although NS1 is not a necessary component of viral replication, it has been shown to enhance viral protein production in infected cells (de la Luna *et al.*, 1995). NS1 has been shown to bind simultaneously to the eukaryotic initiation factor 4G1 (eIF4G1), a large scaffolding protein that is part of the translation initiation machinery. NS1 also binds the cytoplasmic polyadenylate binding protein (PABP1) (Aragon *et al*, 2000; Burgui *et al.* 2003), another member of the translation initiation machinery. Because NS1 is also able to bind specifically to the 5' untranslated region (5'UTR) of viral mRNA (Park & Katze, 1995), it is hypothesized that NS1 is able to enhance the translation of viral mRNA by recruiting the translation initiation machinery specifically to the viral mRNA transcripts. This strategy has the added effect of titrating the translation machinery away from the host mRNA, thereby inhibiting the host innate immune response by preventing the production of the response proteins (Fig. 7).

An alternate strategy employed by NS1 to enhance viral replication is to activate the PI3-k/AKT signaling pathway by activating phosphoinositide 3 kinase (PI3-k). NS1 has been shown to activate PI3-k both, by binding directly to the p85 subunit of PI3-k (Hale *et al.* 2008; Li *et al.* 2008; Shin *et al*, 2007), as well as by binding to Crk/CrkL (Heikkinen *et al.*

Figure 7. NS1-mediated modulation of translation initiation. (A) Normal translation initiation in the absence of NS1. eIF4E recruits the eIF4G1 scaffolding protein. PABP1, bound to the poly(A) tail of the mRNA also binds to eIF4G1. Additional translation initiation factors, and eventually the ribosomal subunits are recruited and translation begins. **(B)** NS1 is able to bind eIF4G1 and PABP1 in a non-competitive manner, thereby not inhibiting their interaction with one another. Simultaneous binding of viral mRNA (v-mRNA) by NS1 increases the affinity of the translation initiation complex for viral mRNA, while also enhancing the stability of the complex. Thereby, NS1 specifically enhances the translational efficiency of viral mRNA.

A

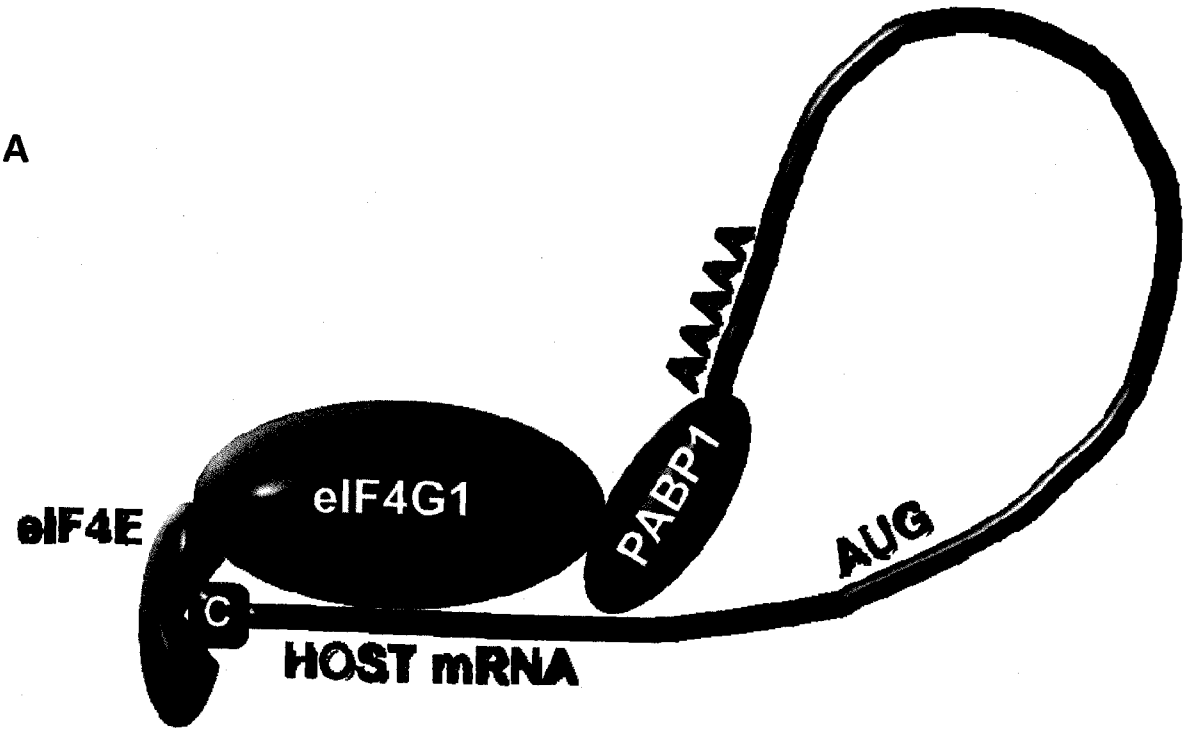

B

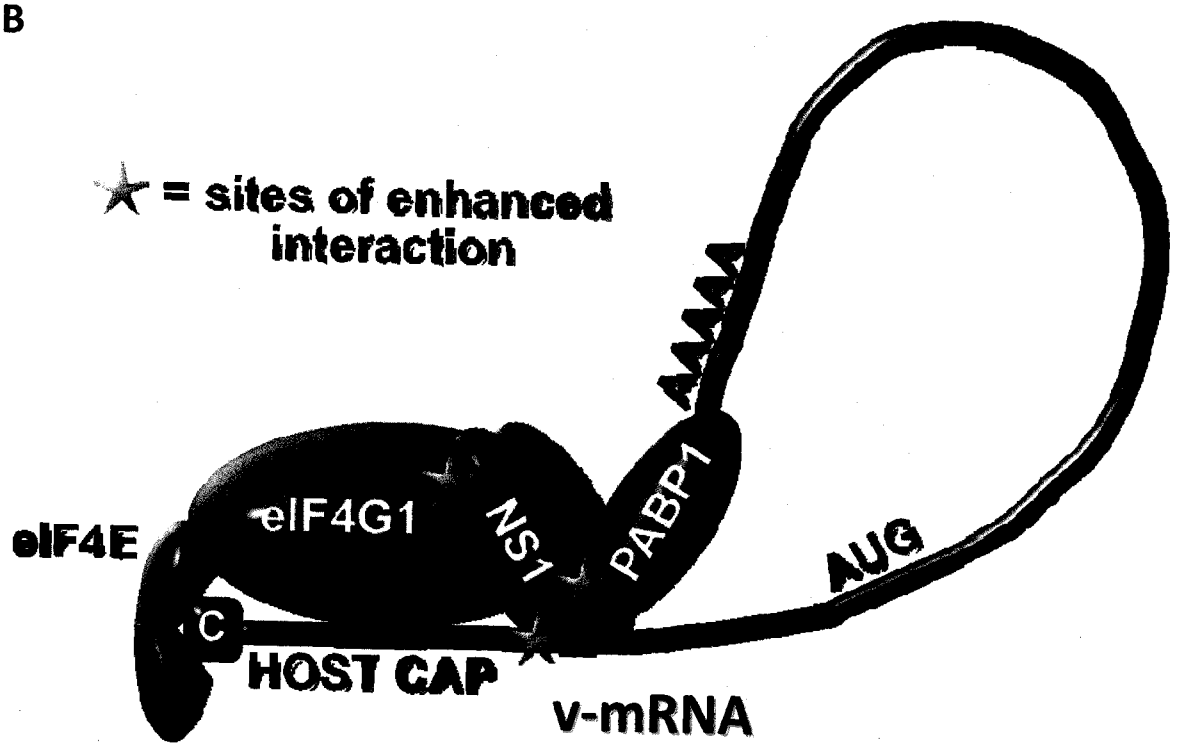

2008), a modulator of the PI3-k/AKT pathway. Once activated, the PI3-k/AKT signaling pathway has numerous diverse effects, most notably increasing cell growth, proliferation, and survival (Vanhaesebroeck *et al.*, 2001). Thus, by activating PI3-k, NS1 enhances cellular metabolism, thereby increasing the amount of 5'-capped pre-mRNA, ribosomes, and other host proteins and cellular resources needed to enhance viral replication. NS1 also increases the concentration of 5'-capped pre-mRNA available for use in viral mRNA transcription by binding to the poly(A) ssRNA tails, thereby inhibiting nuclear export of host mRNA (Qiu & Krug, 1994).

A third potential strategy by which NS1 may enhance viral replication efficiency is through its capacity to bind hStaufen (Falcon *et al.* 1999). Although the function of hStaufen has not yet been elucidated, Staufen, the drosophila homolog of hStaufen, binds to the double-stranded tertiary structure of specific mRNA transcripts and acts as an engine to transport these mRNA transcripts along microtubules. Staufen is active during embryonic development and is critical for mRNA localization and transcriptional control (Ferrandon *et al.*, 1994; St Johnston *et al.*, 1991). The hStaufen protein has also been shown to bind dsRNA and microtubules and is therefore thought to play a similar role in humans (Marion *et al.*, 1999). In addition, hStaufen is associated with polysomes, further supporting this hypothesis (Villace *et al.*, 2004). Although the significance of NS1's ability to associate with hStaufen is not yet known, NS1 may, theoretically, utilize hStaufen to shuttle viral mRNA directly to polysomes to enhance translation.

One final strategy to enhance viral replication that may be used by highly pathogenic FluAV strains is to attract macrophages and neutrophils to the site of infection. Although this may seem counter-productive, both HPAI and the Spanish flu have been shown to induce the expression of pro-inflammatory cytokines such as IL-6, IL-8, CCL2, and CCL5 (Kobasa *et al.*, 2007; Perrone *et al.*, 2008). IL-8, CCL2, and CCL5 also function as chemokines which serve to direct neutrophils and macrophages to the site of infection. Indeed significantly high levels of neutrophils and macrophages have been noted within the lungs of mice infected with HPAI or the Spanish flu compared against those infected with low pathogenicity FluAV strains (Perrone *et al.*, 2008). Furthermore, these studies have also shown that the HPAI and the Spanish flu are able to successfully replicate within macrophages and neutrophils *in vitro*, suggesting that these highly pathogenic FluAV strains are actively recruiting these cells types to the lungs to provide additional host cells for replication (Perrone *et al.*, 2008).

1.5 The Type I Interferon Response to Influenza A Infection

Upon entering a host cell, FluAV is immediately challenged by the host's innate immune anti-viral response which is primarily mediated by the type one IFN response. There are many potential triggers to the IFN response, but one potent trigger is the presence of the dsRNA that is created as a byproduct of FluAV infection. The dsRNA is recognized by cellular sentinel proteins such as toll-like receptor 3 (TLR3) and retinoic acid inducible gene 1 (RIG-1), which in turn lead to the downstream autophosphorylation of

dimerized interferon regulatory factor 3 (IRF3). Phosphorylated IRF3 forms a complex with CREBBP, which then moves into the nucleus and activates transcription of IFN by binding to the IRF promoter (Alexopoulou *et al.*, 2001; Marie *et al.*, 1998; Sen and Sarker, 2005; Weaver *et al.*, 1998). Once IFN-β is transcribed and translated, the mature protein is exported into the extracellular space where it is free to bind to the IFN-α and IFN-β receptor (IFNAR) found on the cytoplasmic membranes of the infected cell and its neighbours, thereby eliciting an antiviral state in the surrounding uninfected cells as well. Once bound by IFN-α or IFN-β, IFNAR utilizes the JAK/STAT signaling pathway to phosphorylate the STAT1 and STAT2 proteins. Phosphorylated STAT1 and STAT2 form a heterodimer and recruit IRF9 to complete the trimeric interferon-stimulated gene transcription factor (ISGF). ISGF quickly moves into the nucleus and binds to the numerous interferon stimulated response elements (ISREs) that precede the various IFN-α/β inducible genes (ISGs). Through this mechanism IFN-α/β induction results in the production of greater than 300 anti-viral proteins including IRF7. IRF7 is another transcription factor that binds to the IRF promoter, further enhancing the transcription of IFN-β and creating a positive feedback loop to sustain the anti-viral state (Biron and Sen, 2001; Takeda and Akira, 2004; Marie *et al.*, 1998; Smith, 2005) (Fig. 8a).

Other notable IFN-inducible proteins include: dsRNA-activated protein kinase R (PKR), 2',5'-oligoadenylate synthetase (OAS), RNase L, and MxA GTPase. Both PKR and OAS are activated by various forms of viral RNA that is created during infection. Activated PKR inhibits translation by phosphorylating, and thereby deactivating, eIF-2α – a necessary component of translation initiation (Biron and Sen, 2001; Samuel, 2001). Activated OAS

Figure 8. The interferon-induced innate immune response. (A) Simplified diagram of the immediately relevant portions of the interferon cascade in response to influenza A infection. **(B)** NS1 antagonizes the IFN cascade by: inhibiting IRF3 activation through dsRNA sequestering and RIG-I binding; inhibiting the translation of IFN-β and IFN-inducible genes by preventing splicing, polyadenylation, and mRNA export through its interaction with CPSF30, PABII, u6 snRNA, and poly(A) RNA; and also inhibits the activation of IFN-inducible PKR protein, both by inhibiting its induction, and by directly binding and inactivating the protein. Proteins and genetic elements are depicted and/or indicated by their common acronyms. Green arrows indicate casual activation. Red barred lines indicate inhibition. Influenza A is depicted in red near the center of the figure.

A

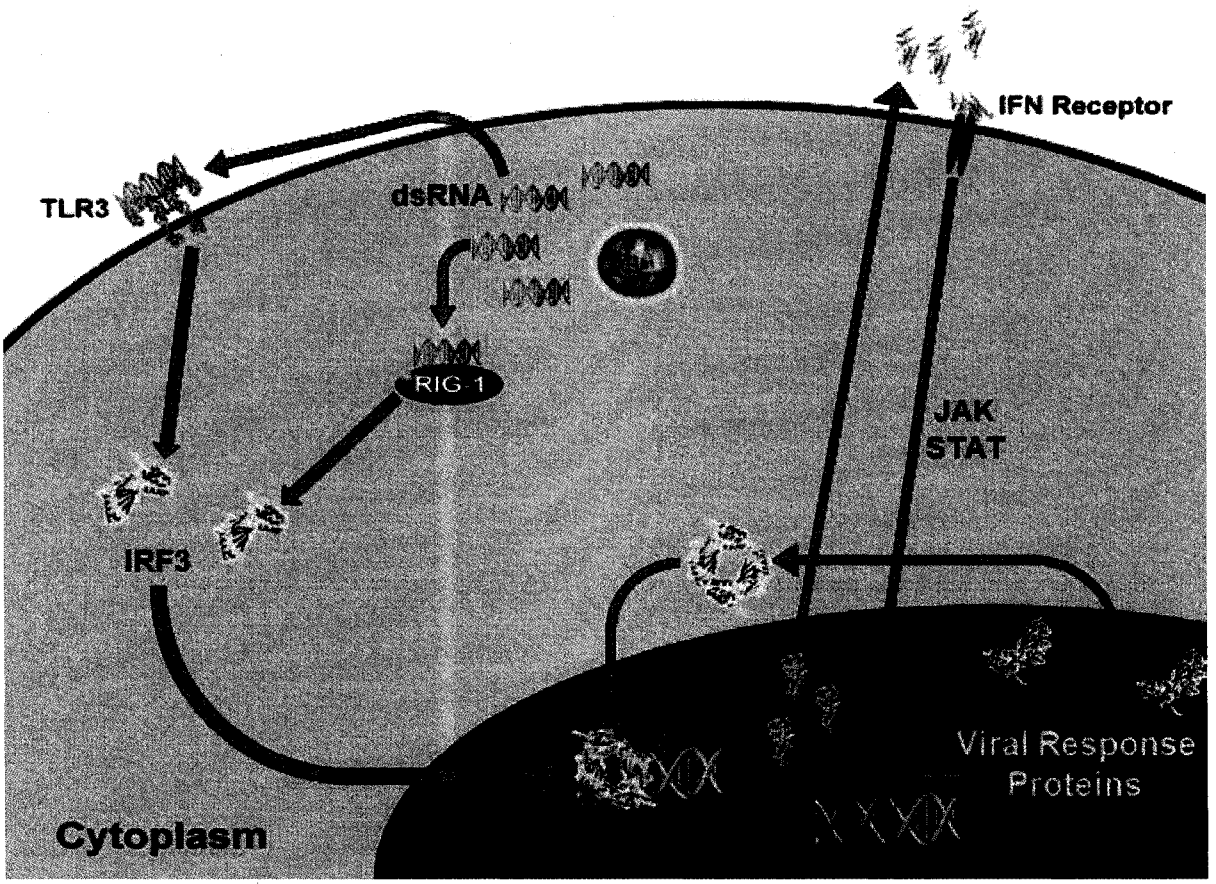

B

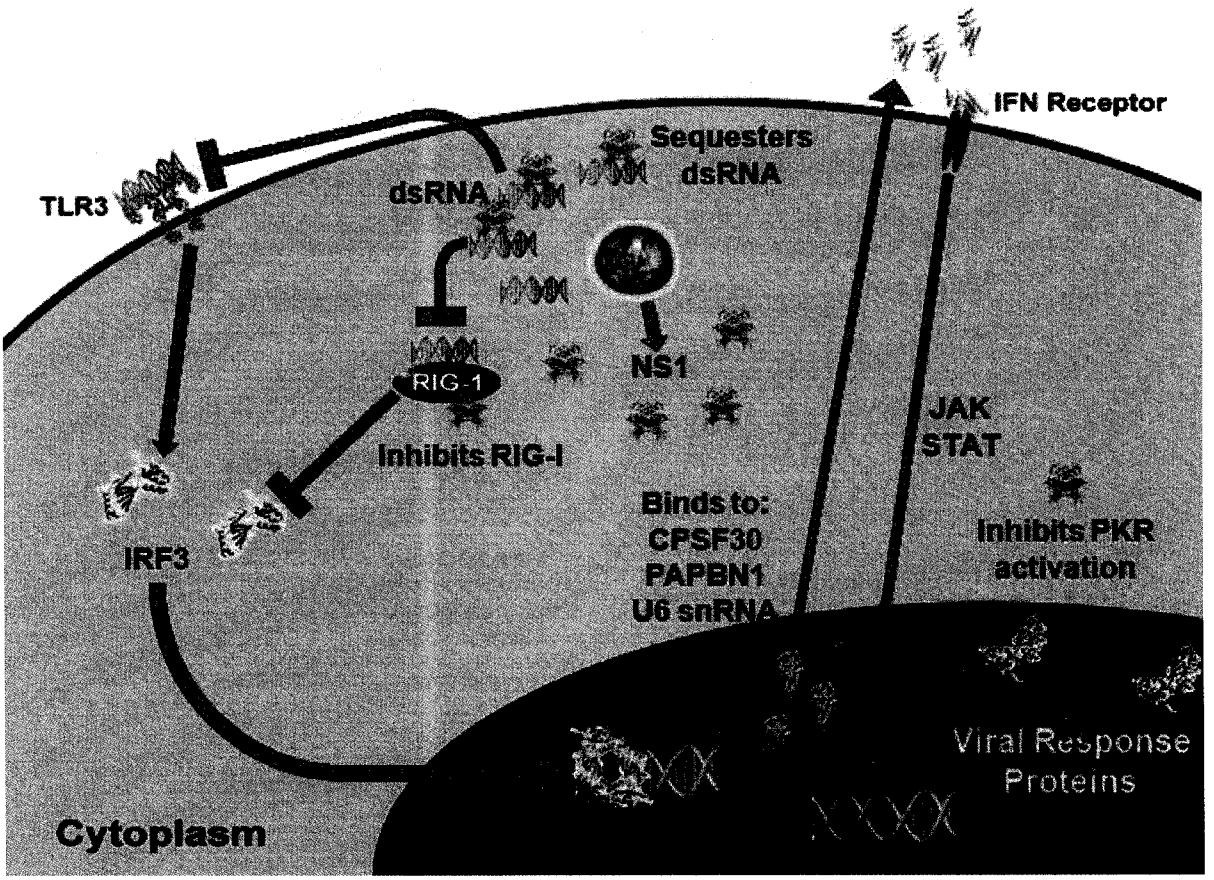

moves to activate the endonuclease RNase L which, in turn, homodimerizes and begins cleaving mRNA and ribosomal RNA (Biron and Sen, 2001; Samuel, 2001). Thus the combined effect of PKR, OAS, and RNase L is a general inhibition of protein translation, thereby slowing the viral spread by reducing cellular metabolism and preventing the synthesis of viral proteins. The MxA GTPase is a cytoplasmic IFN-inducible protein that is able to recognize and bind RNPs. MxA sequesters the bound RNPs in the cytoplasm away from the virus assembly site, preventing the formation of new viral particles. Additionally, MxA prevents RNPs from entering the nucleus where they can replicate. FluAV is especially sensitive in MxA inhibition (Haller *et al.*, 1998; Haller & Kochs, 2002; Staeheli *et al.,* 1993). Other important results of the IFN-induced anti-viral state include the expression of pro-inflammatory chemokines which attract immune cells (including macrophages, neutrophils, and lymphocytes) to the infected area, while also up-regulating the presentation of viral antigen to these attracted immune cells.

1.6 The Effect of NS1 on the Type I Interferon Response

Given the hostile environment that FluAV must endure during the IFN-induced anti-viral state, the NS1 gene has evolved numerous methods to antagonize the IFN response.

The first strategy employed by NS1 is to hide the virus' presence from the host by binding and sequestering dsRNA, thereby inhibiting the dsRNA-dependent activation of RIG-I and TLR3 (Hatada *et al.* 1992). Sequestration of dsRNA also inhibits the activation of PKR and OAS (Hatada *et al.*, 1999; Lu *et al.*, 1995). Furthermore, NS1 is also able to bind activated RIG-I directly, thereby inhibiting the downstream activation of IRF3 (Mibayashi *et*

al. 2007). By preventing host sentinel proteins from detecting dsRNA, NS1 thus prevents the activation of IRF3 and the resultant induction of IFN-β and the IFN cascade.

NS1 also acts as an IFN antagonist in the nucleus where it inhibits the poly-adenylation of host pre-mRNA by binding to PABPN1 and CPSF30. By inhibiting the poly-adenylation of host pre-mRNA transcripts, the virus inhibits the production mature host mRNA and, thereby inhibits the production of IFN as well as all of the IFN-inducible proteins at the post-transcriptional processing level. Simultaneously, sequestering the pre-mRNA to the nucleus by inhibiting poly-adenylation ensures a substantial supply of the host mRNA 5'-caps that are located on the partially formed pre-mRNA and are needed by the virus to prime the transcription of it's own mRNA (Chen *et al.* 1999; Nemeroff *et al.* 1998). Still in the nucleus, NS1 also inhibits pre-mRNA splicing by binding to U6 and U6atac snRNAs (Wang & Krug, 1998), as well as the nuclear export of mature host mRNA by binding to the poly(A) tails (Qiu & Krug, 1994; Wang & Krug, 1998). The combined effect of all these nuclear functions is a generalized inhibition of host gene expression at the transcriptional level. This inhibition is then further compounded at the level of translation by the preferential expression of viral mRNA that occurs due to the interaction of NS1 with PABP1 and eIF4G1. Because IFN-β is not present in a cell under normal conditions, the NS1-mediated inhibition of host gene expression inhibits IFN-β expression. Furthermore, the generalized inhibition extends to the expression of all of the IFN-inducible genes, greatly inhibiting the induction of the anti-viral state within the infected cell. Thus, NS1 antagonizes the IFN response by inhibiting the expression of all host genes, including IFN-β and the IFN-inducible genes. However, this generalized inhibition of all host genes may also hinder viral

replication by preventing the expression of host genes that are needed by the virus (Fig. 8b).

Interestingly, more recent investigations have demonstrated that FluAV may demonstrate more precise control over the IFN response, specifically down-regulating the expression of IFN-β and IFN-inducible genes. This specific inhibition of IFN-inducible genes has been linked to the NS1 protein (Geiss *et al.*, 2002), specifically the NS1 interaction with RIG-I (Matikainen *et al.*, 2006; Siren *et al.*, 2006). Highlighting the immunomodulation ability of FluAV are the highly pathogenic HPAI and Spanish flu strains, which are able to significantly suppress the expression of IFN-α and β and many IFN-inducible genes, while simultaneously and substantially inducing the expression of pro-inflammatory cytokines IL-6, IL-8, CCL2, CCL5, and MCP-1 (Kobasa *et al.*, 2007; Perrone *et al.*, 2008).

Finally, NS1 has been shown to bind PKR directly and, thereby, inhibit PKR activation, even in the presence of dsRNA (Tan, & Katze, 1998; Li *et al.* 2006; Min *et al.* 2007). Thereby, NS1 can prevent the PKR-mediated inhibition of protein translation that would decrease the production of viral proteins.

1.7 Pathogenesis of Influenza A

FluAV is a highly infectious respiratory virus that infects and replicates in the respiratory epithelium. Epithelial infection leads to necrosis of the infected surface epithelium along the respiratory tract which causes inflammation of the trachea and bronchi (tracheobronchitis) (Wright *et al.*, 2007). A more severe primary infection may also spread to infect and necrotize the alveoli (To *et al.*, 2001). Alveolar infection can lead to

viral interstitial pneumonitis as the alveoli are destroyed and the lungs become inflamed and are infiltrated by immune cells and fluid (Guarner *et al.*, 2000)

Common symptoms of the flu are generally derived from the immune response to the virus and include fever, chills, myalgia, malaise, anorexia, headaches, and a dry cough. Less common complications include myositis, gastrointestinal problems, and viremia, while neurological complications have been reported in rare cases. The virus reaches peak titers at approximately two days post infection and viral shedding disappears between days six to eight (Wright *et al.*, 2007).

FluAV mortalities generally occur due to respiratory failure resulting from interstitial pneumonitis or complications arising from secondary bacterial pneumonia (Louria *et al.*, 1959; Petersdorf *et al.*, 1959; Robertson *et al.*, 1958). Elderly and immunocompromised patients are the most at risk to develop interstitial pneumonitis or secondary bacterial pneumonia (Barker and Mullooly, 1980; 12, Simonsen, 1999; Sprenger *et al.*, 1993). Cardiovascular disease, chronic bronchitis, obstructive pulmonary disease, diabetes, and asthma are also factors that increase the risk of developing interstitial pneumonitis or secondary bacterial pneumonia (Wright *et al.*, 2007). The highly pathogenic HPAI and Spanish flu strains display a much greater degree of virulence in humans than the common FluAV strains that have low pathogenicity. Fatality during infection with one of these highly pathogenic FluAV strains is more typically caused by respiratory failure due to viral interstitial pneumonitis (Wright *et al.*, 2007). Those most at risk to develop complications in response to infection with highly pathogenic FluAV strain are young and otherwise healthy adults, aged 15 to 35 years old (Wright *et al.*, 2007). This pneumonitis is caused by the

infiltration of immune cells that are drawn into the lungs by the heightened and aberrant immune response that is modulated by the virus (Kobasa *et al.*, 2007). Thus, the high risk of complications in healthy adults is due to the increased strength of the innate immune response that their bodies are able to mount. The mortality rate of the Spanish flu was 2.5%, compared to the mortality rate of less than 0.1% that is seen in typical human FluAV outbreaks (Wright *et al.*, 2007). The mortality rate of HPAI in human infection is 63% to date (World Health Organization).

1.8 Evolution in the Influenza A Virus

Due to the fact that all known human HA and NA subtypes are maintained in birds, it is hypothesized that all mammalian FluAV strains are derived from the avian FluAV virus reservoir. This hypothesis has gained further support from phylogenic analysis (Webster *et al.*, 1992). New subtypes of FluAV are generally introduced into the human population from the avian reservoir by a process termed "antigenic shift". There have been four antigenic shifts in the past 100 years: the H1N1 subtype emerged in 1918, H2N2 emerged in 1957, H3N2 in 1968, and a much less pathogenic strain of H1N1 emerged in 1977 (Webster *et al.*, 1992). The newly introduced FluAV subtypes are antigenically distinct from endogenous human FluAV strains and, therefore, cause pandemics due to their high infection rates in the immunologically naïve human population.

Antigenic shift generally results from a reassortment between human and avian FluAV strains. Reassortment is the process by which the genomic RNA segments from more than one progenitor virus are sorted into the same virion during viral replication. The result

is a new virus containing a complete genome consisting of individual genomic segments from two or more parent viruses (Wright *et al.*, 2007). Reassortment is possible due to the segmented nature of the FluAV genome, and may occur when a cell is co-infected with two or more separate FluAV strains. Reassortment is the process by which the H2N2 and H3N2 subtypes entered into the human population, and is also responsible for the development of the H1N2 subtype from endogenous human subtypes (Wright *et al.*, 2007).

A second, albeit rare, mechanism for the emergence of a new human FluAV subtype is through the direct transmission of an avian FluAV to humans, followed by its establishment in the human population. Interspecies transfer by means of direct transmission is uncommon, likely due to the decreased fitness that an avian FluAV strain faces in a foreign host as compared against the indigenous host-adapted strains (Webster *et al.*, 1992). Thus interspecies direct transmission may only be viable for highly pathogenic FluAV strains that are able to overcome this deficiency. Although the evidence is not conclusive, phylogenic analysis suggests that the highly pathogenic 1918 Spanish H1N1 FluAV was introduced into humans by direct transmission from an avian strain (Basler *et al.*, 2001; Reid *et al.*, 1999; Reid *et al.*, 2000; Reid *et al.*, 2002; Reid *et al.*, 2004; Taubenberger *et al.*, 2005). There is currently concern that the highly pathogenic H5N1 avian strain may also evolve into a pandemic human virus through direct transmission.

Exclusive of reassortment, the evolution of human FluAV strains progress in response to selective pressures at a rate of 0.004 base substitutions per nucleotide per year (Webster *et al.*, 1992). The speed of mutation in human FluAV strains is likely due to viral adaptation to the (relatively) new human host because evolutionary rates are substantially

slower in avian FluAV strains (Webster *et al.*, 1992), in which they are nearly static. The evolutionary rate of FluAV also differs between the individual genetic segments, with the envelope protein genes (HA, NA, and M2) evolving much faster than the other genes. Evolution within the envelope proteins generally map to antigenic sites and are likely to be primarily the result of selective pressure imposed by the adaptive immune system (Webster *et al.*, 1992). Interestingly, the two NS genes also evolve at different rates, with the NS1 gene changing faster than the NS2 (Webster *et al.*, 1992), likely due to the dynamic immunomodulatory nature of the NS1 protein. The evolution of virulence in FluAV results from conditions that provide a vast supply of susceptible hosts, thereby favouring the viruses that can replicate and spread the most quickly. Increased viral replication may be derived from mutations that enhance the efficiency of replication, as well as from mutations that allow the virus to escape host antiviral responses. These evolved viruses are more virulent because faster viral replication and increased immunosuppression generally come at the cost of increased host pathogenesis. Such virulence-promoting conditions currently exist in modern high-density poultry farming. It is this environment which is the most likely source of the current H5N1 HPAI lineage in Asia.

1.9 Project Background

1.9.1 The Mouse Model for Influenza Virulence

The genetic basis of virulence is difficult to study in human FluAV strains because all clinical isolates of these viruses are of similar pathogenicity (Kilbourne, 1959). However, although FluAV is partially host restricted, a fundamental basis of infection is common

across different species (Suarez *et al.*, 1998). Therefore investigation into the genetic basis of virulence in a model species may provide insights that are also applicable to human FluAV strains. To this extent, the mouse model is a valuable tool for the study of human FluAV virulence due to the pathological similarities between the interstitial pneumonia that occurs in both species (Ward, 1997; Sweet & Smith, 1980). Furthermore the mouse model is especially suitable to this study because the NS1 binding partners that are being investigated, CPSF30-F2/F3 (the NS1-binding region of CPSF30) and PABP1, are highly conserved between humans and mice (100% and >99% respectively). Thus adaptive mutations to the NS1 protein acquired through serial passage in mice will likely have similar effects on NS1's capacity to bind PABP1 and CPSF30 in both species.

Previously, mice were subjected to high-dose serial passaging of the prototype human A/HK/1/68 (H3N2) virus (HK-wt) in order to simulate the conditions of high population density that select for increased virulence (Brown *et al.* 2001). After 20 sequential passages, the lethal median dose (LD_{50}) decreased from greater than $10^{7.7}$ plaque-forming units (pfu) in the avirulent HK-wt to as low as $10^{2.7}$ pfu in the mouse-adapted (HK-MA) strains, marking a 10^5-fold increase in virulence. Sequence analysis of the MA strains revealed numerous sites of independently selected mutations that localized to all eight segments of the genome, suggesting that the control of virulence in FluAV is multigenic. This multigenic control of virulence supports the findings of other studies (Brown and Bailly, 1999; Brown, 1990; Smeenk and Brown, 1994; Smeenk *et al.*, 1996). However, in order to understand the genetic basis of virulence, the significance of each mutation must be examined in isolation. Therefore, because the HK-MA viruses displayed

increased IFN resistance and viral protein production (E.G. Brown, unpublished data), the NS1 gene was selected for further investigation.

1.9.2 Properties of the NS1 Variants

Examination of the NS1 gene yielded seven specific mutation sites that were independently and repeatedly selected: aa23, aa98, aa103, aa106, aa180, and aa226 (Table 2, Fig. 9). The repeated occurrence of mutations at some of these sites and the clustering of mutations in specific regions strongly suggests that these areas are involved in the increased viral virulence. Furthermore, V23A, F103L, M106I, and V226I are convergent mutations in that identical mutations have been selected independently in the highly pathogenic HPAI and Spanish flu viruses (Table 2). Similarly, the L98S, F103L, and M106V mutations are sites of directional mutation with regards to the HPAI and the Spanish flu in that these strains contain mutations at the same residues, but that these mutations result in different amino acid substitutions (Table 2). Finally, aa103 and aa106 have been specifically identified as critically important in stabilizing the binding between NS1 and CPSF30 and, thereby, inhibiting the production of IFN-β (Koch *et al.*, 2007; Twu *et al.*, 2007). These findings lend additional support for the importance of these sites in viral virulence.

To examine the effect of the NS1 mutations during infection in isolation recombinant viruses were created for each of the NS1 variants (rWSN viruses). These recombinant viruses consisted of an isogenic A/WSN/33 backbone, into which the WSN NS1 gene was substituted with the NS1 gene from HK-wt or one of the HK-MA viruses. During both *in vivo* infection of mice and *in vitro* infection of murine eukaryotic cell lines, the

Table 2. Convergent mutations acquired in NS1 gene of the HK/1/68 (H3N2) virus upon mouse adaptation after 20 passages. (A) The site of the mutation is noted along the top and the corresponding amino acids substitutions are bolded and underlined. The entire affected codon is shown for clarity. **(B)** The resultant amino acid substitutions are presented with the site of the mutations noted along the top. Mutations marked with "*" have been previously shown to alter CPSF30 binding capacity (Twu *et al.*, 2007). Mutations marked with "¥" occur in a region that has been previously shown to affect PABP1 binding capacity (Burgui *et al.*, 2003). The amino acids that are present at the corresponding sites in the highly pathogenic avian influenza and 1918 Spanish flus are listed in the bottom two rows. Cells marked "-" denote no deviation from HK-wt.

Denotes a mutation in the PABPN1 binding domain
Denotes a mutation in the eIF4G1 binding domain
Denotes a mutation in the CPSF30 binding domain
Denotes a mutation in the PABPC1 binding domain

A

Viral Strain	NS1 Variant	Nucleotide Position						
		68	293	307	[illegible]	[illegible]	[illegible]	676
HK/1/68 (H3N2)	HK-wt	GTA	TTG	[illegible]	[illegible]	[illegible]	[illegible]	GTT
HK-MA20 (H3N2)	HK-23A	GCA	-	-	-	-	-	-
HK-MA20c (H3N2)	HK-103L	-	-	CTG	-	-	-	-
HK-MA41 (H3N2)	HK-106V	-	-	-	[illegible]	[illegible]	[illegible]	-
HK-MA51 (H3N2)	HK-106I	-	-	-	[illegible]	[illegible]	[illegible]	-
HK-MA53 (H3N2)	HK-106I + 98S	-	TCG	-	[illegible]	[illegible]	[illegible]	-
HK-MA63 (H3N2)	HK-180A	-	-	-	[illegible]	[illegible]	[illegible]	-
HK-MA103 (H3N2)	HK-226I	-	-	-	[illegible]	[illegible]	[illegible]	ATT

B

Viral Strain	NS1 Variant	Amino Acid Position						
		23	98	[illegible]	[illegible]	[illegible]	[illegible]	226
HK/1/68 (H3N2)	HK-wt	V	L	-	-	-	-	V
HK-MA20 (H3N2)	HK-23A	A	-	-	-	-	-	-
HK-MA20c (H3N2)	HK-103L	-	-	-	L	-	-	-
HK-MA41 (H3N2)	HK-106V	-	-	-	-	V	-	-
HK-MA51 (H3N2)	HK-106I	-	-	-	-	I	-	-
HK-MA53 (H3N2)	HK-106I + 98S	-	S	-	-	I	-	-
HK-MA63 (H3N2)	HK-180A	-	-	-	-	-	A	-
HK-MA103 (H3N2)	HK-226I	-	-	-	-	-	-	I
HK/97 (H5N1)	HPAI	A	M	-	-	-	-	I
BM/18 (H1N1)	Spanish Flu	A	M	-	-	-	-	I

Figure 9. Three-dimensional functional map of the Influenza A NS1 protein. NS1 is presented here in one of the proposed homodimerized forms (Bornholdt & Prasad, 2006 and Chein *et al.*, 1997). Relevant active binding sites mapped on NS1 are colour-coded and labeled in the legend to the right. The sites of convergent evolution seen in mouse-adapted HK/1/68 (H3N2) strains are indicated by the green space filling diagrams and the corresponding amino acid residue number. The 226 mutation could not be shown because the NS1 effector domain used to solve the crystal structure is truncated and ends at residue 206. The crystal structures of the NS1 RNA-binding and effector domains were solved independently of each other. The RNA-binding domain is the uppermost structure, while the effector domain is located below. The connecting 3' residues of the RNA-binding domains and 5' residues of the effector domains are marked with black arrows.

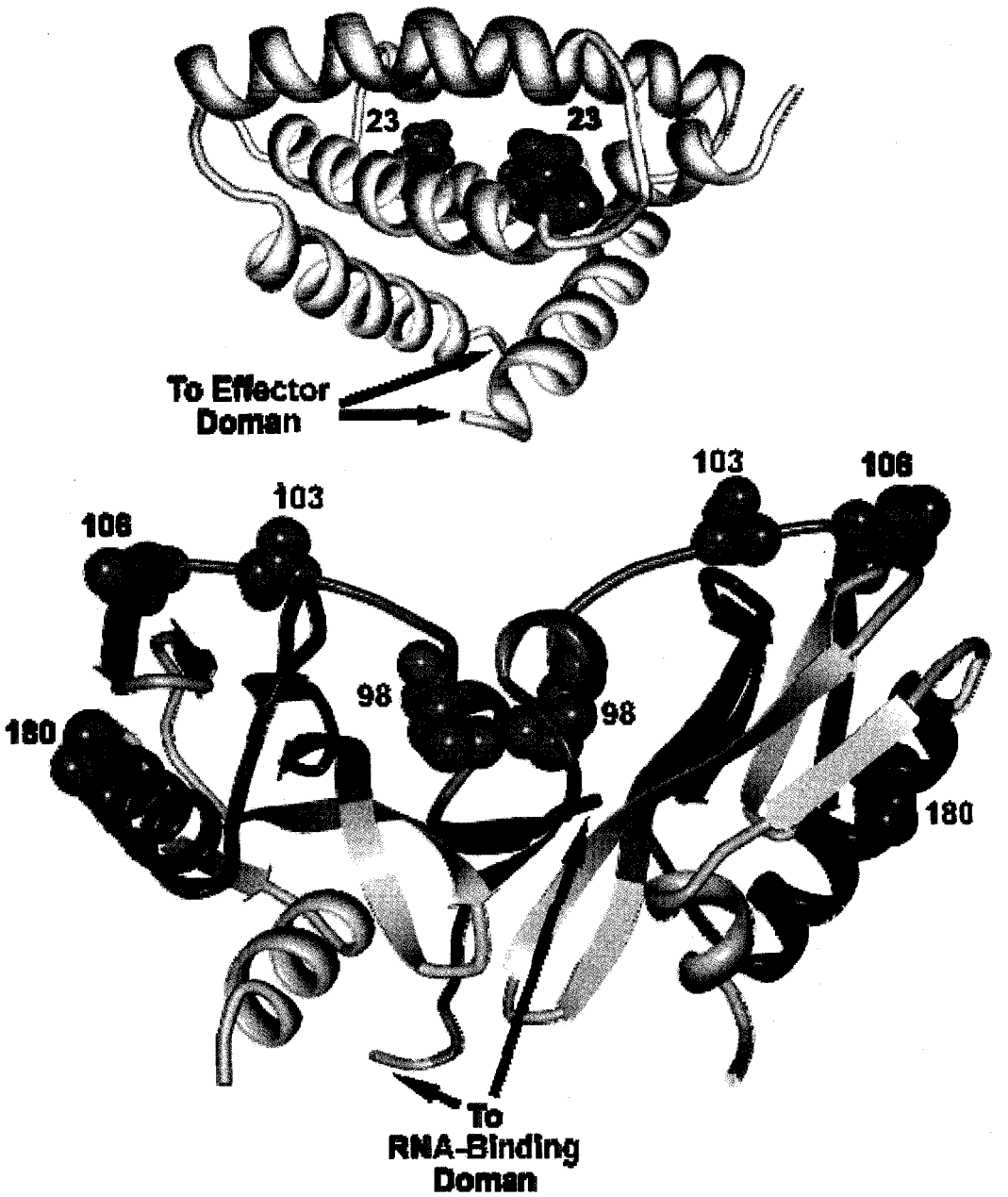

PABP1/PKR Binding Domain
eIF4G1 Binding Domain
CPSF30 Binding Domain
PI3K Binding Sites
MA Mutations

rWSN-103L, rWSN-106I, and rWSN-98S+106I recombinant viruses displayed a greater resistance to IFN-β than the rWSN-wt control. Similarly, these rWSN viruses also showed an increase in viral protein production (E.G. Brown, unpublished data). Both of these phenotypes are seen in the naturally occurring HPAI and Spanish FluAVs, thereby lending greater support to the hypothesis that NS1 is a critical virulence factor (Kobasa *et al.*, 2007; Perrone *et al.*, 2008). Interestingly, the rWSN-MA viruses also induced IFN-β to a greater extent than rWSN-wt, and the V23A and M106V mutations were growth attenuating to various degrees (Table 3). This increase in IFN-β production may be due, in part, to mutations at the aa103 and aa106 which have been previously shown to play a role in stabilizing the NS1-CPSF30 binding. Mutations at these sites that lead to a loss of CPSF30 binding have been shown to increase IFN-β induction and to also cause growth attenuation when expressed in recombinant viruses (Das *et al.*, 2008; Koch *et al.*, 2007; Twu *et al.* 2006; Twu *et al.* 2007). Thus, it is apparent that these specific mutations in the NS1 drastically alter the specific aspects of immunosuppression, IFN resistance, and protein production of FluAV variants that possess these mutations. However, the molecular mechanisms by which the NS1 mutations alter these abilities are not yet understood. Due to the phenotype of increased viral protein production in the HK-MA viruses and the integral role of the NS1-PABP1 interaction in enhancing viral protein production, it is likely that the MA mutations are affecting the PABP1 and/or eIF4G1 binding affinity of NS1 in some manner. Similarly, due to the increased interferon resistance exhibited by the mouse-adapted viruses combined with the localization of numerous mutations to specific sites that are known to

Table 3. The effects of the mouse-adapted NS1 mutations on viral growth, IFN induction, IFN resistance, and protein production in recombinant WSN viruses. (Derived from E.G.Brown, unpublished data) Changes are presented as percentages relative to the result obtained for rWSN-wt. Experiments could not be performed on the rWSN-23A and rWSN-106V strains due to their attenuation. Experiments have not yet been performed on the rWSN-180A and rWSN-226I strains.

Strain	Viral Growth in MDCK Cells	Increase in IFN Induction in M1 Cells	Increase in IFN Resistance in M1 Cells Pretreated with IFN-β	Increase in Protein Production in A549 cells without IFN	Increase in Protein Production with IFN Pretreatment
rWSN-wt	-	-	Sensitive	-	-
rWSN-23A	Unrescuable	Not Rescued	Not Rescued	Not Rescued	Not Rescued
rWSN-103L	Comparable to wt	270%	Significantly Resistant	400%	570%
rWSN-106V	Attenuated 1,000-fold	Insufficient titer for experiment	Significantly Resistant	Insufficient titer for experiment	Insufficient titer for experiment
rWSN-106I	Comparable to wt	400%	Significantly Resistant	380%	730%
rWSN-98S+106	Comparable to wt	200%	Significantly Resistant	150%	250%
rWSN-180A	Experiments not yet performed				
rWSN-226I	Experiments not yet performed				

be important in CPSF30-binding, it is likely that the MA mutations are affecting NS1's CPSF30-binding ability.

1.10 Hypothesis

Adaptive mutations found in mouse adapted highly virulent FluAV strains may increase viral protein production by increasing the binding affinity of NS1 to PABP1. Similarly, these mutations may increase the interferon resistance of the mouse-adapted strains by increasing the binding affinity for CPSF30.

1.11 Objectives

A) Express and purify the HK-wt and HK-MA NS1 proteins.

In order to examine differences in binding affinity between the HK-wt and HK-MA NS1 proteins, these proteins had to first be expressed and purified to examine the protein phenotype in the absence of the other viral proteins.

B) Examine the differences in CPSF30 binding affinity between HK-wt and the HK-MA variant NS1 proteins by coimmunoprecipitation.

C) Examine the differences in PAPB1 binding affinity between HK-wt and the HK-MA variant NS1 proteins by GST pulldown.

MATERIALS AND METHODS

2.1 Cell Lines and Viruses

COS-1 cells (African green monkey kidney fibroblast-like cell line expressing the simian virus 40 T antigen) and 293T cells (human embryonic kidney epithelial cell line expressing the simian virus 40 T antigen) were grown and maintained in minimal essential medium (MEM) supplemented to 10% with fetal bovine serum (FBS) in a 3.5% CO_2 atmosphere at 37°C.

DH5α escheria coli (*E. coli*) was chosen for plasmid propagation due to it's deficiency in endonuclease and reconbinase A production, thereby allowing for higher fidelity of cloned plasmids. BL21 was chosen for bacterial protein expression because it lacks the lon and ompT proteases, thereby allowing for more efficient protein expression. Additionally the BL21(DE3) strain contains a chromosomal copy of T7 polymerase under expressional control by lavU5, allowing for expressional control of proteins transcribed from the T7 promoter by modifying the IPTG level of the media. Finally, the BL21(DE3)pLysS strain contains the pLysS plasmid expressing T7 lysozyme which provides tighter control of T7 promoter-controlled expression by binding to low levels of T7 polymerase that may be constitutively expressed in the absence of IPTG despite the lacU5 control. DH5α, BL21(DE3), and BL21(DE3)pLysS *E. coli* were grown in Luria-Bertani (LB) broth or on LB agar plates. Both the LB broth and plates were supplemented 300 μg/mL ampicillin (amp) and/or 100 μg/mL chloramphenicol (cm) where necessary. Bacterial cultures were stored at -80°C in LB broth supplemented with 20% glycerol.

NS1 genes were derived from A/Hong Kong/1/68 (H3N2) Influenza and its mouse-adapted progenies; HKMA20, HKMA 20c, HKMA41, HKMA51, HKMA53, HKMA63, and HKMA103.

2.2 Protein Expression Vectors

2.2.1 Construction of the NS1 Protein Expression Vectors

Eight separate pHH21 plasmids, each containing one of the eight studied NS1 variants, were obtained from Dr. Earl Brown at the University of Ottawa, Ottawa, Canada. From these constructs, the NS1 genes were amplified by PCR with the NS1 TOPO primers (Appendix II) which added a 5' NdeI restriction site and 6x-His tag, as well as a 3' EcoR1 site. PCR conditions: 94°C for 4 minutes, followed by 30 cycles of (94°C for 30 sec, 52°C for 30 sec, 72°C for 4 min and 30 sec) and finally 72°C for 10 min.

2.2.1.1 Topo Cloning

NS1 genes amplified from pHH21 were recombined into the pDrive Topo cloning vector (Qiagen) using the Topo TA cloning kit (Invitrogen) as per the manufacturer's protocol.

2.2.1.2 Subcloning of the NS1 Genes

NS1 genes were subcloned from pDrive into pET17b using the NdeI and EcoRI restriction sites. pET17b allows for bacterial expression from the T7 promoter.

2.2.2 PABP1-GST Expression Vector

The pGEX2T-PABP1-GST expression vector was donated by Dr. Juan Ortín at the Centro Nacional de Biotecnología in Madrid, Spain. These vectors allow for bacterial expression of PAPB1-GST from the Ptac promoter.

pGEX4T-GST is commercially available from Amersham Biosciences.

2.2.3 CPSF30 Expression Vectors

pCAGGs-CPSF30-Flag and pCAGGS-CPSF30-F2/F3-Flag were donated by Dr. Adolfo Garcia-Sastre at the Mt. Sinai School of Medicine in New York, USA.

pCAGGS allows for eukaryotic expression of the cloned protein from the SV40 promoter.

2.2.4 eIF4G1 Expression Vectors

pcDNA3-HA-eIF4G1, pET15g-eIF4G1-Flag, and pGEX-eIF4G1-His were donated by Dr. Nahum Sonenberg at the Rosalind and Morris Goodman Cancer Centre in Montreal, Canada.

pcDNA3-HA-eIF4G1 allowed bacterial expression of HA-tagged eIF4G1 from the T7 promoter, as well as eukaryotic expression of the protein from the CMV promoter. pET15g-eIF4G1-Flag allowed bacterial expression of Flag-tagged eIF4G1 from the T7 promoter. Finally, pGEX-eIF4G1-His allowed bacterial expression of 6x-His-tagged eIF4G1 from the Ptac promoter.

2.3 Plasmid Purification

2.3.1 MiniPrep

Colonies were picked from LB plates containing 300 μg/mL ampicillin (amp) and used to inoculate 3 mL of LB broth which also contained 300 μg/mL amp. Inoculated cultures were incubated O/N at 37°C with shaking at 225 rpm. Following incubation, a miniprep was performed using the QIAprep Spin Miniprep Kit (Qiagen) according to the manufacturer's protocol.

2.3.2 MiniPrep – Boiling Lysis Method

Colonies were picked from LB plates containing 300 μg/mL ampicillin (amp) and used to inoculate 3 mL of LB broth which also contained 300 μg/mL amp. The inoculated LB broth cultures were incubated O/N at 37°C with shaking at 225 rpm. Following incubation, the bacteria were pelleted from the culture by 30 seconds of centrifugation at 14,000 rpm. All supernatant was then removed by gentle aspiration. The pelleted bacteria were resuspended in 350 μL of STET containing 50 mg/mL lysozyme and placed in a boiling water bath for 30 seconds. The bacterial lysate was then centrifuged at 14,000 rpm for 15 minutes, after which the supernatant was poured into a new microcentrifuge tube. The DNA was precipitated from the supernatant with 34 μL of 3M sodium acetate (pH 5.2) and 420 μL of isopropanol. The precipitated DNA was pelleted by centrifugation at 14,000 rpm for 10 minutes, washed once with 1 mL of 70% ethanol, and then air-dried for 15 minutes at

room temperature. Finally, the pelleted nucleic acids were dissolved in 50 µL of TE (pH 8.0) and stored at -20°C.

2.3.3 MidiPrep

An inoculation loop of frozen bacterial stock was used to inoculate 50 mL of LB broth containing 300 µg/mL amp, which was then incubated O/N at 37°C with shaking at 225 rpm. Following incubation, a midiprep was performed using the Wizard Plus Midiprep DNA Purification System (Promega), according to the manufacturer's protocol.

2.3.4 MaxiPrep

An inoculation loop of frozen bacterial stock was used to inoculate 150 mL of LB broth containing 300 µg/mL amp, which was then incubated O/N at 37°C with shaking at 225 rpm. Following incubation, a maxiprep was performed using the GenElute HP Plasmid Maxiprep Kit (Sigma) according to the manufacturer's protocol.

2.4 Restriction Digestion

2.4.1 Single Digestions

Restriction endonucleases were used to screen cloned plasmids. NheI digestions were carried out in a 50 µL solution containing 2 µg of plasmid DNA, 5 units of NheI (Fermentas), and 5 µL 10x Tango Buffer (Fermentas) in distilled water. EcoRI digestions proceeded in a 50 µL reaction containing 2 ug of plasmid DNA, 10 units of EcoRI (New

England Biolabs), and 5 µL 10x NEBuffer 4 (New England Biolabs) in distilled water. All single digestion reactions were incubated for 2 hours at 37°C.

2.4.2 Double Digestions

Double digestions were used to excise the His-NS1 fragment from the pDrive-His-NS1 plasmids and also to digest the pET17b vector in preparation for insertion of the His-NS1 fragments. Double digestion with NheI and EcoRI were carried out in two steps. First, 2 µg of plasmid DNA was incubated at room temperature for 2 hours in a 60 µL solution containing 5 units NheI (Fermentas), and 6 µL 10x Tango buffer (Fermentas) in distilled water. Following the initial incubation, an additional 6 µL of Tango buffer was added along with 10 units EcoRI (New England Biolabs) and the solution was incubated for a further 2 hours at 37°C.

2.5 Ligation

Ligation reactions to insert the His-NS1 DNA fragments into pET17b were carried out in 12 µL solutions containing 7 µL of NheI and EcoRI digested His-NS1 DNA fragment (≈ 500 ng), 2 µg of NheI and EcoRI digested pET-17b expression vector, 2 units of T4 DNA Ligase (Roche), and 2 µL 5x Ligase Reaction Buffer (Roche). The ligation reaction was incubated at room temperature for 4 hours.

2.6 Transformation of chemically competent *E. coli*

100 µl of chemically competent DH5α, BL21(DE3), or BL21(DE3)pLysS *E. coli* was incubated for 30 minutes on ice in the presence of 10 ng of the desired plasmid. The

transformation mixture was then heat-shocked for 45 seconds in a 42°C water bath before being returned to the ice for an additional 2 minutes. 900 µl of room temperature S.O.C. Medium was then added and the transformation mixture was incubated for 1 hour at 37°C with shaking at 225 rpm. Finally, 50 µl and 150 µl of the transformation mixture was plated onto LB plates containing 300 µg/mL amp (as well as 100 µg/mL chloramphenicol (cm) for BL21(DE3)pLysS transformations) and incubated O/N at 37°C.

2.7 Cracking Gel

Cracking gels were employed to efficiently screen a large number of colonies for the presence of the desired NS1 DNA insert in the pET17b plasmid. Ten to twenty colonies were picked and resuspended individually in 7 µL of suspension buffer. Each resuspended colony was then loaded into a well in a 0.8% agarose gel and 10 µL of lysis buffer was added to each. After a 10 minute incubation at room temperature, the gel was submerged in TBE buffer and subjected to electrophoresis at 110 V until the bromophenol marker had migrated 2/3 the length of the gel. The presence or absence of the NS1 DNA insert was confirmed by size comparison against a wild-type pET17b plasmid control.

2.8 Gel Extraction of DNA

Gel extraction was used to separate His-NS1 DNA fragments from linear pDrive following double digestion and also to separate linear pET17b-His-NS1 from the circularized template following PCR site-directed mutagenesis. DNA samples were purified by electrophoresis on a 0.8% agarose gel in TBE buffer. The desired DNA band was excised

using a razor blade under long wavelength ultra-violet light (BLAK-RAY long wave ultra-violet lamp). Purification of the DNA from the extracted gel was performed with the QIAquick Gel Extraction Kit (Qiagen) according to the manufacturer's protocol.

2.9 PCR Site-directed Mutagenesis

Site directed mutagenesis was used to correct undesired mutations that occurred in the HK-wt, HK-103L, HK-106I, and HK-106I+98S NS1 genes during cloning. A pair of specific primers were designed to correct each mutation (see Appendix II) and used to amplify corrected pET17b-His-NS1 plasmids from the mutated plasmid templates. PCR conditions: 94°C for 4 minutes, followed by 30 cycles of (94°C for 30 sec, 43°C for 30 sec, 72°C for 4 min and 30 sec) and finally 72°C for 10 min. The linear corrected constructs were then separated from the mutated template plasmids by agarose gel extraction for subsequent ligation and transformation.

2.10 5' Phosphorylation and Ligation

A two step phosphorylation and ligation reaction was performed to circularize linear PCR-amplified plasmids following PCR site-directed mutagenesis. 24 µL of gel-purified PCR Product DNA was incubated for 30 minutes at 37°C in a solution containing 3 µL of 10x T4 DNA Ligase Buffer (Roche) and 2 units of PNK (Pharmacia) in ddH_2O (30 µL total volume). Next the solution was incubated at 70°C for 15 minutes in order to deactivate the PNK and then cooled to room temperature. Finally, 2 units of T4 DNA Ligase (Roche) were added and the solution was incubated for an additional 2 hours at room temperature.

2.11 Prokaryotic Protein Expression

2.11.1 Mini-induction

Overnight cultures were created by inoculating 3 ml of LB broth containing the appropriate antibiotics (300 µg/mL amp for DH5α and BL21(DE3), 300 µg/mL amp and 100 µg/mL cm for BL21(DE3)pLysS) with *E. coli* containing the expression vector for the desired protein. The cultures were then incubated O/N at 37°C with shaking at 225 rpm. After this incubation, 100 µl from the overnight culture was used to inoculate a fresh, pre-warmed, 3 ml LB broth culture containing the same antibiotics. The new 3 ml culture was shaken at 225 rpm and 37°C until the culture reached an optical density at λ = 600 nm ($O.D._{600}$) of between 0.3 and 0.6. At this point 1 ml of the culture was removed, centrifuged at 6,000 rpm for 1 minute, and resuspended in a volume of 2x SDS sample buffer equal to $O.D._{600}$ x 100 µl to represent an uninduced sample. The remaining culture was induced with 1 mM IPTG for 3 hours at 37°C with shaking at 225 rpm. After induction the $O.D._{600}$ was measured

again and 1 ml of the induced culture was centrifuged at 6,000 rpm for 1 minute and then resuspended in a volume of 2x SDS sample buffer equal to $O.D._{600}$ x 100 µl to represent an induced sample. Samples were analyzed for the presence of the desired protein by SDS-PAGE followed by coomassie blue staining.

2.11.2 Mega-induction

Overnight cultures were created by inoculating 25 ml of LB broth containing 300 µg/mL amp and 100 µg/mL cm, with BL21(DE3)pLysS *E. coli* containing the appropriate expression vector (pET17b-His-NS1for NS1 expression, pGEX-2T-PABP1 for PABP1-GST expression, pGEX-4T for GST expression, and pGEX-eIF4G1-His for eIF4G1 expression). The cultures were then incubated O/N at 37°C with shaking at 225 rpm. Following this incubation, the entire overnight culture was used to inoculate 500 ml of fresh, pre-warmed, LB broth containing the same antibiotics. The 500 ml culture was incubated at 37°C with shaking at 225 rpm until the culture reached an $O.D._{600}$ of between 0.5 and 0.6. At this point 1 ml of the culture was removed, centrifuged at 6,000 rpm for 1 minute, and resuspended in a volume of 2x SDS sample buffer equal to $O.D._{600}$ x 100 µl to represent an uninduced sample. The remaining culture was induced with IPTG (10 µM IPTG for NS1 induction or 1 mM IPTG for PABP1, eIF4G1, and GST induction) and incubated for specific times at specific temperatures (16 hours at room temperature for NS1 expression, 3 hours at 37°C for PABP1 and GST expression, or 3 hours at 30°C for eIF4G1 expression). After induction the $O.D._{600}$ was measured again and 1 ml of the induced culture was centrifuged at 6,000 rpm for 1 minute and resuspended in a volume of 2x SDS sample buffer equal to $O.D._{600}$ x 100 µl

to represent an induced sample. The cultures were then chilled on ice before being subjected to centrifugation at 4,000 rpm for 20 minutes at 4°C. The supernatant was then discarded and the pelleted cells were resuspended in 20 mL of NS1, PABP1, or eIF4G1 Lysis Buffer and lysed by 5 minutes of sonication on ice interspersed with a 30 second rest period following each minute of sonication. The bacterial lysate was then centrifuged for 20 minutes at 10,000 rpm and 4°C. Next, the supernatant was removed as the soluble fraction, and the pellet was resuspended in 10 mL of Insoluble Fraction Urea Buffer. 50 µL samples were taken from each of the soluble and insoluble fractions and mixed with 50 µL of 2x SDS sample buffer. All samples were then analyzed by SDS-PAGE and coomassie staining and/or western blotting to verify protein expression.

2.12 Protein Purification

2.12.1 Ni-NTA Batch purification of NS1 and eIF4G1

Recombinant His-NS1 and His-eIF4G1 were purified from the soluble fraction of the crude bacterial cell lysate by binding their His tags to Ni-NTA agarose (Qiagen) for 2 hours at room temperature in NS1 Lysis Buffer or eIF4G1 Lysis Buffer, respectively, supplemented with 20 mM imidazole. The Ni-NTA agarose was then transferred to a column and washed twice with 25 mL of NS1 or eIF4G1 Lysis buffer supplemented with 50 mM imidazole. Finally, the His-NS1 or His-eIF4G1 proteins were eluted in 20 mL of NS1 or eIF4G1 Lysis buffer supplemented with 1 M imidazole and collected in 3 mL fractions. Individual fractions were then analyzed for the presence of the desired purified protein by SDS-PAGE,

followed by coomassie blue staining or western blot. The eluted fractions determined to contain purified protein were pooled and dialyzed against PBS at pH 8.5.

2.12.2 PABP1

2.12.2.1 Glutathione Sepharose Purification

Expressed PABP1-GST and GST proteins were individually column purified from the soluble fraction of the crude cell lysate using Glutathione Sepharose 4B Resin (Amersham Biosciences) according to the manufacturer's protocols. The presence of purified protein in the eluted fractions was detected by SDS-PAGE followed by coomassie blue staining. Elution fractions determined to contain purified protein were pooled and dialyzed against PBS at pH 7.4.

2.12.2.2 High Performance Liquid Chromatography (HPLC)

PABP1-GST was further purified by high performance liquid chromatography (HPLC) in an ÄKTA Purifier (Amersham Biosciences). PABP1-GST was bound to a HiTrap SP FF cationic exchange column (GE Healthcare) and eluted using a 50 mL gradient from 0 to 1 M [NaCl] collected in 1 mL fractions. The presence of purified protein in the eluted fractions was detected by spectrophotometry and confirmed by SDS-PAGE followed coomassie blue staining. Eluted fractions determined to contain purified protein were pooled and dialyzed against PBS at pH 7.4.

2.13 Protein Quantification

2.13.1 Bradford Assay

Small-scale Bradford assays were performed in 96-well plates. 20 µL of Protein Assay Dye Reagent (Bio-Rad) was added to 80 µL samples of purified protein at various dilutions. Reactions were incubated for 5 minutes at room temperature, and then the A_{595} was measured using a Spectra plate reader (Tecan) with WinSelect 2.2 software (Tecan). Protein concentration was quantified against a standard curve created using a range of known concentrations of BSA.

2.13.2 Densitometry

Kodak X-OMAT LS film was exposed to HRP western blots and developed with a Kodak X-OMAT 2000A Processor. The developed images were then scanned into digital TIFF format at 600 DPI using a Brother MFC-420cn multi-function scanner. Band density was quantified from the digital images using UN-SCAN-IT Gel 6.1 software (Silk Scientific Corporation).

2.14 Western Blotting

2.14.1 Horse-radish Peroxidase (HRP) Detection of Proteins

Following SDS-PAGE, proteins were transferred onto a PVDF membrane (Millipore) and incubated for 1 hour at room temperature in Blocking Buffer. Membranes were then incubated for a further 1 hour at room temperature with a 1:1,000 dilution of primary Ab (murine α-Flag, murine α-PABP1, rabbit α-eIF4G1, or rabbit α-NS1) in fresh Blocking Buffer.

After washing the membranes 3 times in Wash Buffer, they incubated for 1 hour at room temperature with a 1:10,000 dilution of an appropriate HRP-conjugated secondary Ab in Blocking Buffer. Membranes were then washed 3 times in Wash Buffer, reacted in SuperSignal West Pico Chemiluminescent Substrate (Pierce), and exposed to Kodak X-OMAT LS film.

2.13.2 Alkaline Phosphatase (AP) Detection of Blots

Following SDS-PAGE, proteins were transferred onto a PVDF membrane and incubated for 1 hour at room temperature with 5% skim milk in PBS. Membranes were then incubated for a further 1 hour at room temperature with a 1:1,000 dilution of primary Ab (murine α-Flag, murine α-PABP1, rabbit α-eIF4G1, or rabbit α-NS1) and 5% skim milk in fresh PBS. After washing the membranes 2 times in PBS and 1 time in TBS, the membranes were incubated for 1 hour at room temperature with a 1:10,000 dilution of an appropriate AP-conjugated secondary Ab and 5% skim milk in TBS. Membranes were then washed 3 times in TBS and reacted in 10 mL of AP Buffer containing 330 µL of 10 g/L NBT and 33 µL of 50 g/L BCIP. When protein bands were visible, the membrane was washed for 10 minutes in Stop Solution.

2.15 Autoradiography

S^{35}-labelled proteins generated by *in vitro* TnT were separated by SDS-PAGE, and the resulting acrylamide gel was bathed in a fixative solution (25% methanol, 7% glacial acetic

acid) for 20 minutes, followed by a 15 minute rinse in 100% methanol. The gel was then given 2 one hour washes in DMSO, followed by a 1 hour bath with 22% PPO in DMSO. The gel was then rinsed under running water for 1 hour, dried onto 3mm chromatography paper (Whatman) with a Gel Slab Drier (Bio-Rad), and exposed to Kodak X-OMAT LS film for 48 to 240 hours at -80°C. Films were developed with a Kodak X-OMAT 2000A Processor.

2.16 Eukaryotic Transfection

Six well plates containing eukaryotic cell lines at 90-95% confluency were transfected with 4 μg of either pcDNA3-HA-eIF4G1, pCAGGS-CPSF30-Flag, or pCAGGS-CPSF30-F2/F3-Flag plasmids and 15 μL of Lipofectamine 2000 (Invitrogen) per well according to the manufacturer's protocol.

2.17 Cell Line Infection with FluAV

Eukaryotic cell lines were grown in 6-well plates to 100% confluency and then washed twice in warmed PBS before being infected with one of the HK-MA or rWSN viruses (viral titres were previously established) at MOI = 2. Infection proceeded for 8 or 16 hours, after which the cells were lysed into 1 mL of Extraction Buffer and clarified by 15 minutes of centrifugation at 10,000 g.

2.18 *In vitro* Transcription and Translation

Both eIF4G1 and NS1 were individually expressed *in vitro* from 1 µg of the pcDNA3-HA-eIF4G1 and pET17b-His-NS1 plasmids respectively. Proteins were expressed using the TNT T7 Quick Coupled Transcription/Translation System (Promega) according to the manufacturer's protocol for Methionine, L-[^{35}S]-labelled proteins. Proteins were labeled with Methionine, L-[^{35}S], 1,000 Ci/mmol from Perkin Elmer as per the Promega T7 Quick Coupled Transcription/Translation System protocol.

2.19 NS1-PABP1 Pulldown Experiments

A predetermined amount of NS1 and 3 µg of PABP1-GST or 1 µg of GST (negative control) were incubated together in Burgui's Binding Buffer with 10% BSA for 2 hours at room temperature in the presence of a 10 µL bed of Glutathione Sepharose 4B Resin (Amersham Biosciences). The resin was then washed 3 to 5 times with Burgui Binding Buffer before being denatured in 50 µL of 2x SDS sample buffer and analyzed by SDS-PAGE and HRP western blot.

2.20 Coimmunoprecipitation Experiments

2.20.1 NS1-CPSF30 Coimmunoprecipitation

A predetermined amount of NS1 was mixed with 200 µL of clarified crude cell lysate from pCAGGS-CPSF30-Flag or pCAGGS-CPSF30-F2/F3-Flag transfected cells and incubated together in Extraction Buffer III for 2 hours at room temperature in the presence of 15 µL of Protein G DynaBeads (Invitrogen) and 1 µg of α-Flag M1 Monoclonal Antibody (Sigma). The DynaBeads were then washed 4 times with Extraction Buffer III before being denatured in 50 µL of 2x SDS sample buffer and analyzed by SDS-PAGE and HRP western blot.

2.20.2 NS1-eIF4G1 Coimmunoprecipitation

A 50 µL eIF4G1 TnT reaction was mixed with either a predetermined amount of NS1, or a 50 µL NS1 TnT reaction, and incubated together in Binding Buffer for 1 hour at 4°C. Antibodies were prebound to 15 µL of Protein G DynaBeads (Invitrogen) by mixing with 1 µg of either rabbit α-NS1 serum (Brown Lab) or purified rabbit α-eIF4G1 Ab (Bethyl Laboratories) and incubating in Binding Buffer for 1 hour at room temperature. The DynaBeads were then washed 3 times with Binding Buffer before being added to the eIF4G1 and NS1 mixture with incubation for an additional 2 hours at 4°C. After incubation, the DynaBeads were washed 4 times with ice cold Binding Buffer before being denatured in 50 µL of 2x SDS sample buffer and analysis by SDS-PAGE and HRP western blot.

RESULTS

3.1 Construction of Plasmids for Synthesis of Recombinant NS1 Proteins

The first step was to produce the purified HK-wt and HK-MA NS1 proteins for use in the subsequent pulldowns and coimmunoprecipitations. Therefore, the various NS1 genes were cloned into the pET17b plasmid for protein expression from the pHH21 vectors in which they were stored by Dr, Brown. To achieve this, PCR primers were designed to amplify the NS1 genes, while also encoding an N-terminal His tag on each NS1 protein, as well as 5' NdeI and 3' EcoRI restriction sites flanking the NS1 gene (See Appendix II). These amplified NS1 genes were then Topo cloned into the pDrive Topo-cloning vector where they were propagated in *E. coli*. Finally, the NS1 genes were subcloned into pET17b, using the NdeI and EcoRI restriction sites, for bacterial expression from a T7 promoter. See Figure 10 for an overview of the pET17b-His-NS1 expression vector design. Eight separate pET17b-His-NS1 vectors were constructed to individually express HK-wt NS1 or one of the seven HK-MA NS1 variants.

Following construction, each of the pET17b-His-NS1 vectors were screened, first by restriction analysis and then by sequencing, to ensure that the fidelity of NS1 genetic sequence was maintained throughout cloning. Sequencing revealed undesired mutations in the HK-wt NS1, HK-103L, HK-106V, HK-106I, and HK-106I+98S genes. These mutations were corrected by site-directed PCR mutagenesis and the corrections were confirmed by sequencing.

Figure 10. Cloning strategy for construction of the pET17b-His-NS1 expression vectors. The HK-wt NS1 gene, as well as the HK-MA NS1 genes, were PCR amplified with primers that were designed to add a 3' terminal EcoRI restriction site, a 5' terminal NdeI restriction site, and a 5' 6x His tag (see Appendix II). PCR amplified His-NS1 genes were first inserted into pDrive via topoisomerase assisted cloning, which was then propagated in DH5α *E. coli,* before being cloned into pET17b for expression from the T7 promoter.

NS1 gene from HK-MA FluAV amplified by PCR
from original pHH21 constructs

5' terminal NdeI restriction site and 6x His tag,
and 3' terminal EcoR1 Restriction site were
added to the NS1 genes with modified PCR primers

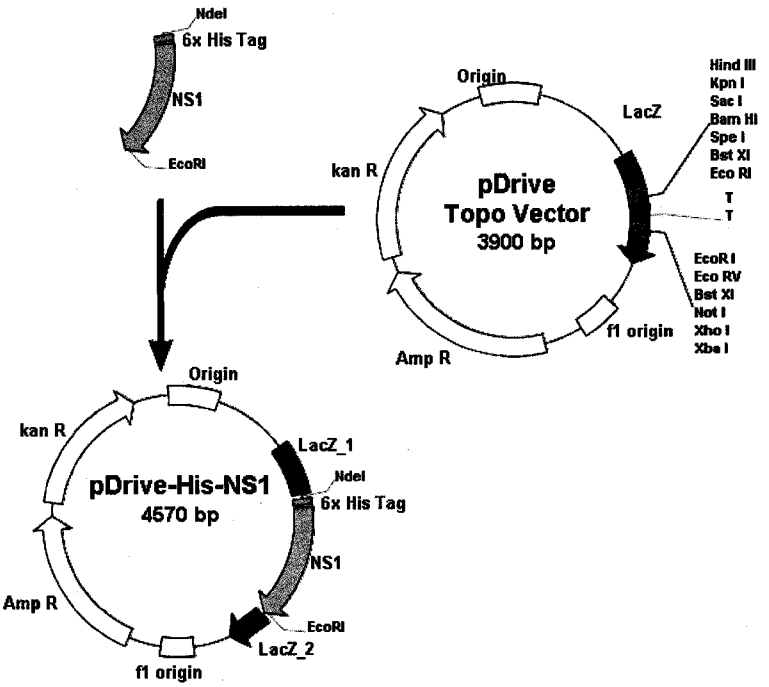

PCR fragments are cloned into pDrive vector
via Topoisomerase-assisted cloning

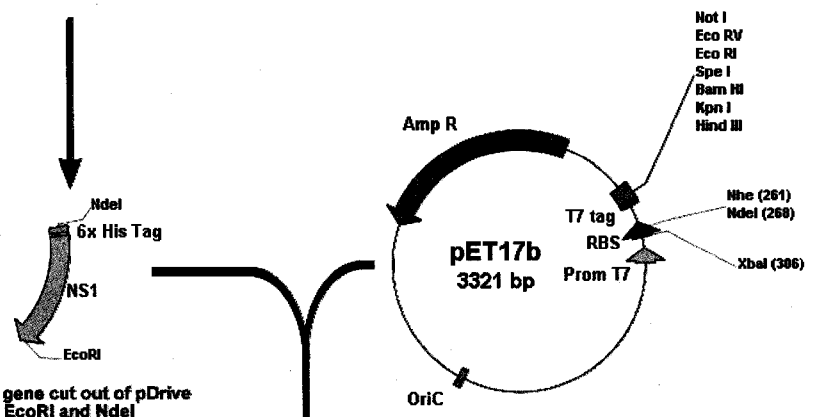

NS1 gene cut out of pDrive
with EcoRI and NdeI

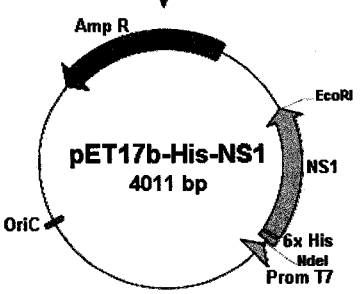

NS1 gene cloned into pET17b vector
for expression from a T7 promoter

3.2 Optimizing NS1 Protein Expression

Following creation of the pET17b-His-NS1 vectors, the optimal induction conditions for the expression of soluble NS1 protein from these vectors in BL21(DE3) *E. coli* were determined by utilizing the HK-wt NS1 as an archetype. Induction of HK-wt NS1 expression was first attempted for 3 hours at 30°C with 10 μM [IPTG] because these conditions had been previously employed to successfully induce NS1 expression from a similar construct (Aragon et al., 2000). However, upon examination of the soluble fraction of the bacterial lysate, there was an undetectable amount of soluble HK-wt NS1 and most of the protein existed in an insoluble form (Fig. 11a). Additionally, HK-wt NS1 was observed to be expressed constitutively in the absence of IPTG, as evidenced by the presence of NS1 in the "T=0" uninduced bacterial lysate sample (Fig. 11a). Various induction temperatures were subsequently tested, including room temperature and 37°C, with identical results to the 30°C induction condition (Fig. 11a). To confirm that NS1 expression was constitutive, these induction conditions were repeated in the absence of IPTG. Even without IPTG present to induce NS1 expression, NS1 was still expressed at levels comparable to those induced with 10 μM IPTG (Fig. 11a). In BL21(DE3) *E. coli*, the lac operon controls the expression of T7 polymerase, which in turn transcribes the NS1 gene from the expression vector. Therefore, constitutive expression of NS1 suggests leakiness in the lac operon of this particular strain of BL21(DE3), which may have affected the production of soluble forms of NS1. However, expression of HK-wt NS1 in a separate BL21(DE3) strain that was obtained from an alternate source also yielded insoluble, but not soluble NS1.

Figure 11. Determining the optimal induction conditions for the expression of soluble NS1. Expression of soluble NS1 was initially attempted in BL21 *E. coli*. **(A)** A 3 hour induction with 10 μM IPTG did not yield soluble NS1 when induced at 30°C, 37°C, or at room temperature. **(B)** The addition of 1% glucose to the expression media did not yield soluble NS1, nor did induction with 1 mM IPTG. **(C)** Overnight expression at room temperature did not yield soluble NS1 when induced from BL21 *E. coli*, but soluble NS1 was produced from BL21(DE3)pLysS *E. coli* under the same conditions. The greatest amount of soluble NS1 was expressed in BL21(DE3) pLysS when induced overnight at room temperature with 10 μM IPTG. Samples are fractional lysates separated by SDS PAGE and stained with Coomassie or AP western blot with α-NS1 at 1:1000 dilution. The "T=0" samples were taken prior to induction, while the "T=3H" and "T=16H" samples were taken at 3 and 16 hours post-induction respectively. The "Soluble" and "Insol." samples were taken from the respective soluble and insoluble fractions of the bacterial cell lysate.

A

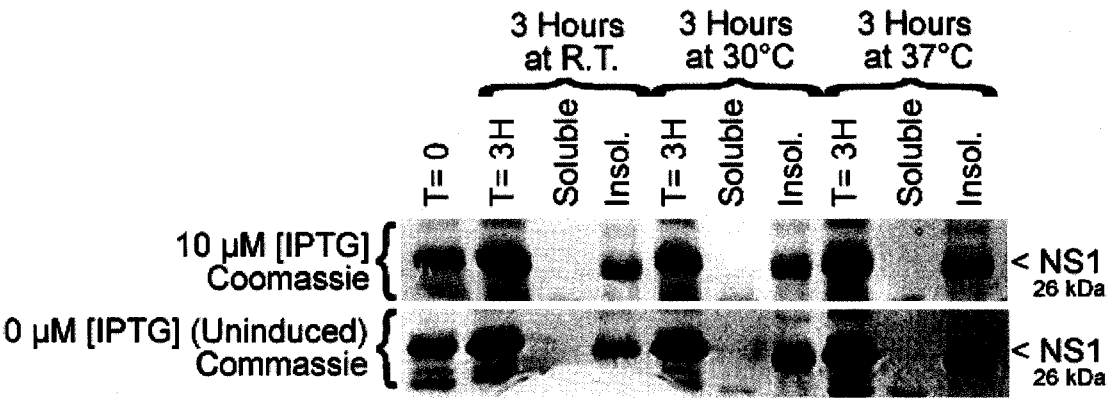

B

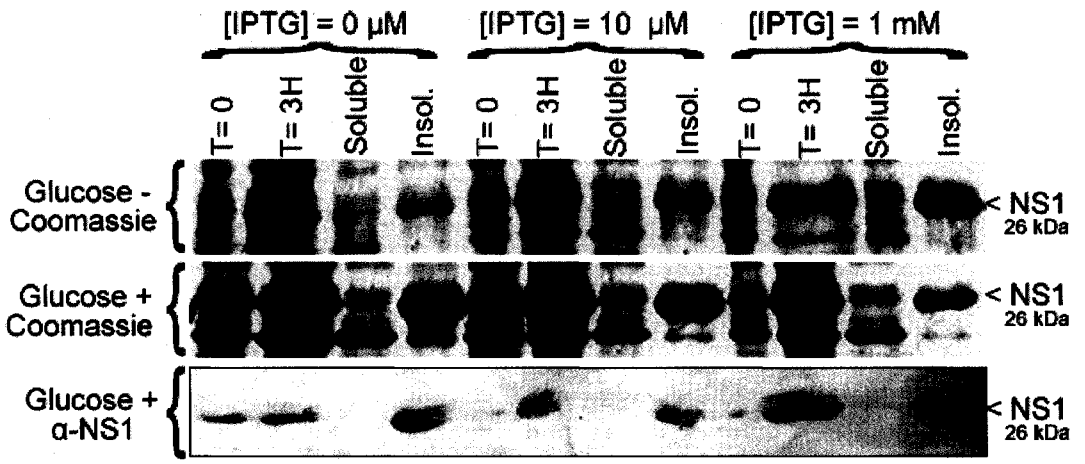

C

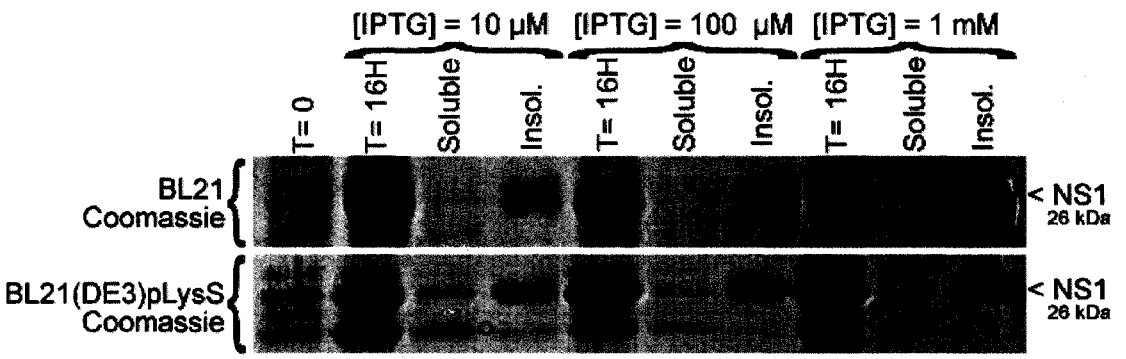

Constitutive NS1 expression may have resulted in high levels of insoluble protein by over-expressing NS1, resulting in precipitate formation due to saturating concentrations of NS1 in the cytoplasm. Therefore, to further restrict constitutive expression of T7 polymerase from the lac operon, 1% glucose was added to the expression media (Amersham Biosciences, 2003). While the addition of glucose appeared to reduce the level of constitutive NS1 expression, both Coomassie staining and western blotting revealed that the glucose did not significantly improve expression of soluble NS1 (Fig. 11b).

HK-wt NS1 expression was then attempted in the BL21(DE3)pLysS *E. coli* strain, which provides greater control over the expression of T7 promoter-controlled genes by means of the T7 lysozyme gene found in the pLysS plasmid. When expressed, T7 lysozyme binds to and inhibits the transcriptional activity of T7 polymerase. Therefore, the T7 lysozyme should inhibit the activity of small amounts of constitutively expressed T7 polymerase and, thereby, reduce the level of uninduced NS1 expression. Additionally, overnight inductions of NS1 at lower temperatures (room temperature) were performed in attempt to slow the rate of NS1 expression by reducing the cellular metabolism of the host. These overnight inductions yielded no soluble NS1 when attempted in BL21(DE3). However, expression in BL21(DE3)pLysS under the same conditions provided a great deal of soluble NS1 (Fig. 11c). The optimal HK-wt NS1 induction conditions in BL21(DE3)pLysS were experimentally determined to be 16 hours at room temperature with 10 μM [IPTG] (Fig. 11c). Following the successful expression of soluble HK-wt NS1, the seven HK-MA NS1

variants were individually expressed from BL21(DE3)pLysS *E. coli* and under the same conditions as HK-wt NS1.

3.3 NS1 Purification

Expressed HK-wt NS1 was successfully purified from bacterial lysate by means of the N-terminal his tag (Fig. 12). Following the successful purification of HK-wt NS1, the seven HK-MA NS1 variants were individually purified by the same means. Next, the purified NS1 protein preparations were dialyzed against PBS (pH7.4), upon which the HK-MA NS1 variants were seen to precipitate from solution. Comparison of NS1 solubility in response to pH revealed optimum NS1 solubility at approximately pH 8.5 (Table 4).

pH	Relative Precipitate Level
6.0	Slight Precipitate
7.0	Strong Precipitate
7.4	Strong Precipitate
8.0	Slight Precipitate
9.0	No Precipitate

Table 4. Relative solubility in NS1 in relation to buffer pH. The condition for the optimal solubility of purified NS1 is achieved at a pH of between 8 and 9. Relative solubility was determined by the visual opacity of the solution.

3.4 Cleavage and Polyadenylation Specificity Factor 30-NS1 Coimmunoprecipitation

3.4.1 Coimmunoprecipitation from 293T Cells Following Transfection and Infection

A preliminary experiment to probe the interaction between NS1 and CPSF30 was modeled using the published coimmunoprecipitations performed by Twu *et al.* (2007). For

Figure 12. Ni-NTA agarose purification of NS1. NS1 was purified from bacterial cell lysate with a Ni-NTA agarose column via the N-terminal His tag. NS1 was eluted from the Ni-NTA agarose with 20 mL of buffer containing 1M imidazole collected in 3 mL fractions (labeled "Elution 1-7"). The majority of the NS1 was eluted early in elution fractions 1 and 2. The "T=0" sample was taken prior to induction, while the "T=16H" sample was taken at 16 hours post-induction. The "Soluble" and "Insol." samples were taken from the respective soluble and insoluble fractions of the bacterial cell lysate. Soluble fraction flow through and the column washes are labeled "F.T." and "Wash 1 & 2" respectively.

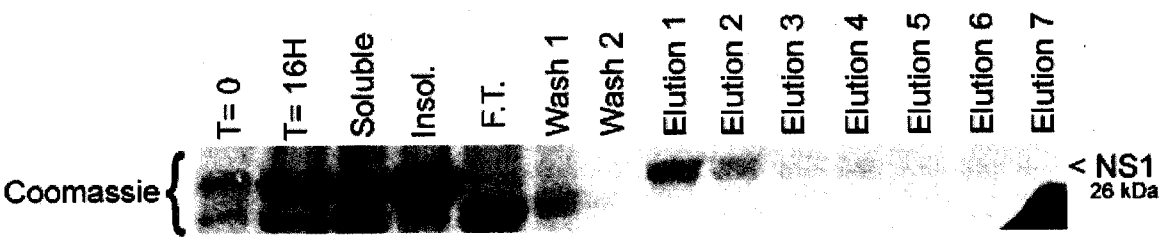

this experiment 293T cells were transfected with the pCAGGs-CPSF-F2/F3-Flag vector expressing an N-terminally flag-tagged 61-amino-acid sequence comprising the second and third zinc fingers (F2/F3) of the CPSF30 protein. The CPSF30-F2/F3 protein fragment has been shown to constitute the NS1 binding domain of the CPSF30 protein and to be sufficient for binding to NS1 (Twu *et al.*, 2006). After transfection and a 24 hour incubation period to allow for CPSF30-F2/F3 expression, the 293T cells were infected with HK-wt at a moi of 2 for 8 or 16 hours. The cells were then lysed and CPSF30-F2/F3 was immunoprecipitated from the crude cell lysate by α-Flag Abs. Figure 13b shows the presence of coimmunoprecipitated NS1 (Figure 13 a & b, lane 3). However, there is also a significant amount of NS1 in the untransfected negative control, suggesting that NS1 is non-specifically binding with the protein G beads and/or the α-Flag antibody used in the CoIP.

DOC was then added to the CoIP Extraction Buffer (which was used in the CoIP to bind and wash the proteins) to increase the binding stringency (as performed by Twu *et al.* 2007). The addition of DOC to the Extraction Buffer suppressed non-specific NS1 binding, but also inhibited NS1 from being coimmunoprecipitated by CPSF30-F2/F3 in the 8 hour infection condition (Fig. 13b). However, HK-wt NS1 was successfully coimmunoprecipitated with CPSF30-F2/F3 at 16 hours post-infection without any non-specific binding (Fig. 13b).

Following the successful coimmunoprecipitation of HK-wt NS1 with CPSF30-F2/F3 from HK FluAV infected cells, the above experiment was repeated (16 hour infection with DOC in the extraction buffer) with the HK-MA and rWSN viruses. These experiments failed in that NS1 was absent from all of the CoIPs, including the repeated HK-wt infection

Figure 13. Coimmunoprecipitation of NS1 with CPSF30-F2/F3 from pCAGGS-CPSF30-F2/F3-Flag transfected and HK-wt Influenza A infected 293T cell lysate. (A) CPSF30-F2/F3 was able to pull NS1 from crude cell extract in the absence of DOC from the extraction buffer (lane 3). However, the high levels of non-specific NS1 binding in the negative control (lane 1) invalidate this result as the product if NS1 binding to CPSF30 F2/F3. **(B)** When DOC was added to the extraction buffer, CPSF30-F2/F3 was not able to pull NS1 from crude cell extract following an 8 hour infection with HK-wt Influenza A, but was able to do so after a 16 hour infection with the same virus. CoIP was performed on the samples labeled "α-Flag CoIP", while samples labeled "Crude Cell Lysate" correspond to 1:20 dilutions of the untreated 293T cell lysates used in the CoIPs. "α-NS1" and "α-Flag" denote HRP western blots performed with the respective α-NS1 and α-Flag primary antibodies.

A

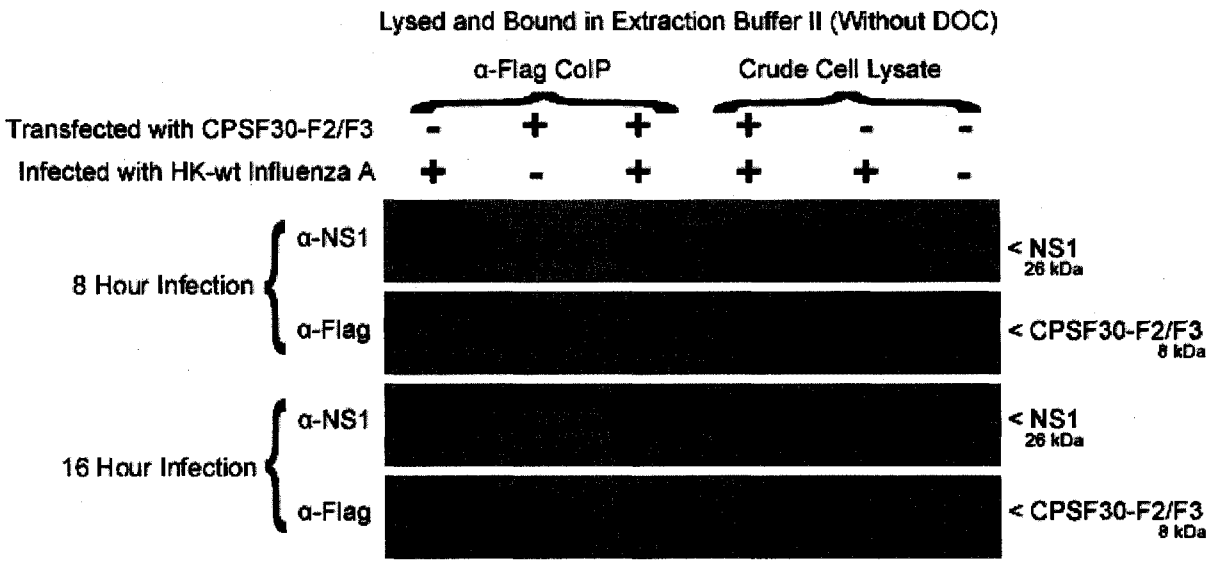

B

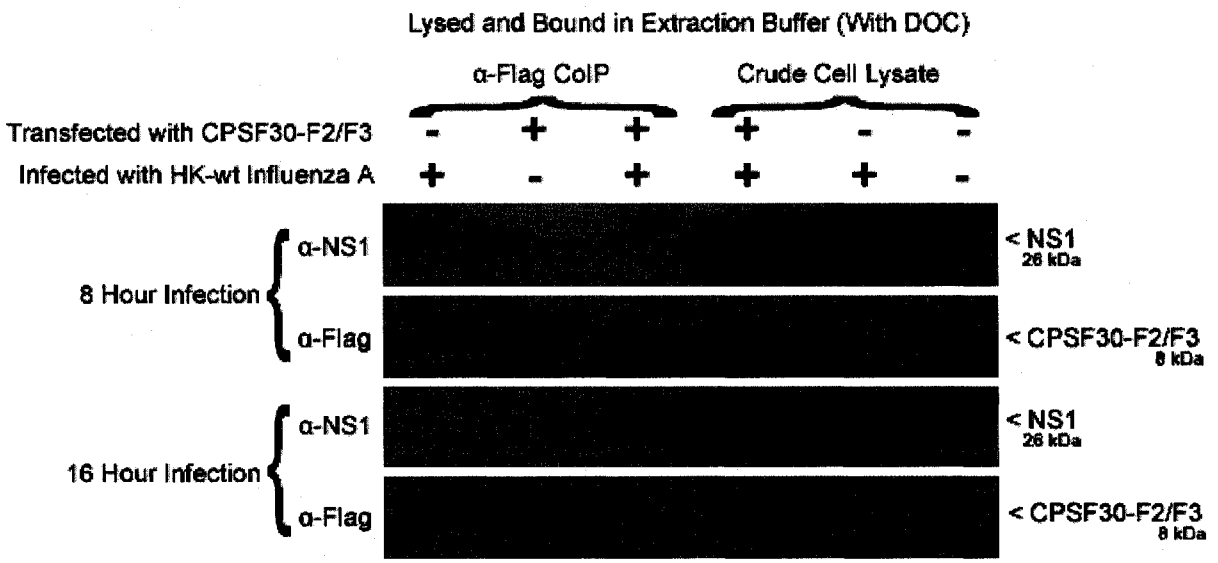

condition, indicating difficulties in the reproducibility of this approach.

Unfortunately, the rWSN-106V viral strain was growth attenuated and, thus, there was insufficient viral stock to perform the transfection-infection CoIP experiments on this mutant. Also, the MA-180A and MA-226I mouse-adapted FluAV strains, and the rWSN-23A, rWSN-180A, and rWSN-226I, HK-MA NS1 recombinant WSN FluAV strains were not available for analysis. Finally, due to differences in viral protein expression levels between the MA and rWSN strains (Brown, unpublished data), the amount of NS1 input into each CoIP likely varied among the mutants. For these reasons, the transfection-infection experiments were abandoned in favour of CoIPs with standardized amounts of purified NS1 mixed with the lysate of transfected cells expressing CPSF30-F2/F3.

3.4.2 Coimmunoprecipitation of Purified NS1 with CPSF30

To perform the *in vitro* CoIPs, crude cell lysate from pCAGGs-CPSF-F2/F3-Flag transfected 293T cells was mixed with a predetermined amount of purified 6X-His-tagged NS1. CPSF30-F2/F3-Flag was then precipitated from the solution by means of an α-Flag antibody bound to Protein A beads and the resulting precipitate was examined for the presence of NS1 by SDS-PAGE and HRP western blot with rabbit α-NS1 Ab. HK-wt NS1 was again used as a prototype to determine optimal CoIP conditions. In the preliminary attempt at this experiment HK-wt NS1 was pulled down by the CPSF30-F2/F3-bound Protein A beads. (Fig. 14a, Lane 3). However, there was an unacceptable level of non-specific

Figure 14. Coimmunoprecipitation of purified NS1 with CPSF30-F2/F3 from pCAGGS-CPSF30-F2/F3-Flag transfected 293T cell lysate. (A) CoIP of purified NS1 with CPSF30-F2/F3 was initially unsuccessful due to the low NS1 signal from the CoIP (lane 3 and 4) and relatively high level of non-specific NS1 binding background (lane 2). **(B)** The amount of NS1 pulled down by CPSF30-F2/F3 in the CoIP was increased by the addition of 10% glycerol ("Gly.") and by the addition 10% BSA. "CPSF30-F2/F3" and "HK-wt NS1" refer the presence or absence of the respective CPSF30-F2/F3 and HK-wt NS1 protein in the CoIP. "1:20 NS1 LC" corresponds to a 1:20 dilution loading control of the purified NS1 protein used in the CoIP. "EB" refers to the extraction buffer used in the CoIP and "α-NS1" denotes HRP western blot performed with α-NS1 as the primary antibody.

A

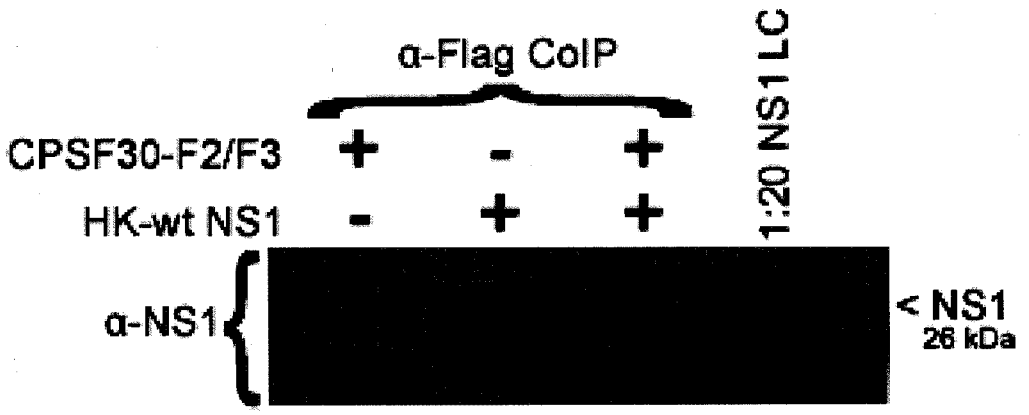

B

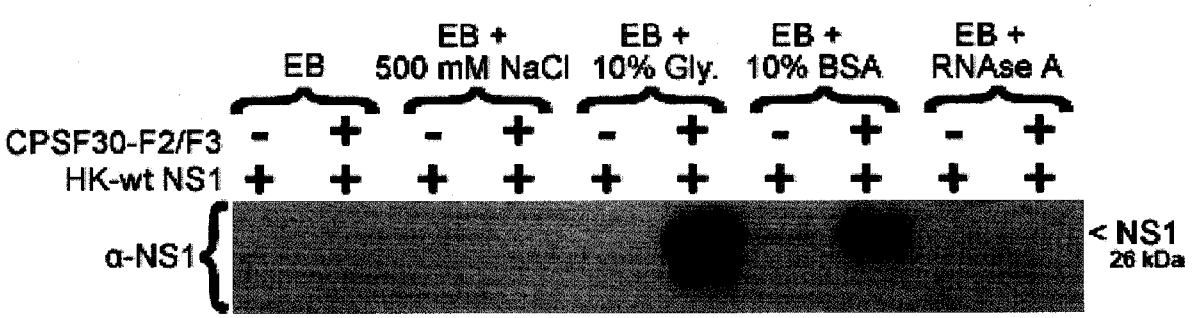

association of HK-wt NS1 with the Protein A beads in the absence of CPSF30-F2/F3 (Fig. 14a, Lane 2). Therefore the Extraction Buffer was further refined to reduce the non-specific NS1 binding.

The different Extraction Buffer conditions that were tested included: an increase in the NaCl concentration to increase binding stringency, the addition of 10% glycerol to stabilize protein structure and enhance CPSF30-NS1 binding capacity, 10% BSA to competitively inhibit non-specific protein binding, and RNase A to reduce any non-specific binding that may be mediated by RNA bridging between NS1 and other RNA-binding proteins. Additionally, the Protein A agarose beads used in the preliminary CoIP of purified NS1, as well as the infection-transfection CoIPs, were switched to Protein G DynaBeads because the protein G beads provided a higher affinity for the mouse α-Flag M1 monoclonal IgG_1 that was used for immunoprecipitation. While the 500 mM NaCl and RNAse A conditions seemed to have no effect on the amount of pulled down HK-wt NS1, both the 10% glycerol and the 10% BSA conditions strongly increased the amount of NS1 that was pulled down without increasing non-specific NS1 binding (Fig. 14b). The 10% glycerol and 10% BSA conditions were combined into a new buffer (Extraction Buffer III) which was used to successfully coimmunoprecipitate the HK-wt and HK-MA NS1s from crude cell lysate by means of CPSF30-F2/F3 (Fig. 15).

The CPSF30-F2/F3 CoIPs of the HK-wt and various HK-MA NS1 proteins were completed with various amounts of input NS1 (2 μg, 1 μg, 0.5 μg, or 0.1 μg) in order to generate affinity curves for the CPSF30 association and this experiment was performed in

Figure 15. Coimmunoprecipitation of HK-wt and all HK-MA variant NS1 proteins with CPSF30-F2/F3. (A) α-NS1 HRP western blots show that CPSF30-F2/F3 was able to pull down both HK-wt NS1 and the HK-23A NS1 variant in a CoIP, while all of the other HK-MA NS1 variants were not pulled down by CPSF30-F2/F3. **(B)** Densitometry data was calculated from non-saturated exposures of panel A, corrected for differences in the input NS1 loading controls, and used to plot association curves. The difference in the HK-wt and HK-23A curves is not significant as determined by the T-test (P=0.22). **(C)** HRP and AP western blots showing a side-by-side comparison of the 2.0 μg input NS1 CoIPs display the input NS1 and CPSF30-F2/F3 loading controls, as well as the α-Flag pulldown control. **(D)** Densitometry data was calculated from non-saturated exposures of panel C and adjusted for differences in the input NS1 loading controls to highlight the deficiency of all HK-MA NS1 variants (with the exception of HK-23A) in their ability to bind CPSF30-F2/F3. "CPSF30" refers to the presence or absence of CPSF30-F2/F3 in the pulldown, while "NS1 (μg)" denotes the amount of purified NS1 protein input into the respective pulldown. Both "LC" (A) and "Input NS1" (C) correspond to a 1:20 dilution (0.1 μg total) loading control of the purified NS1 protein used in the pulldown. "Input CPSF" (C) corresponds to a 1:20 dilution of the pCAGGS-CPSF30-F2/F3-Flag transfected 293T cell lysate used in the pulldown. Densitometry Data is presented relative to 100% binding at the 2 μg HK-wt NS1 CoIP condition. More saturated HRP exposures were selected for display to increase graphical clarity. This experiment was performed in triplicate to yield statistical results.

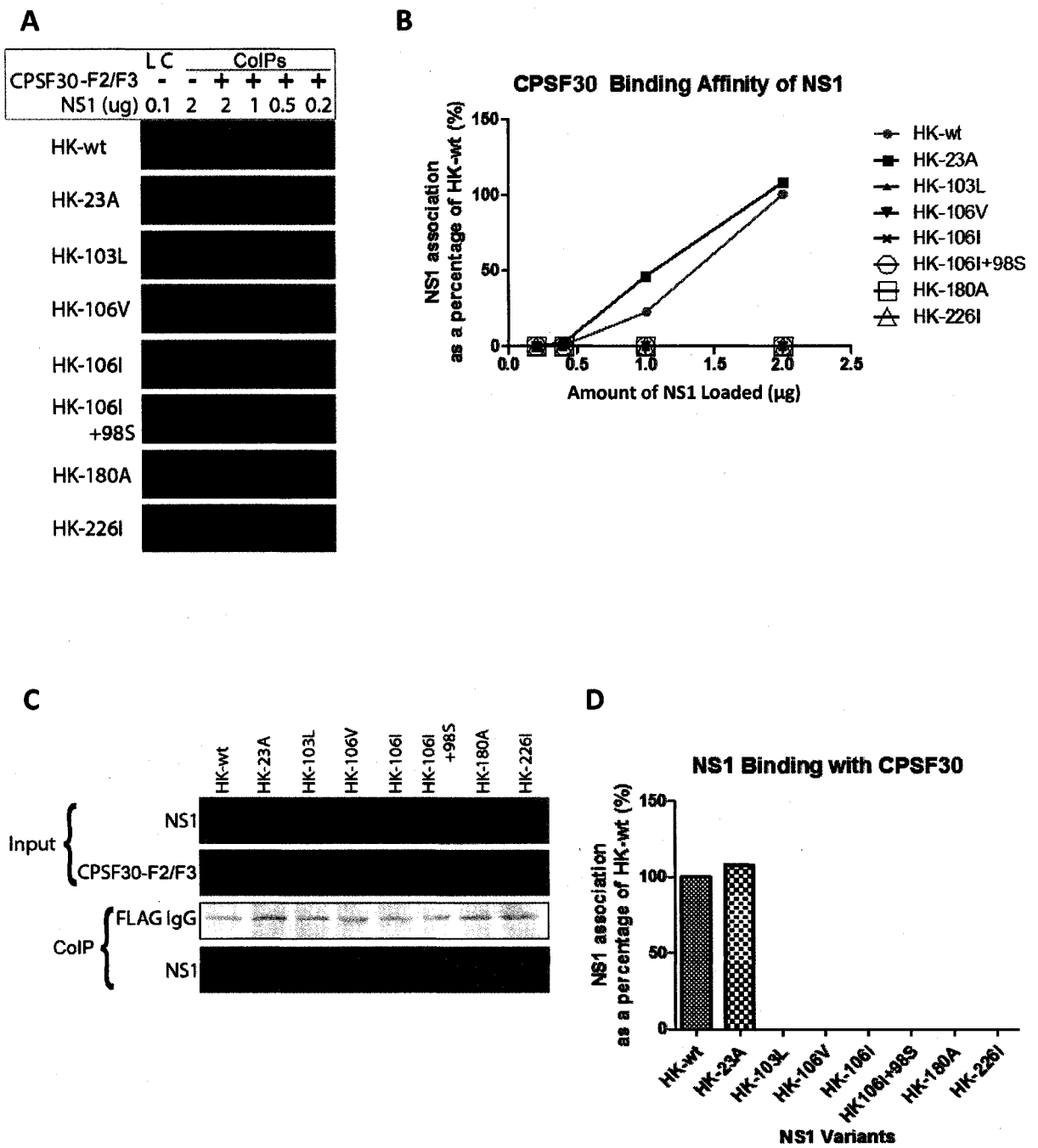

triplicate. From these curves, it can be seen that the HK-23A mutation did not significantly affect CPSF30-F2/F3 binding (determined by T-test, P=0.22). However, all of the other HK-MA NS1 mutants (HK-103L, HK-106V, HK-106I, HK-106I+98S, HK-180A, and HK-226I) were not able to bind CPSF30-F2/F3 at all (Fig. 15). We also analyzed the pulldown of NS1 protein from samples that contained 2 μg of input NS1 each to further demonstrate the differences in binding against the identical loading and pulldown controls (Fig. 15c). This data indicates that all of the NS1 mutations disrupted the ability of the NS1 protein to bind to CPSF30 except for HK-23A.

3.5 PABP1 Expression and Purification

Expression of the PABP1-GST fusion protein was initially attempted from DH5α *E. coli*. Although PABP1-GST was successfully expressed in DH5α, the relatively low proportion of soluble to insoluble PABP1-GST prompted an attempt at expression in BL21(DE3) and BL21(DE3)pLysS *E. coli* strains (Fig. 16a). Upon examining expression in these cells, it was determined that the optimal *E.coli* strain for the expression of soluble PABP1-GST was BL21(DE3)pLysS (Fig. 16b).

Following expression of PABP1-GST, purification of the protein was performed with Glutathione Sepharose 4B resin (GS). Purification of PABP1-GST in this manner yielded numerous co-purified bands, all of which were of smaller molecular weight than PABP1-GST as assayed by SDS-PAGE (Fig. 17a). In an attempt to reduce the association of these co-purified proteins with the GSR, the binding stringency was increased by; increasing the buffer's ionic strength, decreasing the binding time, decreasing the temperature to 4°C, and

Figure 16. Defining the optimal induction conditions for the expression of soluble PABP1-GST. (A) PABP1-GST expressed most efficiently in BL21(DE3)pLysS *E. coli*. **(B)** The majority of the PABP1-GST protein expressed in BL21(DE3)pLysS was soluble. The "T=0" samples were taken prior to induction, while the "T=3H" were taken at 3 hours post-induction. The "Soluble" and "Insol." samples were taken from the respective soluble and insoluble fractions of the bacterial cell lysate. "DH5α", "BL21", and "BL21(DE3)pLysS" denote the respective *E. coli* strains used for expression.

A

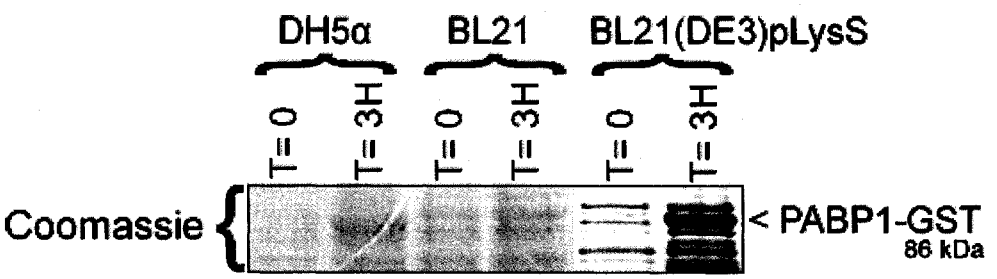

B

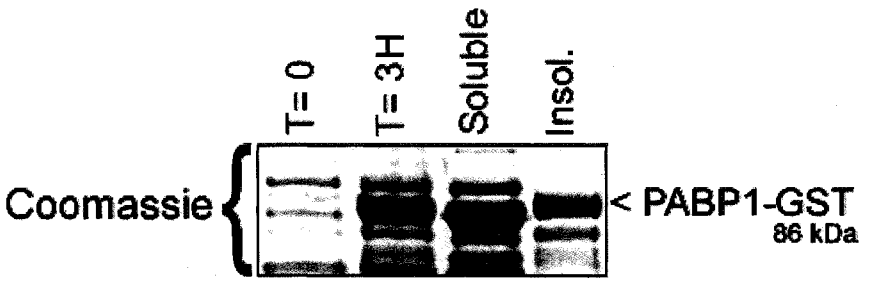

Figure 17. Glutathione Sepharose column purification of PABP1-GST. (A) PABP1-GST was expressed and pulled down from the soluble fraction of the bacterial lysate, but the protein was not present as a single band as indicated by the presence of numerous additional bands in the elution fractions. **(B)** The addition of RNase A to the purification did not reduce the number of additional bands present in the eluant. **(C)** These co-purified bands were GST-PABP1 degradation products because they were detectable by AP western blots with both α-PABP1 and α-GST primary antibodies. The PABP1-GST protein was eluted from the Glutathione Sepharose resin in several fractions (labeled "Elution 1-6"). The "T=0" sample was taken prior to induction, while the T=3H sample was taken at 3 hours post-induction. The "Soluble" and "Insol." samples were taken from the respective soluble and insoluble fractions of the bacterial cell lysate. Soluble fraction flow through and the column washes are labeled "F.T." and "Wash 1, 2, &3" respectively. "α-PABP1" and "α-GST" denote AP western blots performed with the respective α-PABP1 and α-GST primary antibodies.

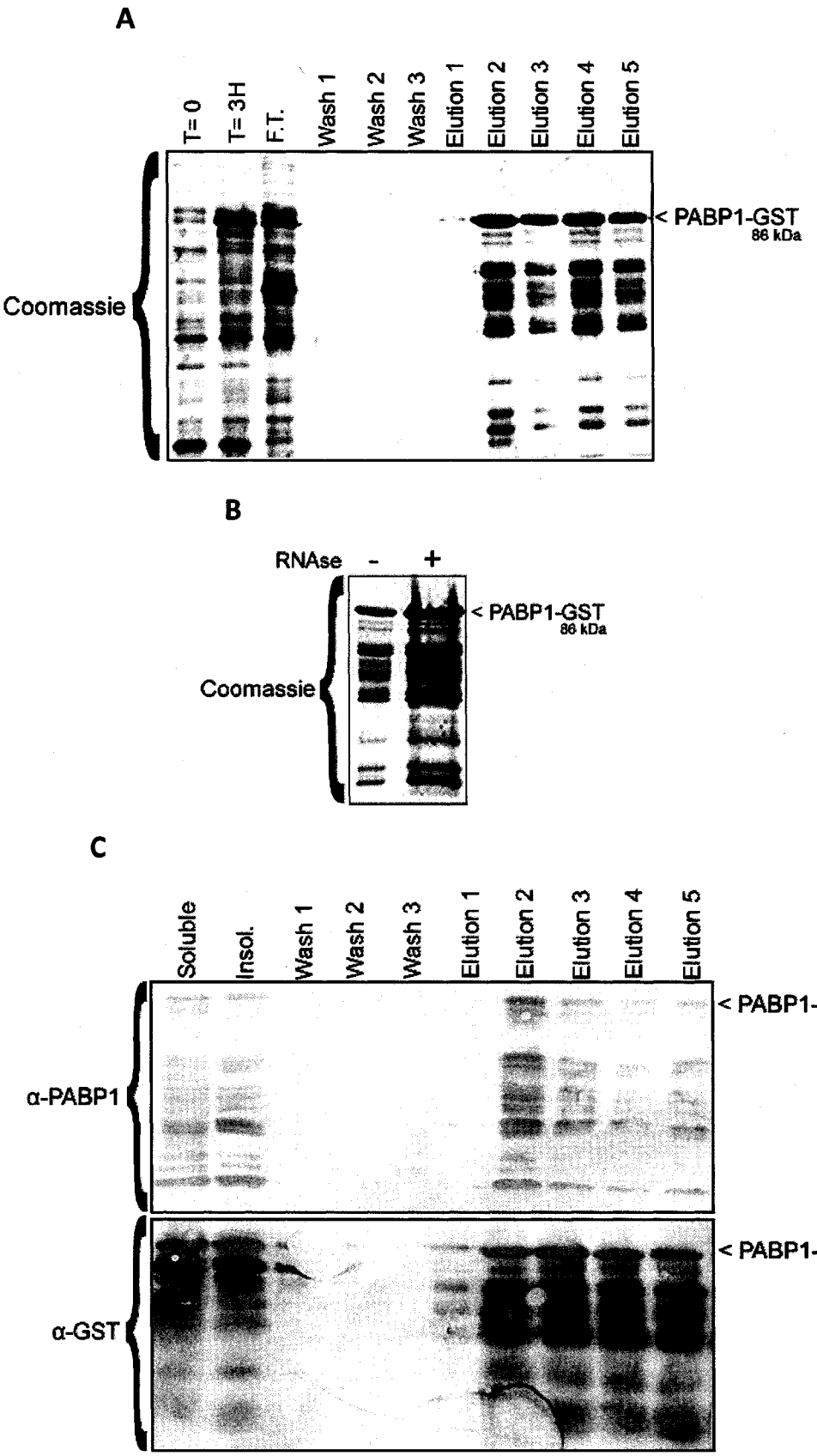

increasing the number and duration of the washes. Additionally, because PABP1 is RNA-binding, a RNase-A treated purification was performed in order to determine if the co-purification of the unwanted proteins was mediated by RNA bridging with the PABP1 protein (Fig. 17b). None of these attempted strategies inhibited the co-purification of the unwanted bands. Next, α-GST and α-PABP1 western blots were performed on the GSR-purified PABP1-GST in an attempt to identify the co-purified bands. These blots showed that both α-GST and α-PABP1 were able to bind the co-purified bands (Fig. 17c), thereby indicating that these multiple bands correspond to PABP1-GST degradation products.

Because full length PABP1-GST could not be completely purified on the basis of immunopurification or the GST tag, ionic exchange high performance liquid chromatography (HPLC) was utilized to separate the full length PABP1-GST from its degradation products on the basis of isoelectric point. Based on amino acid composition, the isoelectric point of PABP1-GST was approximated at 9.41. Therefore, the GSR-purified PABP1-GST sample was applied to a cationic exchange column in distilled H_2O (pH 7.0) and eluted by gradually increasing the ionic strength of the H_2O with NaCl. Through this technique, PABP1-GST was successfully purified by separation from its degradation products at a NaCl concentration of approximately 0.5 M, which corresponded with the 23rd, 24th, and 25th elution fractions (Fig. 18, lanes 7-9).

Figure 18. High Performance Liquid Chromatography purification of PABP1-GST. PABP1-GST was bound to a cationic exchange column and eluted using a [NaCl] gradient from 0 to 1 M. Elution fractions were collected in several intervals (labeled "Elution 1 – 50") PABP1-GST was successfully purified by HPLC at approximately 0.5 M [NaCl] (elution fractions 23-25). The majority of the smaller co-purified bands did not effectively bind the column (Elution 1 - 3), while the larger bands were eluted at fraction 26 along with the majority of the PABP1-GST. Elution fractions 7 – 22 and 29 – 50 did not contain any detectable bands.

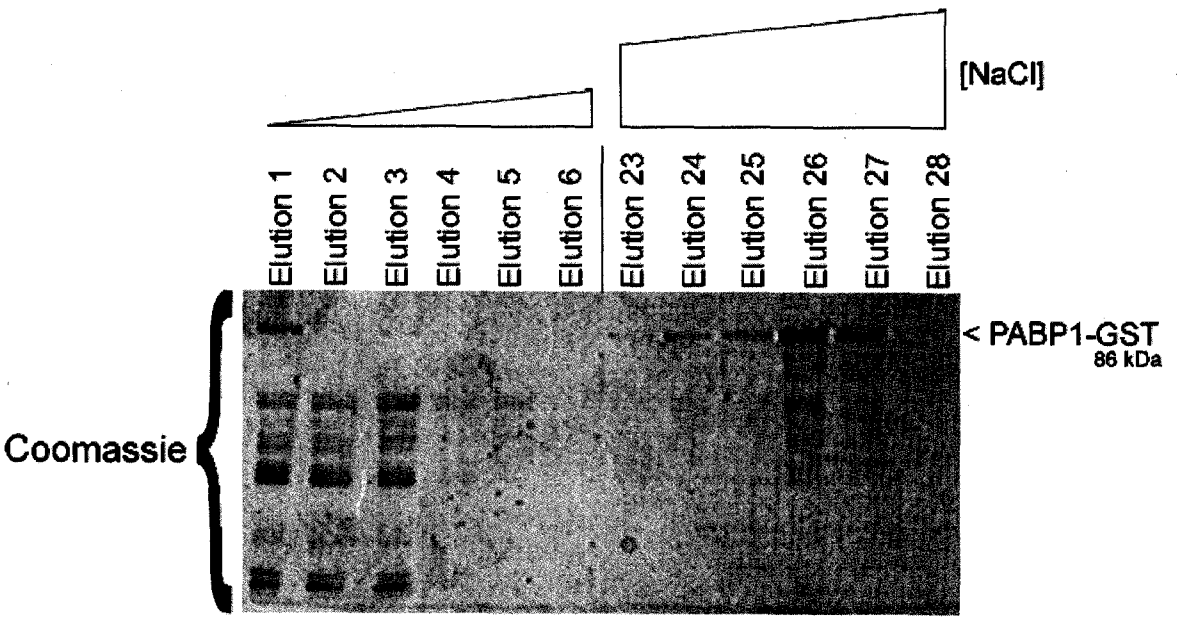

3.6 PABP1-NS1 Glutathione Sepharose Pulldown

Using purified PABP1-GST, it was possible to reproduce the PABP1-NS1 pulldown experiments as previously performed by Burgui *et al.* (2003). 3μg of PABP1-GST and 1μg of HK-wt NS1 were bound together in Burgui's Binding Buffer for 4 hours at room temperature in the presence of GSR-beads and subsequently pelleted with the beads and washed 3 times in the same buffer before being denatured by boiling in 2x SDS sample buffer for analysis by SDS-PAGE and HRP western blot. This attempt to reproduce Burgui's pulldown was successful; however there was a small amount of background association between HK-wt NS1 and the GST plus GSR-beads in the absence of PABP1-GST (Fig. 19, lane 1). In order to reduce the background NS1 binding, the binding/wash buffer composition and the binding and wash conditions were experimentally refined. The optimal conditions for the pulldown of HK-wt NS1 with PABP1-GST were, thereby, determined to be a 2 hour binding time at room temperature in Burgui's Binding Buffer supplemented with 10% BSA, followed by 3 washes with the same buffer.

Using the above conditions, HK-wt NS1 did not bind to GST + GSR-beads however, several of the HK-MA NS1 variants demonstrated persistent background binding to this complex. Of special note was the significant level of background binding that occurred between the HK-106V NS1 variant and the GST + GSR-beads in the absence of PABP1 (Fig. 20a, row 4). Three additional attempts were made to reduce the background level in HK-106V pulldown by increasing the number of washes to 5, decreasing the binding time and

Figure 19. Glutathione Sepharose pulldown of HK-wt NS1 by PABP1-GST. PABP1-GST was able to pull down HK-wt NS1 from solution with minimal non-specific NS1 binding. "PABP1" refers to the presence or absence of PABP1-GST in pulldown where the "PABP1 –" pulldown was performed in the presence of purified GST as a negative pulldown control. "HK-wt NS1 (μg)" denotes the amount of purified HK-wt NS1 protein input into the respective pulldown. "1:10 NS1 LC" corresponds to a 1:10 dilution loading control of the purified NS1 protein used in the pulldown. "α-NS1" and "α-PABP1" denote HRP western blot performed with the respective α-NS1 and α-PABP1 primary antibodies.

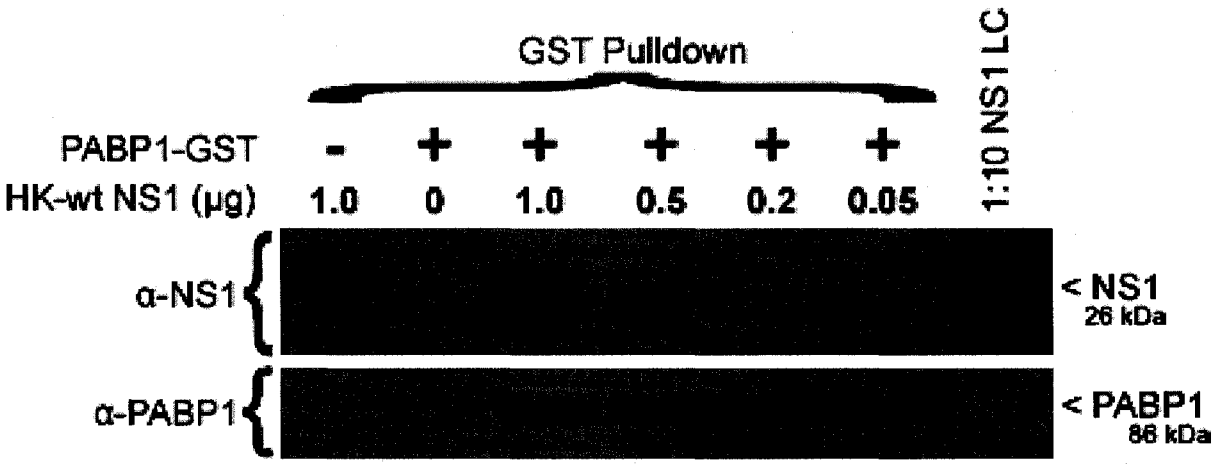

Figure 20. Glutathione Sepharose pulldown of HK-wt and all HK-MA variant NS1 proteins by PABP1-GST. (A) α-NS1 HRP western blots show that PABP1-GST was able to pull down both HK-wt NS1 and all of the HK-MA NS1 variants with the exception of HK-226I. Densitometry data was taken from non-saturated exposures of the 2 μg pulldowns from panel A and adjusted for differences in the input NS1 loading controls **(B)** as well as for the background association of His-NS1 with the glutathione Sepharose resin **(C)**. Panels B and C highlight the differences in PABP1 binding capacity among HK-wt NS1 and the HK-MA NS1 variants. **(D)** Densitometry values were calculated from non-saturated exposures of panel A. These values were corrected for differences in the input NS1 loading controls and for the background association of NS1 with the glutathione Sepharose resin, and were then used to plot binding curves. These curves show no significant difference in the PABP1 binding affinity of the HK-23A NS1 variant above that of HK-wt NS1 (T test P-value = 0.377), as well as a large increase in the PABP1 binding affinity of the HK-103L, HK-106V, HK-106I, and HK-106I+98S NS1 variants. The HK-180A and HK-226I adaptations show decreased binding affinity for PABP1. **(E)** HRP western blots showing a side-by-side comparison of the 1.0 μg input NS1 pulldowns show the input NS1 loading control, as well as the PABP1-GST pulldown control. "PABP1" refers to the presence or absence of PABP1-GST in pulldown where the "PABP1 –" pulldown was performed in the presence of purified GST as a negative pulldown control. "NS1 (μg)" denotes the amount of purified NS1 protein input into the respective pulldown. Both "LC" (A) and "Input NS1" (C) correspond to a 1:20 dilution (0.1 μg total) of the purified NS1 protein used in the pulldown. Densitometry Data is presented relative to 100% binding at the 2 μg HK-wt NS1 CoIP condition. The most saturated HRP exposures were selected for increased graphical clarity. The data shown is representative of three similar experiments performed under different binding conditions, yet yielding similar results.

A

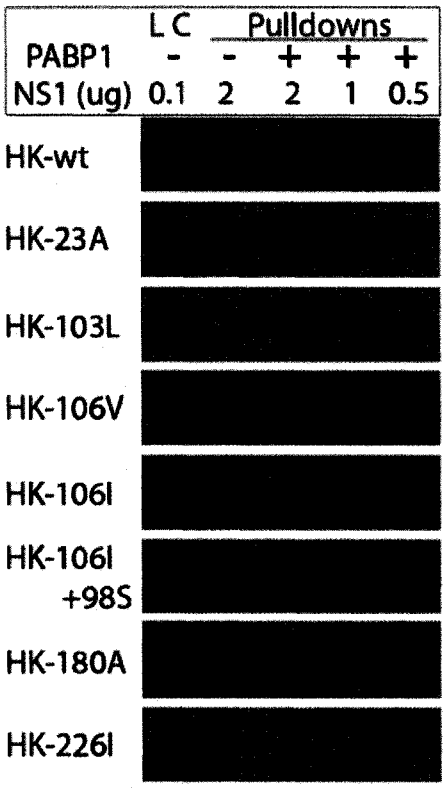

B

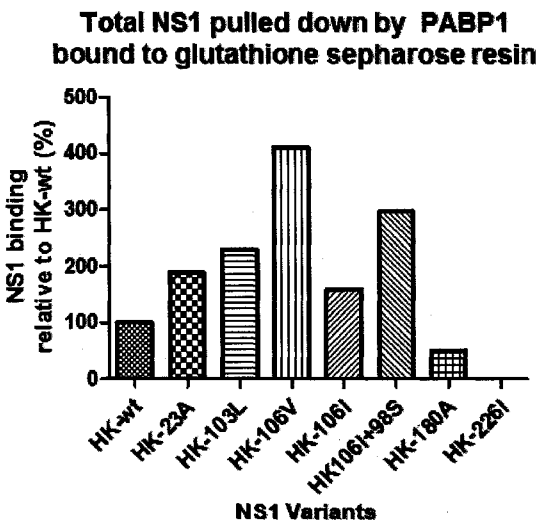

C

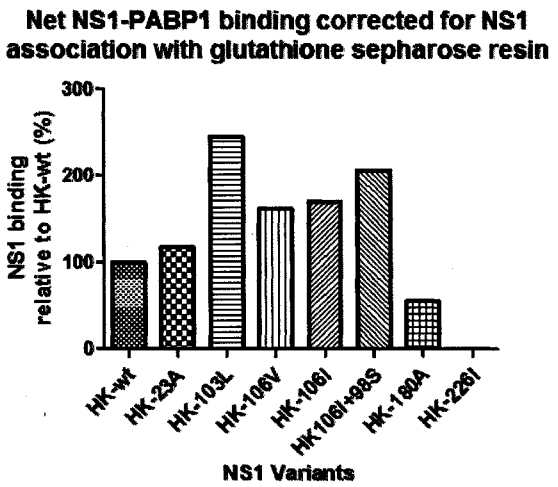

D

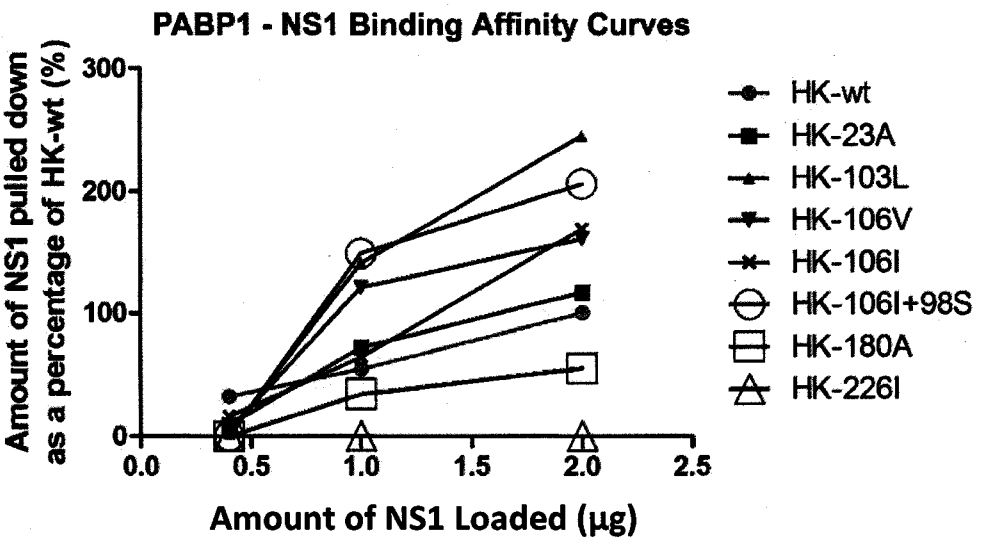

E

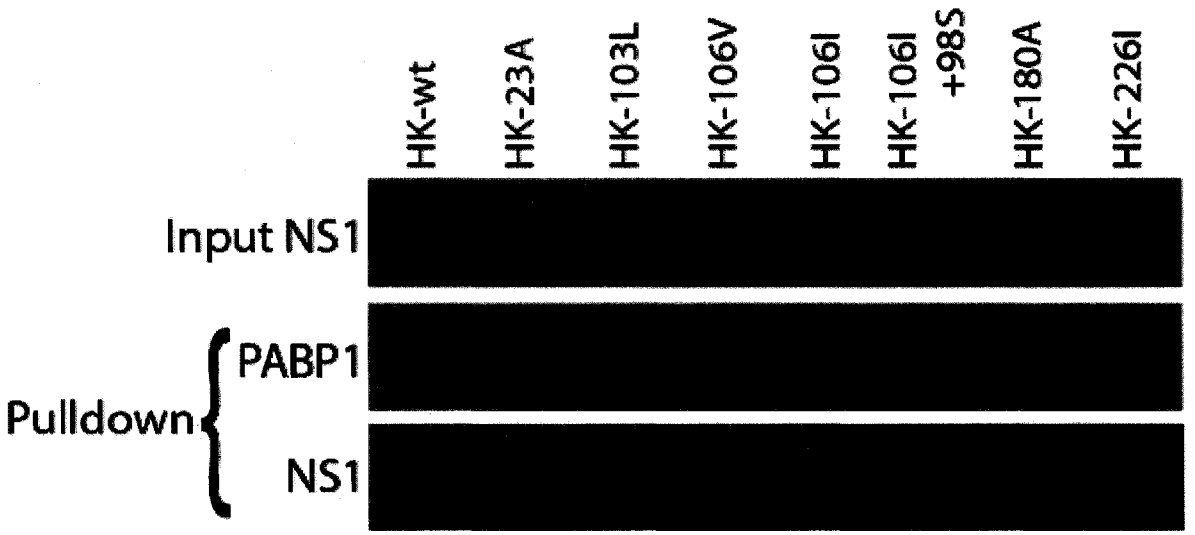

temperature to 1 hour at 4°C, and adding DOC to the binding/wash buffer while simultaneously increasing the ionic strength of the wash buffer by increasing the NaCl concentration. Unfortunately, none of these conditions were able to reduce the background binding of HK-106V NS1 to the GST + GSR-beads. The extent of the HK-106V background binding is emphasized when compared next to the other HK-MA pulldowns (Fig. 20b & e). Therefore, the net binding of HK-106V to PABP1 was extrapolated by deducting the background HK-106V densitometry values from the total HK-106V pulldown values. This calculation was also performed for HK-23A and HK-106I+98S variants, which showed minor non-specific NS1 binding. These adjusted HK-106V, HK-106I+98S, and HK-23A densitometry values were more accurately comparable against the other NS1 pulldown data (Fig. 20c & d).

GSR-bead pulldowns with PABP1-GST were performed using the optimized procedure outlined above for the HK-wt and various HK-MA NS1 proteins. These pulldowns were then repeated with various amounts of input NS1 (2 μg, 1 μg, or 0.5 μg) in order to generate binding affinity curves (Fig. 20a). Examination of these curves (Fig. 20d), suggests that the 103L, 106I, and 106V mutations and the 106I+98 double mutations had a positive effect on the PABP1 binding affinity of their respective NS1 variants. The PABP1 binding affinity of the HK-103L and HK-106I+98S NS1 variants were the greatest, being more than double that of the HK-wt NS1. The HK-106I NS1 variant also showed an increase in its PABP1 binding affinity, where binding to PABP1 was approximately 150% stronger than HK-wt NS1. In contrast, the 180A and 226I mutations had the opposite effect on PABP1 binding

affinity. The HK-180A NS1 variant bound to PABP1 only half as strongly as HK-wt NS1, while the HK-226I NS1 variant was unable to bind to PABP1 at all under these conditions. Finally, the 23A mutation had very little effect on PABP1 binding affinity. The evidence also suggests that the HK-106V NS1 variant also shows an increased binding capacity for PABP1 of approximately 150% that of HK-wt NS1. However, due to the high levels of background associated with pulldowns of the HK-106V NS1, the evidence for this specific mutant cannot be considered conclusive and further investigations are warranted into the PABP1 binding capacity of this mutant.

3.7 Summary of Results

In summary, these experiments show that, in regards to CPSF30-binding, the HK-23A mutant NS1 showed no significant difference from HK-wt NS1, while all of the HK-MA mutations abrogated CPSF30 binding (Table 5). In regards to PABP1-binding, the HK-23A mutant NS1 again showed no significant difference from HK-wt NS1, while the HK-103L, HK-106V, HK-106I, and HK-106I+98S mutants all showed increased binding affinity for PABP1 (Table 5). The HK-180A mutant showed decreased PABP1 binding affinity, while the HK-226I mutation abrogated PABP1 binding (Table 5).

Table 5. Summary of the effect of the adaptive HK-MA NS1 mutations on association with CPSF30 and PABP1. Mapped locations for RNA, PABP1, eIF4G1, CPSF30 (marked "CPSF"), PABII, and PKR interaction are shown. SH2 and SH3 stand for Src homology 2 and 3 domains which are responsible for PI3-k and Crk/CrkL interaction. Also listed are the nuclear localization signals (NLS1 and NLS2) and the nuclear export sequence (NES). The separate RNA-binding and effector domains are marked below. Sites on NS1 functional map that are marked with protein names denote binding sites. Mutation sites where the HK-MA variants differ from HK-wt are marked with arrows and the variant amino acid number.

* Denotes mutations that have been shown to alter CPSF30 binding (Twu et al., 2007).

¥ Denotes mutations occurring in a region known to affect PABP1 binding (Burgui *et al.*, 2003).

- Denotes no deviation from HK-wt

Denotes a mutation in the PABPN1 binding domain

Denotes a mutation in the eIF4G1 binding domain

Denotes a mutation in the CPSF30 binding domain

Denotes a mutation in the PABPC1 binding domain

Denotes a large increase in binding capacity

Denotes a slight increase in binding capacity

Denotes a no change or a slight decrease in binding capacity

Denotes a large decrease in binding capacity

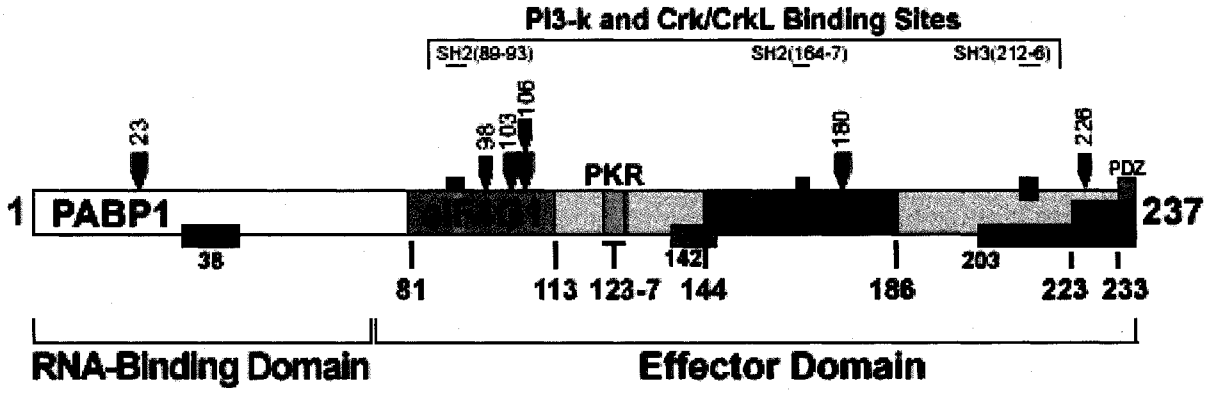

NS1 Variant	Amino Acid Position						Binding Capacity Relative to HK-wt	
	23	98¥	103*¥	106*¥		226	CPSF30	PABP1
HK-wt (H3N2)	V	L	F	M		V	100%	100%
HK-23A	A	-	-	-		-	108%	117%
HK-103L	-	-	L	-		-		45%
HK-106V	-	-	-	V		-		161%
HK-106I	-	-	-	I		-		169%
HK-106I + 98S	-	S	-	I		-		208%
HK-180A	-	-	-	-		-		55%
HK-226I	-	-	-	-		I		
HK/97 (H5N1)	A	M	L	I		I		
HK/03 (H5N1)	A	M	-	-		I		
PR/34 (H1N1)	A	M	S	I		I		
BM/18 (H1N1)	A	M	-	-		I		

DISCUSSION

Through these studies, I have identified several mutations that affect NS1's binding capacity for both PABP1 and CPSF30. Thus, I am seeing a pattern wherein multiple protein functions are affected by single amino acid substitutions. Furthermore these mutations are all generating similar phenotypes in the highly pathogenic mouse adapted FluAV strains. The significance of these findings and possible mechanisms to explain the observed phenotypes will now be discussed.

4.1 The Majority of the MA Mutations Inhibited CPSF30 Binding

Given the role of CPSF30 binding in the inhibition of host gene expression, one striking phenomenon that stands out among the results is inhibition of CPSF30 binding that is common to six of the seven MA NS1 mutants. Previous studies have shown that the F103L and M106I mutations result in the loss of CPSF30 binding (Kochs *et al.* 2007, Twu *et al.* 2007). Therefore, the CPSF30 binding inhibition observed in my experiments for the F103L, M106V, M106I, and M106I + L98S mutants was consistent with the current understanding of NS1 biochemistry. X-ray crystallography has been used to visualize the NS1 dimerization structure that forms upon binding to CPSF30 and has revealed that residues 103 and 106 on both NS1 monomers align to form a CPSF30 binding cleft (Das *et al.*, 2008) (Fig. 21). Thus, our experiments strengthen the evidence identifying the importance of these two residues in CPSF30 binding. Unfortunately, because both the

Figure 21. Dimerization structure seen when NS1 is bound to CPSF30. NS1 is presented here in the homodimerized form associated with CPSF30 binding (Das *et al.*, 2008). Relevant binding sites are colour-coded and labeled in the legend to the right. The sites of convergent evolution seen in mouse-adapted HK/1/68 (H3N2) strains are indicated by the green space filling diagrams and the corresponding amino acid residue number. The F2/F3 finger of the CPSF30 protein is shown as a purple ribbon diagram. The 226 mutation could not be shown because the NS1 effector domain used to solve the crystal structure is truncated and ends at residue 206. The RNA-binding domain is not shown, but the 5' residues of the effector domains that connect to the RNA-binding domain are marked with black arrows.

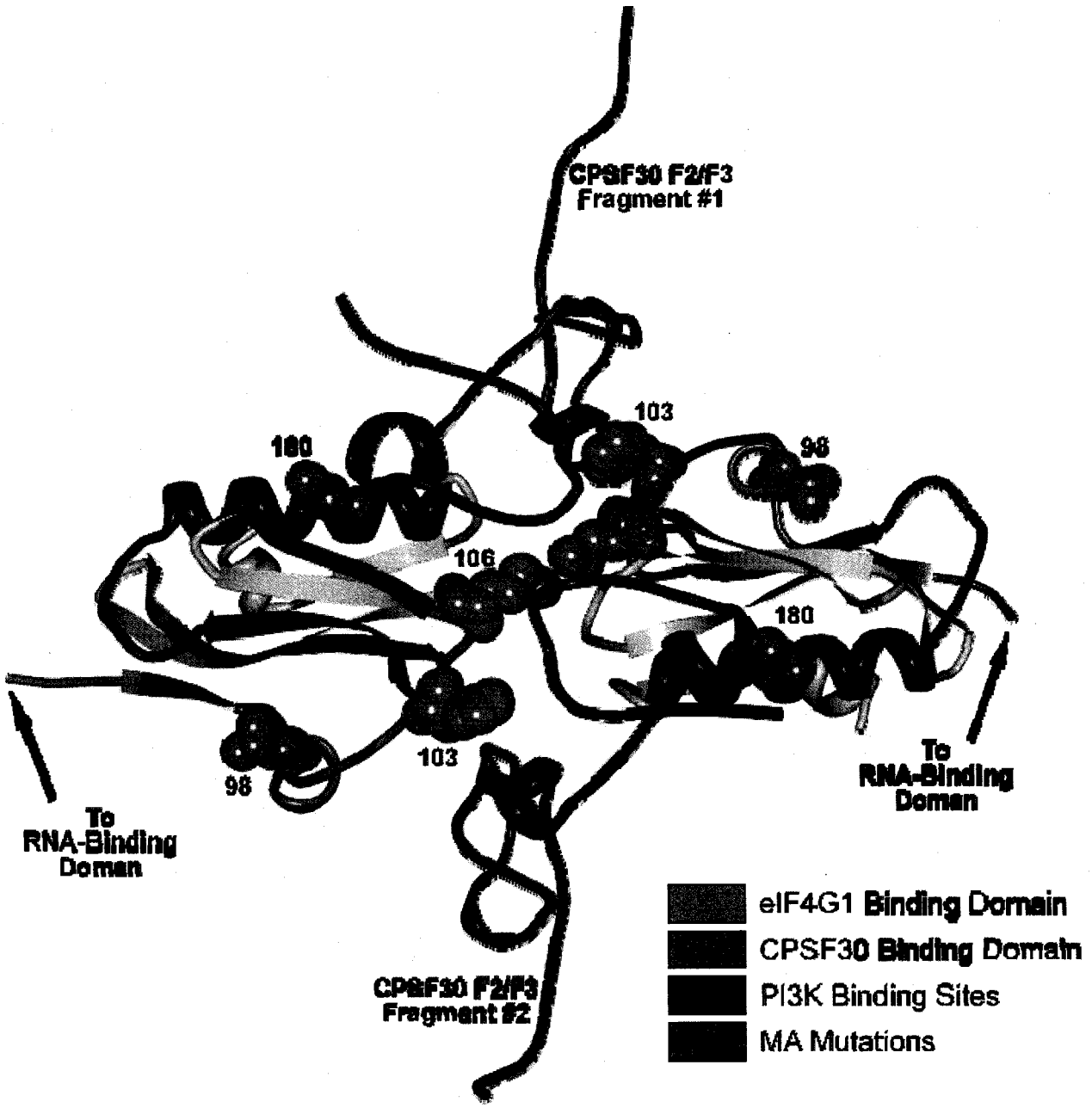

M106I and M106I + L98S variants lost the ability to bind CPSF30, the effect of the L98S mutation could not be assessed on its own. Therefore, the L98S mutation may or may not affect CPSF30 binding. Additional pulldown and association experiments must be performed on a NS1 mutant that possesses the L98S mutation in isolation in order to examine the effect of this mutation CPSF30 binding.

In addition to residues 103 and 106, my evidence indicates that residue 180 is also an important mediator of CPSF30 binding. Residue 180 exists within the 42 residue stretch from aa144 to aa186 which has been mapped to CPSF30 binding. Examination of the structural location of aa180 shows that this residue lies on an α-helix that lies in close proximity to a complimentary α-helix on the CPSF30 protein (Fig. 21). The exchange of a valine (hydropathy index = 4.2) for a less hydrophobic alanine (hydropathy index = 1.8) at this position may inhibit binding by reducing the strength of the hydrophobic interaction with the nearby phenylalanine on the CPSF30 α-helix. Finally, aa226 negates CPSF30 binding, but will be discussed in a later section.

The loss of CPSF30 binding due to six of the seven mutant combinations was surprising because the loss of this interaction has been shown to increase IFN production and attenuate viral production (Kochs *et al.*, 2007; Twu *et al.*, 2006; Twu *et al.*, 2007). Thus, mutations which inhibit CPSF30 binding would appear to be counterproductive to virulence. However, because the results show that numerous functions of the NS1 protein can be affected by single amino acid substitutions, it is reasonable to hypothesize that the loss of CPSF30 binding may be the cost of a mutation that enhances an alternate function of NS1

(such as binding to PABP1 or one of the other NS1 ligands). Although four of the seven mutant NS1 proteins did show an enhanced affinity for PABP1, it is possible that other NS1 functions were also positively affected by these mutations. The V180A mutation is notable in that it had a detrimental effect on both CPSF30 and PABP1 binding. The inhibitory effect of V180A on both of these NS1 functions may suggest that some other function of NS1 is enhanced at the cost of both the CPSF30 and PABP1 binding abilities.

An alternate explanation for the loss of CPSF30 binding may be that it is a form of control over NS1 functionality. CPSF30 binding greatly inhibits polyadenylation of host transcripts, thereby inhibiting IFN-β induction. However, by binding CPSF30, NS1 also inhibits the expression of host proteins that are necessary for viral replication. In quickly replicating high pathogenicity FluA viruses, enhanced host metabolism and protein production may be desirable to allow for more rapid viral replication. Thus, it may be critical for FluAV to develop a manner to control the level of host gene inhibition in response to the immediate needs of viral replication. In support of this model, NS1 variants with mutations at aa103 and 106 that inhibit CPSF30 binding *in vitro* have been shown to effectively bind CPSF30 during infection in their native FluAV strains. Interestingly, NS1 proteins with these same mutantions were not able to bind CPSF30 during infection when they were expressed from a recombinant FluAV strain that did not naturally possess these 103 and 106 NS1mutations (Twu *et al.*, 2007). These findings suggest that mutations at the 103 and 106 sites may be stabilized by one or more additional FluAV proteins, and that additional mutations in alternate genes are able to compensate for the 103 and 106 mutations on NS1

to restore CPSF30 binding. Furthermore, due to the spatial location and demonstrated importance of aa180, it is logical to hypothesize that the loss of CPSF30 binding caused by the V180A mutation may be similarly restored in the presence of a stabilizing protein. The requirement of a stabilizing protein for CPSF30 binding may provide a mechanism through which FluAV is able to control the amount of NS1 that is bound to CPSF30, thereby throttling host protein expression in response to the temporally changing needs of viral replication. Inhibition of CPSF30 binding would also free NS1 to fulfill its other functions (such as PABP1-binding and dsRNA sequestration) without competition from CPSF30. Thus, the loss of CPSF30 binding may contribute to virulence by modulating protein synthesis, while at the same time maintaining IFN inhibition and control over host gene expression through the interaction of NS1 with CPSF30 in coordination with other FluAV proteins. However, further efforts to identify the stabilizing protein(s) and examine the effect of the HK-MA mutations on the interaction of NS1 with its other known binding partners must be performed to support this hypothesis.

4.2 The Majority of the Mutations Affected PABP1 Binding

In addition to their importance in CPSF30 binding, my results demonstrate that residues 98, 103, 106, and 180 are critical components in modulating PABP1 binding affinity. Previous studies have narrowed the essential PABP1 binding region the first 81 N-terminal amino acids. However, this same study identified a region located between residues 82 – 152 that greatly enhanced PABP1 binding (Burgui *et al.*, 2003) (Fig 22).

Figure 22. Functional map of the influenza A NS1 protein with MA mutations mapped. Mapped locations for RNA, PABP1, eIF4G1, CPSF30 (marked "CPSF"), PABII, and PKR interaction are shown. SH2 and SH3 stand for Src homology 2 and 3 domains which are responsible for PI3-k and Crk/CrkL interaction. Also listed are the nuclear localization signals (NLS1 and NLS2) and the nuclear export sequence (NES). The separate RNA-binding and effector domains are marked below the figure. The locations of the identified mouse adapted NS1 mutations are indicated by the black arrows.

Residues 98, 103, and 106 all map to this previously identified enhancement region. Unfortunately, the dimer structure assumed by NS1 upon binding to PABP1 is not yet known. However, in both of the proposed NS1 dimers, residues 98, 103, and 106 are located peripherally on the surface of the dimerized NS1 structure (Fig. 23). Thus these residues may interact directly with PABP1 to stabilize its association with NS1. The function of residue 180 is less obvious in that it can be located either on the periphery of the dimerized NS1 structure, or near the dimerization site, depending on which dimer is assumed to associate with PABP1. Thus, the residue 180 may interact directly with PABP1 wherein the V180A mutation may provide a less stable interaction or, alternatively, the V180A mutation may inhibit dimerization. Native protein PAGE gels may provide further insight into the effect of the V180A mutation on dimerization, while a crystal structure of NS1 bound to PABP1 would greatly clarify these issues.

It has been previously established that an increase in binding affinity between the PABP1 and eIF4G1 proteins stabilize the entire translation initiation complex, thereby enhancing translation (Prevot *et al.*, 2003). Because NS1 is able to bind to both of these proteins, it is likely that mutations that enhance PABP1 binding affinity will enhance translation initiation by stabilizing the eIF4G1 – PABP1 interaction. Furthermore, because NS1 is also able to bind specifically to viral mRNA, this enhanced translation initiation may be specific to viral mRNA, resulting in increased viral protein production (Park & Katze, 1995). Therefore, it is likely that mutations in NS1 that enhance PABP1 binding could increase virulence by enhancing viral protein production. Thus, this enhanced PABP1

Figure 23. Hypothetical dimerization structures of the NS1 effector domain (A) One proposed dimer structure of the NS1 effector domain (Bornholdt & Prasad, 2006). The 98, 103,106, and 180 mutations all map to the periphery of the structure. **(B)** The proposed helix-helix dimer structure of the effector domain (Hale *et al.*, 2008). The 98, 103, and 106 mutations map to the periphery of the structure, while the 180 mutation maps near the dimerization domain. Relevant binding sites are colour-coded and labeled in the legend to the right. The sites of convergent evolution seen in mouse-adapted HK/1/68 (H3N2) strains are indicated by the green space filling diagrams and the corresponding amino acid residue number. The 226 mutation could not be shown because the NS1 effector domain used to solve the crystal structure is truncated and ends at residue 206. However, a portion of the C' terminal unstructured tail from monomer 2 is visible in (B). Amino acid 224 is labeled to suggest the position of the 226 mutation because the mutated site (226) is truncated. The RNA-binding domain is not shown, but the 5' residues of the effector domains that connect to the RNA-binding domain are marked with black arrows.

A

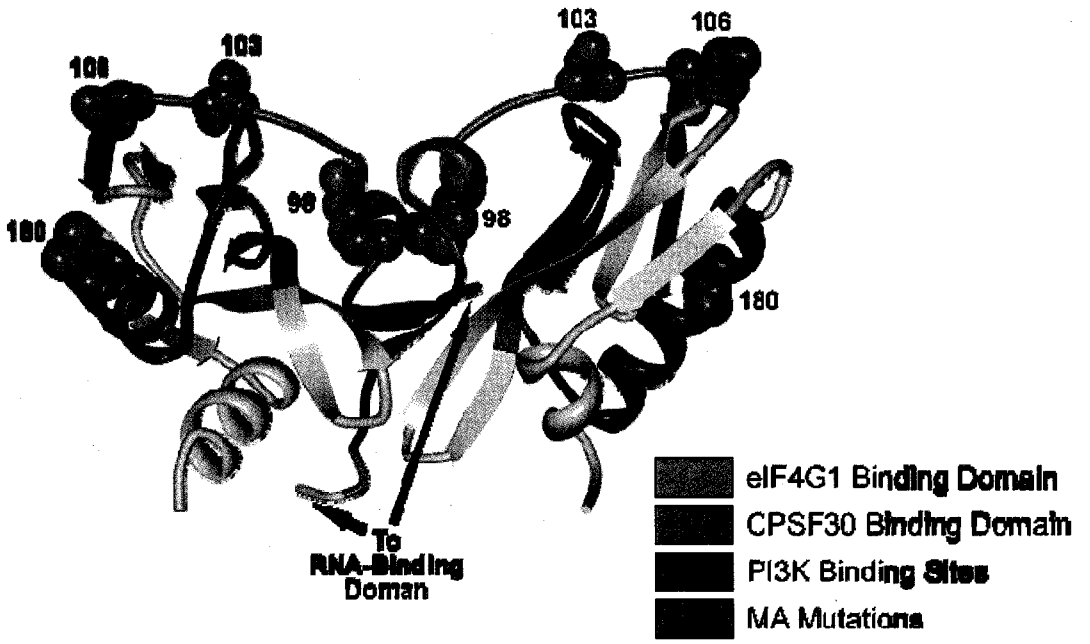

B

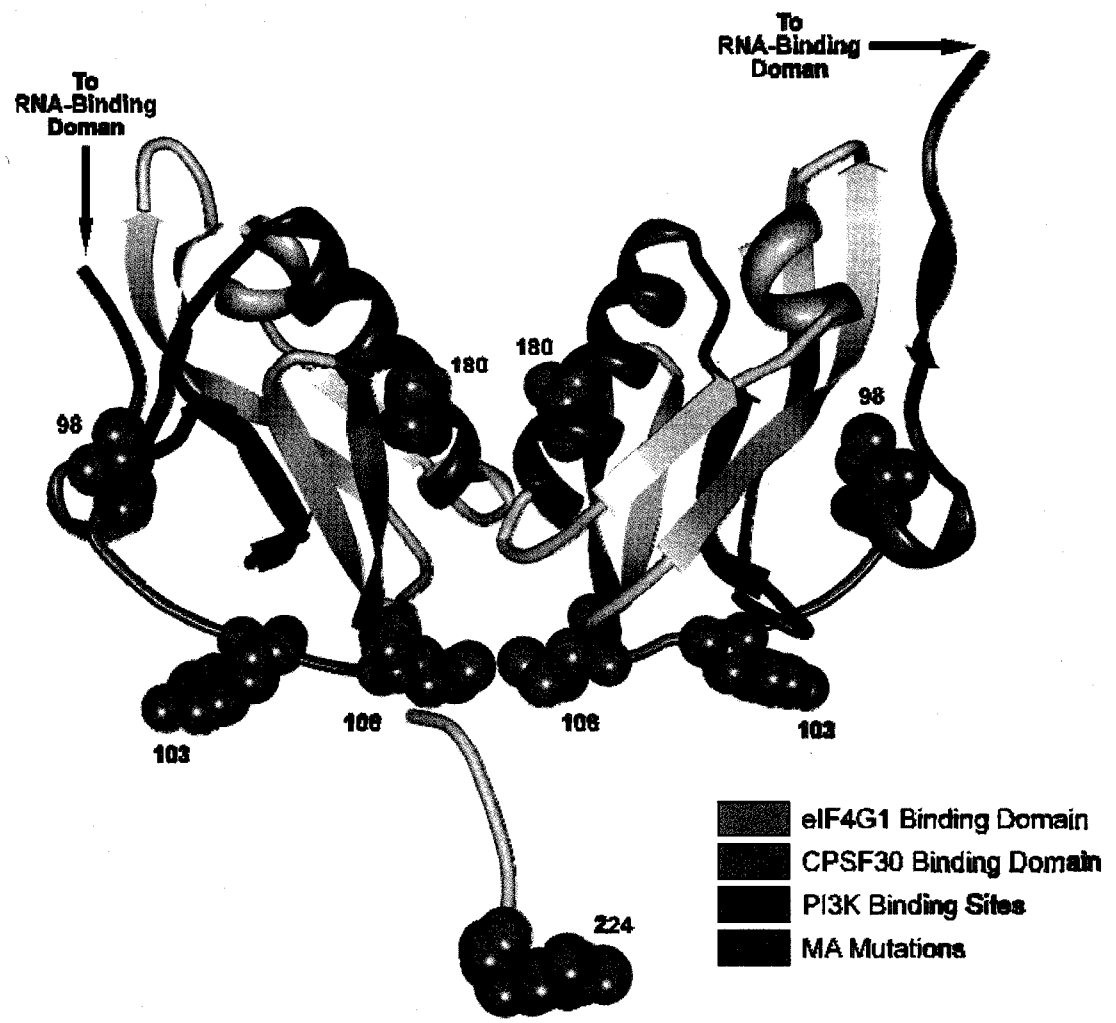

binding affinity is most likely the source of the increased viral protein expression that is seen in the rWSN-103L, rWSN-106I, and rWSN-98S+106I viruses (Table 3). However, *in vitro* translation assays in the presence of the purified mutant NS1 proteins must be conducted to determine whether the enhanced PABP1 affinities rendered by the F103L, M106V, M106I, and L98S mutations translate directly into the increased protein production seen in the viruses. Additionally, the effect of the various mutations on eIF4G1 binding affinity must also be assessed.

Conversely, the V180A mutation had a negative effect on PABP1 affinity. As mentioned above, the loss of PABP1 affinity caused by the V180A mutation may be a sacrifice that is compensated for by the enhancement of alternate viral functions. PABP1 binding affinity may also be restored by stabilizer proteins as is seen for CPSF30 binding. Thus, further binding studies must be performed to elucidate the effect that this mutation may have on the other functions of NS1, while additional coimmunoprecipitations can be designed to examine the PABP1 binding capacity of this mutant in the presence of the other viral proteins.

4.3 The V23A Mutation did not Affect CPSF30 and PABP1 Binding

The V23A mutation did not significantly affect CPSF30 or PABP1 binding capacity. This is not surprising for CPSF30 binding, but is for PABP1 binding because the V23A mutation is located on the overlapping RNA-binding and PABP1 binding domain (Fig. 22).

However, the V23A mutation may still affect virulence by altering the structural stability of the RNA-binding domain homodimer, thereby affecting RNA binding affinity with its multiple roles in controlling IFN induction and IFN responsiveness.

4.4 The V226I Mutation Prevented both CPSF30 and PABP1 Binding

The V226I mutation is interesting in that it inhibited both CPSF30 and PABP1 binding despite being located at the C-terminal end of the NS1 protein, distant from the binding domains for both of these proteins (Fig. 22). Furthermore, truncated NS1 proteins lacking the C-terminal region encompassing aa226, have been shown to fully bind to both PABP1 and CPSF30 (Burgui *et al.*, 2003; Li *et al.*, 2001), suggesting that this region is not necessary to stabilize binding to either of these two proteins. Thus, these findings are consistent with a role for the V226I mutation as a dominant negative mutation that works to inhibit or block PABP1 and CPSF30 binding. The inhibition of these binding functions by the C-terminal tail would, thereby, increase the concentration of unbound NS1 that is available to associate with other binding partners to perform other functions.

The C-terminal region of NS1, downstream of residue 203, forms a disordered tail on the protein. This tail has a high degree of intrinsic flexibility and may move from a disordered to ordered state upon ligand binding (Hale *et al.*, 2008). This disordered tail is also interesting due to its naturally occurring diversity; some FluAV strains carrying a seven residue extension of this tail while others may have up to a 20 residue deletion from this

region (Suarez and Perdue, 1998). Given the structure and diversity of the C-terminal tail, this region may constitute a control domain that modulates NS1 activity by sterically blocking certain binding sites and/or by promoting the formation of NS1 dimer structures that favour the binding of certain ligands over others. The mechanism through which the inhibitory function of this tail is controlled may lie in the PDZ domain located at the extreme C-terminal end of the tail (aa227-30) (Jackson *et al.* 2008; Obenauer *et al.* 2006) (Fig. 22). Binding of the PDZ domain by an unknown host protein could drive a structural change in the C-terminal tail that could modulate its inhibition of binding to other proteins and factors. Due to the prevalence of PDZ domain-containing proteins in the host, such a mechanism would give NS1 the ability to regulate its function in response to protein factors present in the immediate cellular environment. However, this hypothesis is currently highly theoretical. Further studies must be performed to determine the PABP1 and CPSF30 binding capacities of HK-wt NS1 deletion mutants lacking residue 226-37, and also the entire C-terminal tail (aa202 – 237). Additionally, PDZ domain-containing proteins that bind to NS1 have yet to be identified. Once such proteins are identified, the effect of their presence on the binding capacity of NS1 to its various host factors must be determined through pulldown and coimmunoprecipitation studies.

4.5 Identification of NS1 Determinacy Regions that Control Virulence

The seven NS1 mutations identified in the virulent mouse adapted FluAV strains significantly affected the NS1 protein's binding affinity for both PABP1 and CPSF30. The

inhibited CPSF30 binding seen in the NS1 variants with mutations at residues 103 and 106 agrees with previous studies that have identified the functional importance of these two residues in CPSF30 binding. Meanwhile, residues 180 and 226 have been identified as novel modulators of CPSF30 binding. Six of these seven mutations have also been shown to modulate PABP1 binding. Thus we have identified five specific adaptive sites in the FluAV A NS1 protein and provided some insight into the molecular mechanisms that are affected by mutations at these sites. It is highly likely that these specific mutations also affect the affinity of NS1 to other NS1 binding proteins, but further experimentation is necessary to refine this hypothesis.

REFERENCES

Alexopoulou, L., Holt, A.C., Medzhitov, R., and Flavell, R.A. (2001). Recognition of double-stranded RNA and activation of NF-kappaB by Toll-like receptor 3. Nature *413*, 732-738.

Amersham Biosciences (2003). GST Gene Fusion System Handbook. Ed. AA.

Aragon, T., de la Luna, S., Novoa, I., Carrasco, L., Ortin, J., and Nieto, A. (2000). Eukaryotic translation initiation factor 4GI is a cellular target for NS1 protein, a translational activator of influenza virus. Mol Cell Biol *20*, 6259-6268.

Barker, W.H., and Mullooly, J.P. (1980). Impact of epidemic type A influenza in a defined adult population. Am J Epidemiol *112*, 798-811.

Barman, S., and Nayak, D.P. (2000). Analysis of the transmembrane domain of influenza virus neuraminidase, a type II transmembrane glycoprotein, for apical sorting and raft association. Journal of virology *74*, 6538-6545.

Barman, S., Ali, A., Hui, E.K., Adhikary, L., and Nayak, D.P. (2001). Transport of viral proteins to the apical membranes and interaction of matrix protein with glycoproteins in the assembly of influenza viruses. Virus Res *77*, 61-69.

Basler, C.F., and Aguilar, P.V. (2008). Progress in identifying virulence determinants of the 1918 H1N1 and the Southeast Asian H5N1 influenza A viruses. Antiviral Res *79*, 166-178.

Basler, C.F., Reid, A.H., Dybing, J.K., Janczewski, T.A., Fanning, T.G., Zheng, H., Salvatore, M., Perdue, M.L., Swayne, D.E., Garcia-Sastre, A., *et al.* (2001). Sequence of the 1918 pandemic influenza virus nonstructural gene (NS) segment and characterization of recombinant viruses bearing the 1918 NS genes. Proceedings of the National Academy of Sciences of the United States of America *98*, 2746-2751.

Beaton, A.R., and Krug, R.M. (1981). Selected host cell capped RNA fragments prime influenza viral RNA transcription in vivo. Nucleic Acids Res *9*, 4423-4436.

Beaton, A.R., and Krug, R.M. (1986). Transcription antitermination during influenza viral template RNA synthesis requires the nucleocapsid protein and the absence of a 5' capped end. Proc Natl Acad Sci U S A *83*, 6282-6286.

Biron, C.A., and Sen, G.C. Interferons and other cytokines. In: Knipe D.M., Howley P.M., ed. The Field of Virology, forth ed. Lippncott Williams & Wilkins. 2001:321-353.

Bornholdt, Z.A., and Prasad, B.V. (2006). X-ray structure of influenza virus NS1 effector domain. Nat Struct Mol Biol *13*, 559-560.

Boulan, E.R., and Pendergast, M. (1980). Polarized distribution of viral envelope proteins in the plasma membrane of infected epithelial cells. Cell *20*, 45-54.

Brown, E.G. (2000). Influenza virus genetics. Biomed Pharmacother *54*, 196-209.

Brown, E.G. (1990). Increased virulence of a mouse-adapted variant of influenza A/FM/1/47 virus is controlled by mutations in genome segments 4, 5, 7, and 8. Journal of virology *64*, 4523-4533.

Brown, E.G., and Bailly, J.E. (1999). Genetic analysis of mouse-adapted influenza A virus identifies roles for the NA, PB1, and PB2 genes in virulence. Virus research *61*, 63-76.

Brown, E.G., Liu, H., Kit, L.C., Baird, S., and Nesrallah, M. (2001). Pattern of mutation in the genome of influenza A virus on adaptation to increased virulence in the mouse lung: identification of functional themes. Proceedings of the National Academy of Sciences of the United States of America *98*, 6883-6888.

Burgui, I., Aragon, T., Ortin, J., and Nieto, A. (2003). PABP1 and eIF4GI associate with influenza virus NS1 protein in viral mRNA translation initiation complexes. The Journal of general virology *84*, 3263-3274.

Chen, H., Deng, G., Li, Z., Tian, G., Li, Y., Jiao, P., Zhang, L., Liu, Z., Webster, R.G., and Yu, K. (2004). The evolution of H5N1 influenza viruses in ducks in southern China. Proceedings of the National Academy of Sciences of the United States of America *101*, 10452-10457.

Chen, W., Calvo, P.A., Malide, D., Gibbs, J., Schubert, U., Bacik, I., Basta, S., O'Neill, R., Schickli, J., Palese, P., *et al.* (2001). A novel influenza A virus mitochondrial protein that induces cell death. Nat Med *7*, 1306-1312.

Chen, Z., Li, Y., and Krug, R.M. (1999). Influenza A virus NS1 protein targets poly(A)-binding protein II of the cellular 3'-end processing machinery. Embo J *18*, 2273-2283.

Chien, C.Y., Tejero, R., Huang, Y., Zimmerman, D.E., Rios, C.B., Krug, R.M., and Montelione, G.T. (1997). A novel RNA-binding motif in influenza A virus non-structural protein 1. Nat Struct Biol *4*, 891-895.

Compans, R.W., Content, J., and Duesberg, P.H. (1972). Structure of the ribonucleoprotein of influenza virus. Journal of virology *10*, 795-800.

Connor, R.J., Kawaoka, Y., Webster, R.G., and Paulson, J.C. (1994). Receptor specificity in human, avian, and equine H2 and H3 influenza virus isolates. Virology *205*, 17-23.

Couceiro, J.N., Paulson, J.C., and Baum, L.G. (1993). Influenza virus strains selectively recognize sialyloligosaccharides on human respiratory epithelium; the role of the host cell in selection of hemagglutinin receptor specificity. Virus research *29*, 155-165.

Cros, J.F., Garcia-Sastre, A., and Palese, P. (2005). An unconventional NLS is critical for the nuclear import of the influenza A virus nucleoprotein and ribonucleoprotein. Traffic *6*, 205-213.

Das, K., Ma, L.-C., Xiao, R., Radvansky, B., Aramini, J., Zhao, L., Marklung, J., Kuo, R-L., Twu, K., Arnold, E., Krug, R., Montelione, G.T. (2008) Structural basis for suppression of a host antiviral response by influenza A virus. Proceedings of the National Academy of Sciences of the United States of America

Doms, R.W., Lamb, R.A., Rose, J.K., and Helenius, A. (1993). Folding and assembly of viral membrane proteins. Virology *193*, 545-562.

Ellis, T.M., Bousfield, R.B., Bissett, L.A., Dyrting, K.C., Luk, G.S., Tsim, S.T., Sturm-Ramirez, K., Webster, R.G., Guan, Y., and Malik Peiris, J.S. (2004). Investigation of outbreaks of highly pathogenic H5N1 avian influenza in waterfowl and wild birds in Hong Kong in late 2002. Avian Pathol *33*, 492-505.

Falcon, A.M., Fortes, P., Marion, R.M., Beloso, A., and Ortin, J. (1999). Interaction of influenza virus NS1 protein and the human homologue of Staufen in vivo and in vitro. Nucleic Acids Res *27*, 2241-2247.

Ferrandon, D., Elphick, L., Nusslein-Volhard, C., and St Johnston, D. (1994). Staufen protein associates with the 3'UTR of bicoid mRNA to form particles that move in a microtubule-dependent manner. Cell *79*, 1221-1232.

Garcia-Sastre, A., Egorov, A., Matassov, D., Brandt, S., Levy, D.E., Durbin, J.E., Palese, P., and Muster, T. (1998). Influenza A virus lacking the NS1 gene replicates in interferon-deficient systems. Virology *252*, 324-330.

Geiss, G.K., Salvatore, M., Tumpey, T.M., Carter, V.S., Wang, X., Basler, C.F., Taubenberger, J.K., Bumgarner, R.E., Palese, P., Katze, M.G., *et al.* (2002). Cellular transcriptional profiling in influenza A virus-infected lung epithelial cells: the role of the nonstructural NS1 protein in the evasion of the host innate defense and its potential contribution to pandemic influenza. Proceedings of the National Academy of Sciences of the United States of America *99*, 10736-10741.

Glaser, L., Stevens, J., Zamarin, D., Wilson, I.A., Garcia-Sastre, A., Tumpey, T.M., Basler, C.F., Taubenberger, J.K., and Palese, P. (2005). A single amino acid substitution in 1918 influenza

virus hemagglutinin changes receptor binding specificity. Journal of virology *79*, 11533-11536.

Greenspan, D., Palese, P., and Krystal, M. (1988). Two nuclear location signals in the influenza virus NS1 nonstructural protein. J Virol *62*, 3020-3026.

Guarner, J., Shieh, W.J., Dawson, J., Subbarao, K., Shaw, M., Ferebee, T., Morken, T., Nolte, K.B., Freifeld, A., Cox, N., *et al.* (2000). Immunohistochemical and in situ hybridization studies of influenza A virus infection in human lungs. Am J Clin Pathol *114*, 227-233.

Hagen, M., Chung, T.D., Butcher, J.A., and Krystal, M. (1994). Recombinant influenza virus polymerase: requirement of both 5' and 3' viral ends for endonuclease activity. J Virol *68*, 1509-1515.

Hale, B.G., Barclay, W.S., Randall, R.E., and Russell, R.J. (2008). Structure of an avian influenza A virus NS1 protein effector domain. Virology.

Hale, B.G., Batty, I.H., Downes, C.P., and Randall, R.E. (2008). Binding of influenza A virus NS1 protein to the inter-SH2 domain of p85 suggests a novel mechanism for phosphoinositide 3-kinase activation. J Biol Chem *283*, 1372-1380.

Haller, O., Frese, M., and Kochs, G. (1998). Mx proteins: mediators of innate resistance to RNA viruses. Rev Sci Tech *17*, 220-230.

Haller, O., and Kochs, G. (2002). Interferon-induced mx proteins: dynamin-like GTPases with antiviral activity. Traffic *3*, 710-717.

Hatada, E., and Fukuda, R. (1992). Binding of influenza A virus NS1 protein to dsRNA in vitro. The Journal of general virology *73 (Pt 12)*, 3325-3329.

Hatada, E., Saito, S., and Fukuda, R. (1999). Mutant influenza viruses with a defective NS1 protein cannot block the activation of PKR in infected cells. J Virol *73*, 2425-2433.

Heikkinen, L.S., Kazlauskas, A., Melen, K., Wagner, R., Ziegler, T., Julkunen, I., and Saksela, K. (2008). Avian and 1918 Spanish influenza a virus NS1 proteins bind to Crk/CrkL Src homology 3 domains to activate host cell signaling. J Biol Chem *283*, 5719-5727.

Huang, X., Liu, T., Muller, J., Levandowski, R.A., and Ye, Z. (2001). Effect of influenza virus matrix protein and viral RNA on ribonucleoprotein formation and nuclear export. Virology *287*, 405-416.

Hsu, M.T., Parvin, J.D., Gupta, S., Krystal, M., and Palese, P. (1987). Genomic RNAs of influenza viruses are held in a circular conformation in virions and in infected cells by a terminal panhandle. Proceedings of the National Academy of Sciences of the United States of America *84*, 8140-8144.

Isoda, N., Sakoda, Y., Kishida, N., Bai, G.R., Matsuda, K., Umemura, T., and Kida, H. (2006). Pathogenicity of a highly pathogenic avian influenza virus, A/chicken/Yamaguchi/7/04 (H5N1) in different species of birds and mammals. Arch Virol *151*, 1267-1279.

Jackson, D., Hossain, M.J., Hickman, D., Perez, D.R., and Lamb, R.A. (2008). A new influenza virus virulence determinant: the NS1 protein four C-terminal residues modulate pathogenicity. Proceedings of the National Academy of Sciences of the United States of America *105*, 4381-4386.

Johnson, N.P., and Mueller, J. (2002). Updating the accounts: global mortality of the 1918-1920 "Spanish" influenza pandemic. Bulletin of the history of medicine *76*, 105-115.

Kaiser, J. (2006). A one-size-fits-all flu vaccine? Science *312*, 380-382.

Kamps, B.S., Hoffmann, C., and Preiser, W., eds. (2006). Influenza Report (Paris, Flying Publisher).

Kilbourne, E.D. (1959). Studies on influenza in the pandemic of 1957-1958. III. Isolation of influenza A (Asian strain) viruses from influenza patients with pulmonary complications; details of virus isolation and characterization of isolates, with quantitative comparison of isolation methods. J Clin Invest *38*, 266-274.

Kobasa, D., Jones, S.M., Shinya, K., Kash, J.C., Copps, J., Ebihara, H., Hatta, Y., Kim, J.H., Halfmann, P., Hatta, M., *et al.* (2007). Aberrant innate immune response in lethal infection of macaques with the 1918 influenza virus. Nature *445*, 319-323.

Krug, R.M. (1981). Priming of influenza viral RNA transcription by capped heterologous RNAs. Curr Top Microbiol Immunol *93*, 125-149.

Kundu, A., Avalos, R.T., Sanderson, C.M., and Nayak, D.P. (1996). Transmembrane domain of influenza virus neuraminidase, a type II protein, possesses an apical sorting signal in polarized MDCK cells. Journal of virology *70*, 6508-6515.

Lamb, R.A., and Choppin, P.W. (1979). Segment 8 of the influenza virus genome is unique in coding for two polypeptides. Proceedings of the National Academy of Sciences of the United States of America *76*, 4908-4912.

Lamb, R.A., and Choppin, P.W. (1981). Identification of a second protein (M2) encoded by RNA segment 7 of influenza virus. Virology *112*, 729-737.

Lamb, R.A., and Lai, C.J. (1980). Sequence of interrupted and uninterrupted mRNAs and cloned DNA coding for the two overlapping nonstructural proteins of influenza virus. Cell *21*, 475-485.

Lamb, R.A., and Lai, C.J. (1982). Spliced and unspliced messenger RNAs synthesized from cloned influenza virus M DNA in an SV40 vector: expression of the influenza virus membrane protein (M1). Virology *123*, 237-256.

Lamb, R.A., and Lai, C.J. (1984). Expression of unspliced NS1 mRNA, spliced NS2 mRNA, and a spliced chimera mRNA from cloned influenza virus NS DNA in an SV40 vector. Virology *135*, 139-147.

Lamb, R.A., Lai, C.J., and Choppin, P.W. (1981). Sequences of mRNAs derived from genome RNA segment 7 of influenza virus: colinear and interrupted mRNAs code for overlapping proteins. Proceedings of the National Academy of Sciences of the United States of America *78*, 4170-4174.

Li, S., Min, J.Y., Krug, R.M., and Sen, G.C. (2006). Binding of the influenza A virus NS1 protein to PKR mediates the inhibition of its activation by either PACT or double-stranded RNA. Virology *349*, 13-21.

Li, X., and Palese, P. (1994). Characterization of the polyadenylation signal of influenza virus RNA. J Virol *68*, 1245-1249.

Li, Y., Anderson, D.H., Liu, Q., and Zhou, Y. (2008). Mechanism of influenza A virus NS1 protein interaction with the p85beta , but not the p85alpha , subunit of PI3K and upregulation of PI3K activity. J Biol Chem.

Li, Y., Yamakita, Y., and Krug, R.M. (1998). Regulation of a nuclear export signal by an adjacent inhibitory sequence: the effector domain of the influenza virus NS1 protein. Proceedings of the National Academy of Sciences of the United States of America *95*, 4864-4869.

Li, Z., Jiang, Y., Jiao, P., Wang, A., Zhao, F., Tian, G., Wang, X., Yu, K., Bu, Z., and Chen, H. (2006). The NS1 gene contributes to the virulence of H5N1 avian influenza viruses. Journal of virology *80*, 11115-11123.

Lin, S., Naim, H.Y., Rodriguez, A.C., and Roth, M.G. (1998). Mutations in the middle of the transmembrane domain reverse the polarity of transport of the influenza virus hemagglutinin in MDCK epithelial cells. J Cell Biol *142*, 51-57.

Louria, D.B., Blumenfeld, H.L., Ellis, J.T., Kilbourne, E.D., and Rogers, D.E. (1959). Studies on influenza in the pandemic of 1957-1958. II. Pulmonary complications of influenza. J Clin Invest *38*, 213-265.

Lu, Y., Wambach, M., Katze, M.G., and Krug, R.M. (1995). Binding of the influenza virus NS1 protein to double-stranded RNA inhibits the activation of the protein kinase that phosphorylates the eIF-2 translation initiation factor. Virology *214*, 222-228.

Ludwig, S., Wang, X., Ehrhardt, C., Zheng, H., Donelan, N., Planz, O., Pleschka, S., Garcia-Sastre, A., Heins, G., and Wolff, T. (2002). The influenza A virus NS1 protein inhibits activation of Jun N-terminal kinase and AP-1 transcription factors. J Virol *76*, 11166-11171.

MacDonald, N., Weir, E., and Langley, J.M. (2007). Influenza and the influenza vaccine. CMAJ *177*, 1028.

Marie, I., Durbin, J.E., and Levy, D.E. (1998). Differential viral induction of distinct interferon-alpha genes by positive feedback through interferon regulatory factor-7. EMBO J *17*, 6660-6669.

Marion, R.M., Fortes, P., Beloso, A., Dotti, C., and Ortin, J. (1999). A human sequence homologue of Staufen is an RNA-binding protein that is associated with polysomes and localizes to the rough endoplasmic reticulum. Mol Cell Biol *19*, 2212-2219.

Matikainen, S., Siren, J., Tissari, J., Veckman, V., Pirhonen, J., Severa, M., Sun, Q., Lin, R., Meri, S., Uze, G., *et al.* (2006). Tumor necrosis factor alpha enhances influenza A virus-induced expression of antiviral cytokines by activating RIG-I gene expression. Journal of virology *80*, 3515-3522.

Matlin, K.S., Reggio, H., Helenius, A., and Simons, K. (1981). Infectious entry pathway of influenza virus in a canine kidney cell line. J Cell Biol *91*, 601-613.

Matrosovich, M.N., Matrosovich, T.Y., Gray, T., Roberts, N.A., and Klenk, H.D. (2004). Human and avian influenza viruses target different cell types in cultures of human airway epithelium. Proceedings of the National Academy of Sciences of the United States of America *101*, 4620-4624.

Mibayashi, M., Martinez-Sobrido, L., Loo, Y.M., Cardenas, W.B., Gale, M., Jr., and Garcia-Sastre, A. (2007). Inhibition of retinoic acid-inducible gene I-mediated induction of beta interferon by the NS1 protein of influenza A virus. Journal of virology *81*, 514-524.

Min, J.Y., Li, S., Sen, G.C., and Krug, R.M. (2007). A site on the influenza A virus NS1 protein mediates both inhibition of PKR activation and temporal regulation of viral RNA synthesis. Virology *363*, 236-243.

Mould, J.A., Drury, J.E., Frings, S.M., Kaupp, U.B., Pekosz, A., Lamb, R.A., and Pinto, L.H. (2000). Permeation and activation of the M2 ion channel of influenza A virus. J Biol Chem *275*, 31038-31050.

Nayak, D.P., Hui, E.K., and Barman, S. (2004). Assembly and budding of influenza virus. Virus Res *106*, 147-165.

Nemeroff, M.E., Barabino, S.M., Li, Y., Keller, W., and Krug, R.M. (1998). Influenza virus NS1 protein interacts with the cellular 30 kDa subunit of CPSF and inhibits 3'end formation of cellular pre-mRNAs. Molecular cell *1*, 991-1000.

Nemeroff, M.E., Qian, X.Y., and Krug, R.M. (1995). The influenza virus NS1 protein forms multimers in vitro and in vivo. Virology *212*, 422-428.

Neumann, G., Hughes, M.T., and Kawaoka, Y. (2000). Influenza A virus NS2 protein mediates vRNP nuclear export through NES-independent interaction with hCRM1. EMBO J *19*, 6751-6758.

OiE. *Update on Highly Pathogenic Avian Influenza in Animals*. URL: http://www.oie.int/downld/AVIAN%20INFLUENZA/A_AI-Asia.htm Accessed 8 August, 2008.

O'Neill, R.E., Jaskunas, R., Blobel, G., Palese, P., and Moroianu, J. (1995). Nuclear import of influenza virus RNA can be mediated by viral nucleoprotein and transport factors required for protein import. J Biol Chem *270*, 22701-22704.

O'Neill, R.E., Talon, J., and Palese, P. (1998). The influenza virus NEP (NS2 protein) mediates the nuclear export of viral ribonucleoproteins. EMBO J *17*, 288-296.

Palese, P., and Schulman, J.L. (1976). Differences in RNA patterns of influenza A viruses. Journal of virology *17*, 876-884.

Palese, P., and Shaw, M.L. (2007). Orthomyxoviridae: The Viruses and Their Replication. In Field's Virology, D.M.K. PhD, and P.M.H. MD, eds. (Philadelphia, Lippincott Williams & Wilkins), pp. 1647-1678.

Palese, P., Tobita, K., Ueda, M., and Compans, R.W. (1974). Characterization of temperature sensitive influenza virus mutants defective in neuraminidase. Virology *61*, 397-410.

Park, Y.W., and Katze, M.G. (1995). Translational control by influenza virus. Identification of cis-acting sequences and trans-acting factors which may regulate selective viral mRNA translation. J Biol Chem *270*, 28433-28439.

Perrone, L.A., Plowden, J.K., Garcia-Sastre, A., Katz, J.M., and Tumpey, T.M. (2008). H5N1 and 1918 pandemic influenza virus infection results in early and excessive infiltration of macrophages and neutrophils in the lungs of mice. PLoS pathogens *4*, e1000115.

Petersdorf, R.G., Fusco, J.J., Harter, D.H., and Albrink, W.S. (1959). Pulmonary infections complicating Asian influenza. AMA Arch Intern Med *103*, 262-272.

Pinto, L.H., Holsinger, L.J., and Lamb, R.A. (1992). Influenza virus M2 protein has ion channel activity. Cell *69*, 517-528.

Plotch, S.J., Bouloy, M., Ulmanen, I., and Krug, R.M. (1981). A unique cap(m7GpppXm)-dependent influenza virion endonuclease cleaves capped RNAs to generate the primers that initiate viral RNA transcription. Cell *23*, 847-858.

Poon, L.L., Pritlove, D.C., Fodor, E., and Brownlee, G.G. (1999). Direct evidence that the poly(A) tail of influenza A virus mRNA is synthesized by reiterative copying of a U track in the virion RNA template. J Virol *73*, 3473-3476.

Prevot, D., Darlix, J.L., and Ohlmann, T. (2003). Conducting the initiation of protein synthesis: the role of eIF4G. Biol Cell *95*, 141-156.

Qian, X.Y., Chien, C.Y., Lu, Y., Montelione, G.T., and Krug, R.M. (1995). An amino-terminal polypeptide fragment of the influenza virus NS1 protein possesses specific RNA-binding activity and largely helical backbone structure. RNA *1*, 948-956.

Qiu, Y., and Krug, R.M. (1994). The influenza virus NS1 protein is a poly(A)-binding protein that inhibits nuclear export of mRNAs containing poly(A). Journal of virology *68*, 2425-2432.

Qiu, Y., Nemeroff, M., and Krug, R.M. (1995). The influenza virus NS1 protein binds to a specific region in human U6 snRNA and inhibits U6-U2 and U6-U4 snRNA interactions during splicing. RNA *1*, 304-316.

Reactome [*www.reactome.org*] (cited August 2, 2008). Influenza Lifecycle. Available from http://www.reactome.org/cgi-bin/eventbrowser?DB=gk_current&ID=168255

Reid, A.H., Fanning, T.G., Hultin, J.V., and Taubenberger, J.K. (1999). Origin and evolution of the 1918 "Spanish" influenza virus hemagglutinin gene. Proceedings of the National Academy of Sciences of the United States of America *96*, 1651-1656.

Reid, A.H., Fanning, T.G., Janczewski, T.A., Lourens, R.M., and Taubenberger, J.K. (2004). Novel origin of the 1918 pandemic influenza virus nucleoprotein gene. J Virol *78*, 12462-12470.

Reid, A.H., Fanning, T.G., Janczewski, T.A., and Taubenberger, J.K. (2000). Characterization of the 1918 "Spanish" influenza virus neuraminidase gene. Proc Natl Acad Sci U S A *97*, 6785-6790.

Reid, A.H., Taubenberger, J.K., and Fanning, T.G. (2001). The 1918 Spanish influenza: integrating history and biology. Microbes Infect *3*, 81-87.
Robertson, L., Caley, J.P., and Moore, J. (1958). Importance of Staphylococcus aureus in pneumonia in the 1957 epidemic of influenza A. Lancet *2*, 233-236.

Ruigrok, R.W., Barge, A., Durrer, P., Brunner, J., Ma, K., and Whittaker, G.R. (2000). Membrane interaction of influenza virus M1 protein. Virology *267*, 289-298.

Ruigrok, R.W., Calder, L.J., and Wharton, S.A. (1989). Electron microscopy of the influenza virus submembranal structure. Virology *173*, 311-316.

Sakaguchi, T., Tu, Q., Pinto, L.H., and Lamb, R.A. (1997). The active oligomeric state of the minimalistic influenza virus M2 ion channel is a tetramer. Proc Natl Acad Sci U S A *94*, 5000-5005.

Samuel, C.E. (2001). Antiviral actions of interferons. Clin Microbiol Rev *14*, 778-809.

Sen, G.C., and Sarkar, S.N. (2005). Transcriptional signaling by double-stranded RNA: role of TLR3. Cytokine Growth Factor Rev *16*, 1-14.

Schmitt, A.P., and Lamb, R.A. (2005). Influenza virus assembly and budding at the viral budozone. Adv Virus Res *64*, 383-416.

Schulman, J.L., and Palese, P. (1977). Virulence factors of influenza A viruses: WSN virus neuraminidase required for plaque production in MDBK cells. J Virol *24*, 170-176.

Seo, S.H., Hoffmann, E., and Webster, R.G. (2002). Lethal H5N1 influenza viruses escape host anti-viral cytokine responses. Nat Med *8*, 950-954.

Seo, S.H., Hoffmann, E., and Webster, R.G. (2004). The NS1 gene of H5N1 influenza viruses circumvents the host anti-viral cytokine responses. Virus Res *103*, 107-113.

Shin, Y.K., Li, Y., Liu, Q., Anderson, D.H., Babiuk, L.A., and Zhou, Y. (2007). SH3 binding motif 1 in influenza A virus NS1 protein is essential for PI3K/Akt signaling pathway activation. Journal of virology *81*, 12730-12739.

Simonsen, L. (1999). The global impact of influenza on morbidity and mortality. Vaccine *17 Suppl 1*, S3-10.

Simonsen, L., Clarke, M.J., Schonberger, L.B., Arden, N.H., Cox, N.J., and Fukuda, K. (1998). Pandemic versus epidemic influenza mortality: a pattern of changing age distribution. J Infect Dis *178*, 53-60.

Siren, J., Imaizumi, T., Sarkar, D., Pietila, T., Noah, D.L., Lin, R., Hiscott, J., Krug, R.M., Fisher, P.B., Julkunen, I., *et al.* (2006). Retinoic acid inducible gene-I and mda-5 are involved in influenza A virus-induced expression of antiviral cytokines. Microbes and infection / Institut Pasteur *8*, 2013-2020.

Smeenk, C.A., and Brown, E.G. (1994). The influenza virus variant A/FM/1/47-MA possesses single amino acid replacements in the hemagglutinin, controlling virulence, and in the matrix protein, controlling virulence as well as growth. Journal of virology *68*, 530-534.

Smeenk, C.A., Wright, K.E., Burns, B.F., Thaker, A.J., and Brown, E.G. (1996). Mutations in the hemagglutinin and matrix genes of a virulent influenza virus variant, A/FM/1/47-MA, control different stages in pathogenesis. Virus research *44*, 79-95.

Smith, P.L., Lombardi, G., and Foster, G.R. (2005). Type I interferons and the innate immune response--more than just antiviral cytokines. Mol Immunol *42*, 869-877.

Sprenger, M.J., Mulder, P.G., Beyer, W.E., Van Strik, R., and Masurel, N. (1993). Impact of influenza on mortality in relation to age and underlying disease, 1967-1989. Int J Epidemiol *22*, 334-340.

Staeheli, P., Pitossi, F., and Pavlovic, J. (1993). Mx proteins: GTPases with antiviral activity. Trends Cell Biol *3*, 268-272.

Stegmann, T. (2000). Membrane fusion mechanisms: the influenza hemagglutinin paradigm and its implications for intracellular fusion. Traffic *1*, 598-604.

St Johnston, D., Beuchle, D., and Nusslein-Volhard, C. (1991). Staufen, a gene required to localize maternal RNAs in the Drosophila egg. Cell *66*, 51-63.

Suarez, D.L., and Perdue, M.L. (1998). Multiple alignment comparison of the non-structural genes of influenza A viruses. Virus Res *54*, 59-69.

Suarez, D.L., Perdue, M.L., Cox, N., Rowe, T., Bender, C., Huang, J., and Swayne, D.E. (1998). Comparisons of highly virulent H5N1 influenza A viruses isolated from humans and chickens from Hong Kong. J Virol *72*, 6678-6688.

Suzuki, T., Takahashi, T., Guo, C.T., Hidari, K.I., Miyamoto, D., Goto, H., Kawaoka, Y., and Suzuki, Y. (2005). Sialidase activity of influenza A virus in an endocytic pathway enhances viral replication. J Virol *79*, 11705-11715.

Sweet, C., and Smith, H. (1980). Pathogenicity of influenza virus. Microbiol Rev *44*, 303-330.

Takeda, K., and Akira, S. (2004). TLR signaling pathways. Semin Immunol *16*, 3-9.

Talon, J., Horvath, C.M., Polley, R., Basler, C.F., Muster, T., Palese, P., and Garcia-Sastre, A. (2000). Activation of interferon regulatory factor 3 is inhibited by the influenza A virus NS1 protein. Journal of virology *74*, 7989-7996.

Tan, S.L., and Katze, M.G. (1998). Biochemical and genetic evidence for complex formation between the influenza A virus NS1 protein and the interferon-induced PKR protein kinase. J Interferon Cytokine Res *18*, 757-766.

Taubenberger, J.K. (2006). The origin and virulence of the 1918 "Spanish" influenza virus. Proc Am Philos Soc *150*, 86-112.

Taubenberger, J.K., Reid, A.H., Lourens, R.M., Wang, R., Jin, G., and Fanning, T.G. (2005). Characterization of the 1918 influenza virus polymerase genes. Nature *437*, 889-893.

To, K.F., Chan, P.K., Chan, K.F., Lee, W.K., Lam, W.Y., Wong, K.F., Tang, N.L., Tsang, D.N., Sung, R.Y., Buckley, T.A., *et al.* (2001). Pathology of fatal human infection associated with avian influenza A H5N1 virus. J Med Virol *63*, 242-246.

Twu, K.Y., Kuo, R.L., Marklund, J., and Krug, R.M. (2007). The H5N1 influenza virus NS genes selected after 1998 enhance virus replication in mammalian cells. Journal of virology 81, 8112-8121.

Twu, K.Y., Noah, D.L., Rao, P., Kuo, R.L., and Krug, R.M. (2006). The CPSF30 binding site on the NS1A protein of influenza A virus is a potential antiviral target. Journal of virology *80*, 3957-3965.

Vanhaesebroeck, B., Leevers, S.J., Ahmadi, K., Timms, J., Katso, R., Driscoll, P.C., Woscholski, R., Parker, P.J., and Waterfield, M.D. (2001). Synthesis and function of 3-phosphorylated inositol lipids. Annu Rev Biochem *70*, 535-602.

Villace, P., Marion, R.M., and Ortin, J. (2004). The composition of Staufen-containing RNA granules from human cells indicates their role in the regulated transport and translation of messenger RNAs. Nucleic Acids Res *32*, 2411-2420.

Vreede, F.T., Jung, T.E., and Brownlee, G.G. (2004). Model suggesting that replication of influenza virus is regulated by stabilization of replicative intermediates. J Virol *78*, 9568-9572.

Wagner, R., Matrosovich, M., and Klenk, H.D. (2002). Functional balance between haemagglutinin and neuraminidase in influenza virus infections. Rev Med Virol *12*, 159-166.

Wang, W., and Krug, R.M. (1998). U6atac snRNA, the highly divergent counterpart of U6 snRNA, is the specific target that mediates inhibition of AT-AC splicing by the influenza virus NS1 protein. RNA *4*, 55-64.

Wang, X., Li, M., Zheng, H., Muster, T., Palese, P., Beg, A.A., and Garcia-Sastre, A. (2000). Influenza A virus NS1 protein prevents activation of NF-kappaB and induction of alpha/beta interferon. Journal of virology *74*, 11566-11573.

Ward, A.C. (1997). Virulence of influenza A virus for mouse lung. Virus Genes *14*, 187-194.

Webster, R.G., Bean, W.J., Gorman, O.T., Chambers, T.M., and Kawaoka, Y. (1992). Evolution and ecology of influenza A viruses. Microbiol Rev *56*, 152-179.

Weaver, B.K., Kumar, K.P., and Reich, N.C. (1998). Interferon regulatory factor 3 and CREB-binding protein/p300 are subunits of double-stranded RNA-activated transcription factor DRAF1. Mol Cell Biol *18*, 1359-1368.

Wolff, T., O'Neill, R.E., and Palese, P. (1996). Interaction cloning of NS1-I, a human protein that binds to the nonstructural NS1 proteins of influenza A and B viruses. Journal of virology *70*, 5363-5372.

Wolff, T., O'Neill, R.E., and Palese, P. (1998). NS1-Binding protein (NS1-BP): a novel human protein that interacts with the influenza A virus nonstructural NS1 protein is relocalized in the nuclei of infected cells. Journal of virology *72*, 7170-7180.

World Health Organization. *Avian influenza*. URL: http://www.who.int/csr/disease/avian_influenza/en/ Accessed 8 August, 2008.

Wright, P.F., Neumann, G., and Kawaoka, Y. (2007). Orthomyxoviruses. In Field's Virology, D.M.K. PhD, and P.M.H. MD, eds. (Philadelphia, Lippincott Williams & Wilkins), pp. 1692-1732.

Yasuda, J., Nakada, S., Kato, A., Toyoda, T., and Ishihama, A. (1993). Molecular assembly of influenza virus: association of the NS2 protein with virion matrix. Virology *196*, 249-255.

Zheng, H., Lee, H.A., Palese, P., and Garcia-Sastre, A. (1999). Influenza A virus RNA polymerase has the ability to stutter at the polyadenylation site of a viral RNA template during RNA replication. J Virol *73*, 5240-5243.

APPENDIX I : Solutions

Alkaline Phosphatase Buffer:

12 g/L Tris

6 g/L NaCl

1 g/L $MgCl_2$

pH 9.5

Binding Buffer:

150 mM NaCl

10 mM Tris/HCl

1.5 mM MgCl2

0.5% Triton X-100

pH 8.5

Supplement before use with:

1 mM PMSF

1 mM TPCK

1 mM TLCK

Blocking Buffer:

8 mM Na_2HPO_4

2.5 mM NaH_2PO_4

145 mM NaCl

3% Bovine Serum Albumin

0.1% Tween 20

pH 8.5

Burgui Binding Buffer:

5 mM sodium phosphate

150 mM NaCl

1% Triton X-100

2 mM EDTA

pH 8.5

Supplemented before use with:

1 mM PMSF

1 mM TPCK

1 mM TLCK

0.1% β-Mercaptoethanol

Coomassie Staining Solution:

25% Methanol

10% Glacial Acetic Acid

0.1% Coomassie Brilliant Blu

Coomassie Blue Destaining Solution:

25% Methanol

10% Glacial Acetic Acid

Cracking Lysis Solution:

1% SDS

0.2 M NaOH

Cracking Suspension Buffer:

50 mM Tris-HCl

10 mM EDTA

pH 8.0

eIF4G1 Lysis Buffer:

100 mM KCl

20 mM HEPES-KOH

10% Glycerol

pH = 7.5

Supplement before use with:

10 mM β-Mercaptoethanol

10 µL/mL EDTA-free PIC (Bioshop)

Imidazole:

20 mM for Binding

50 mM for Washing

1 M for Elution

Extraction Buffer:

100 mM Tris-HCl

250 mM NaCl

0.5% NP-40

0.5% sodium deoxycholate

pH 8.5

Supplement before use with:

1 mM PMSF

1 mM TPCK

1 mM TLCK

Extraction Buffer II:

150 mM NaCl

1.5 mM MgCl2

10 mM Tris/HCL

0.5% NP-40

pH 8.5

Supplement before use with:

1 mM PMSF

1 mM TPCK

1 mM TLCK

Extraction Buffer III:

100 mM Tris-HCl

250 mM NaCl

0.5% NP-40

0.5% sodium deoxycholate

10% Glycerol

10% BSA

pH 8.5

Supplement before use with:

1 mM PMSF

1 mM TPCK

1 mM TLCK

LB Broth:

10 g/L Tryptone

10 g/L NaCl

5 g/L Yeast Extract

pH 7.5

Sterilize by autoclaving

LB Agar:

15 g/L Agar

10 g/L Tryptone

10 g/L NaCl

5 g/L Yeast Extract

pH 7.5

NS1 Lysis Buffer:

500 mM NaCl

50 mM Tris

5 mM $MgCl_2$

10% Glycerol

0.1% Triton X-100

pH = 8.0

Supplement before use with:

10 mM β-Mercaptoethanol

10 µL/mL EDTA-free PIC (Bioshop)

Imidazole

20 mM for Binding

50 mM for Washing

1 M for Elution

PABP1 Lysis Buffer:

5 mM NaH_2PO_4

150 mM NaCl

2 mM EDTA

1% Triton X-100

pH 7.4

Supplemented before use with:

1 mM PMSF

1 mM TPCK

1 mM TLCK

0.1% β-mercaptoethanol

PBS:

8 mM Na_2HPO_4

2.5 mM NaH_2PO_4

145 mM NaCl

pH 7.4

Sterilize by autoclaving

SDS Sample Buffer (2x)

150 mM Tris

1.2% SDS

30% Glycerol

15% β-mercaptoethanol

0.1% Bromophenol Blue

pH 6.8

Aliquot into 10 mL stock sol. and store at -4°C

SOC Medium:

20 g/L Tryptone

5 g/L Yeast Extract

0.5 g/L NaCl

pH 7.5

Supplemented before use with:

20 mL/L filter-sterilized 1M glucose

STET:

100 mM NaCl

10 mM Tris

1 mM EDTA

5% Triton X-100

pH 8.0

Stop Solution:

PBS with 20 mM EDTA

TAE Buffer:

4.85 g/L Tris

1 mM Na_2EDTA

0.2% Glacial Acetic Acid

pH 8.0

Tank Buffer:

1% SDS

3 g/L Tris

14.4 g/L Glycine

TBE Buffer:

10.8 g/L Tris

5.5 g/L Boric Acid

2 mM Na_2EDTA

pH 8.0

TBS:

50 mM Tris

150 mM NaCl

pH 7.5

TE Buffer

10 mM Tris

1 mM Na_2EDTA

pH 8.0

Wash Buffer:

8 mM Na_2HPO_4

2.5 mM NaH_2PO_4

145 mM NaCl

0.1% Tween 20

pH 7.4

APPENDIX II : Oligonucleotide Primers

All primers were used for PCR Mutagenesis or TOPO Cloning. Primers are written from 5' to 3'. Negative sense primers are denoted with an asterisk.

NS1 Topo Primers:

5' - ATTACATATGCATCACCATCACCATCACCATGGATTCTAACACTGTGTCAAG -3'

*5'- CATGGAATTCTCAATCAGCCATCTTATCTCTTCG -3'

PCR Mutagenesis Primers:

NS1-wt to 20c

5' - GCTCATGCTAATGCCCAAG -3'

*5'- CAGTCCCTTGACAATTCCTC -3'

NS1-wt to 51

5'-TCCCAAGCAGAAAGTGGAAG-3'

*5'-ATTAGCATGAACCAGTCCCTTG-3'

NS1-41 to wt

5'-TAATGCCCAAGCAGAAAGTGG-3'

*5'-GCATGAACCAGTCCCTTGAC-3'

NS1 G225R

5'-CGAGAACAGTTAGGTCAAAAGTTCG-3'

*5'-CCATTTTCCGTTTCTGTTTTGG-3'

APPENDIX III : Plasmid Constructs

pCAGGs-CPSF-F2/F3-Flag:

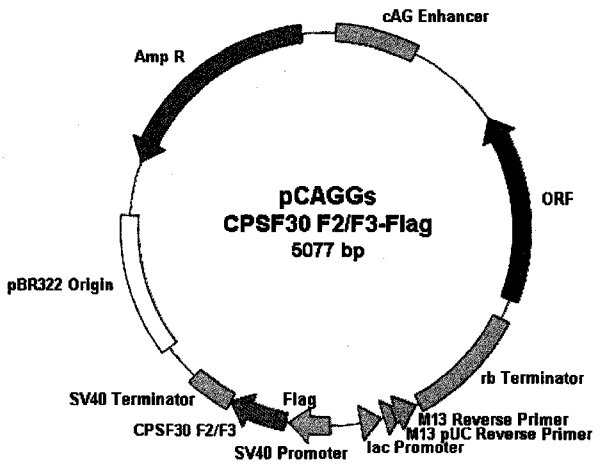

pCAGGS vector expressing N-terminal Flag-tagged CPSF30 F2/F3 fragment from a SV40 promoter followed by a SV40 terminator.

pCAGGs-CPSF30-Flag:

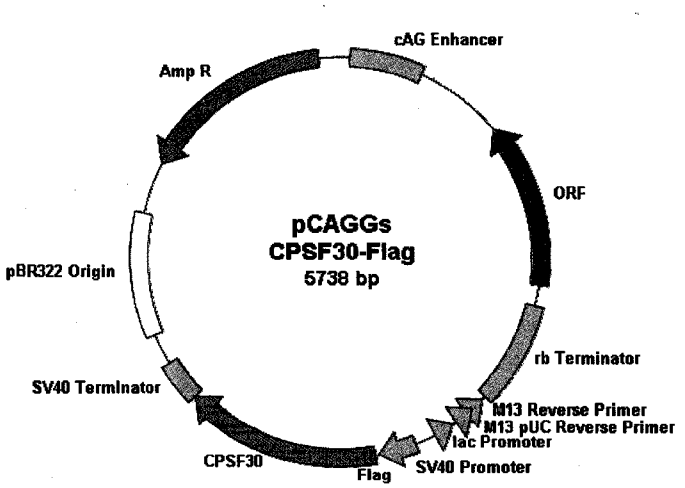

pCAGGS vector expressing N-terminal Flag-tagged CPSF30 from a SV40 promoter followed by a SV40 terminator.

pcDNA3-HA-eIF4G1:

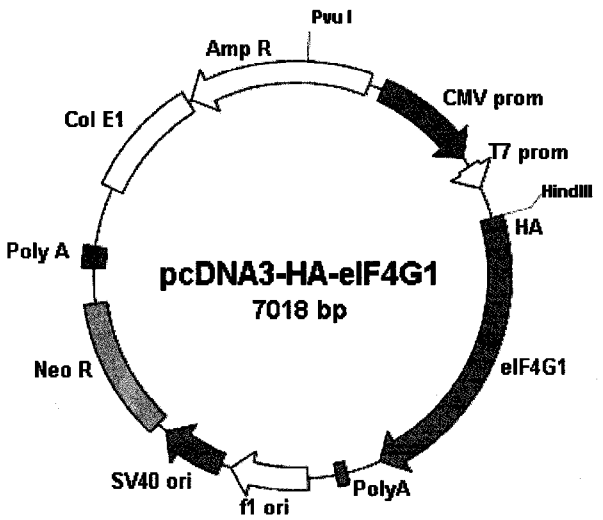

pcDNA3 expressing N-terminal HA-tagged eIF4G1 from both a T7 promoter, and a CMV promoter.

pDrive-His-NS1 variants:

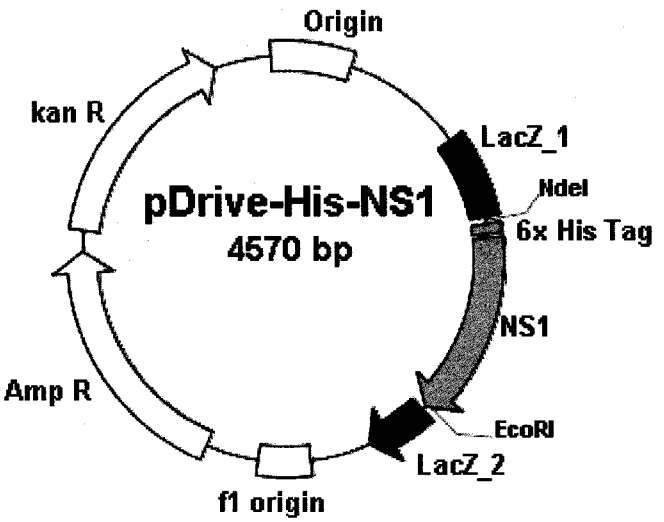

Topo cloning vector containing N-terminal His-tagged NS1 interrupting the LacZ gene.

pET17b-His-NS1 variants:

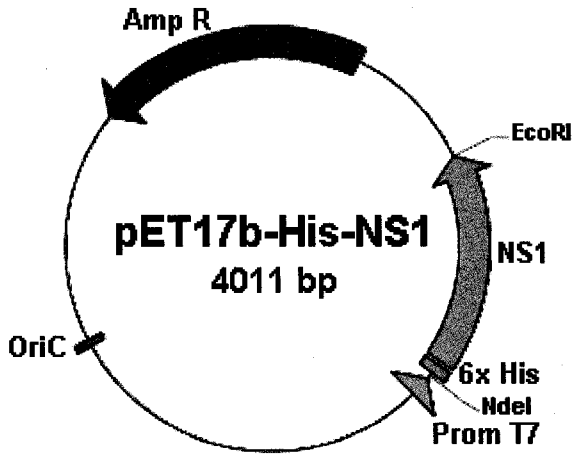

pET17b expressing N-terminal His-tagged NS1 from a T7 promoter.

pET-15G-Flag-eIF4G1:

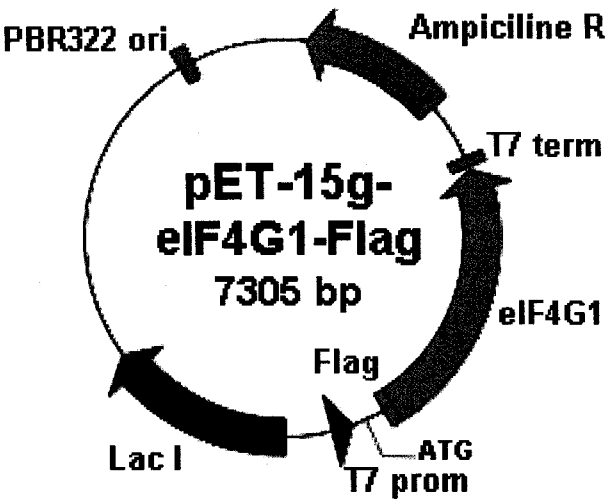

pET15G expressing N-terminal Flag-tagged eIF4G1 from a T7 promoter.

pGEX-2T-PABP1:

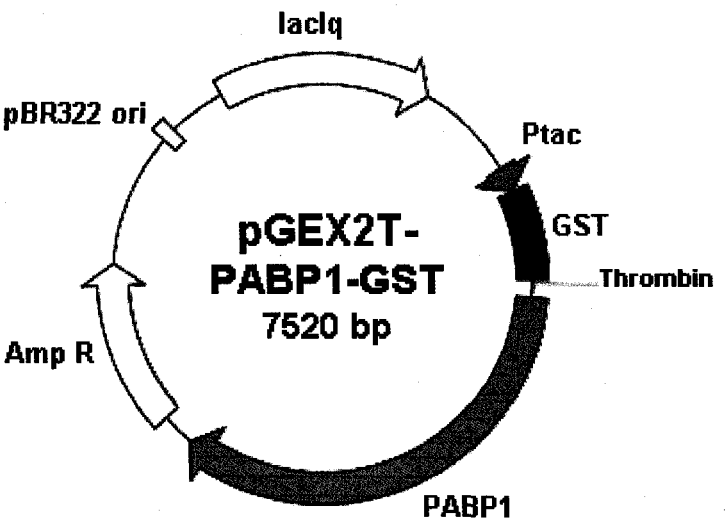

pGEX2T expressing a N-terminal GST-PABP1 fusion protein from a Tac promoter/operator.

pGEX-4T:

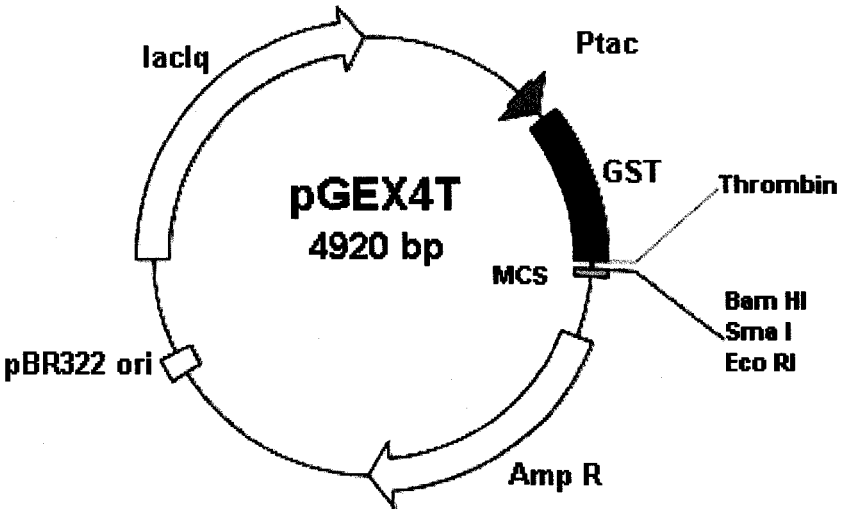

pGEX4T expressing a GST protein from a Tac promoter/operator.

pGEX-His-eIF4G1:

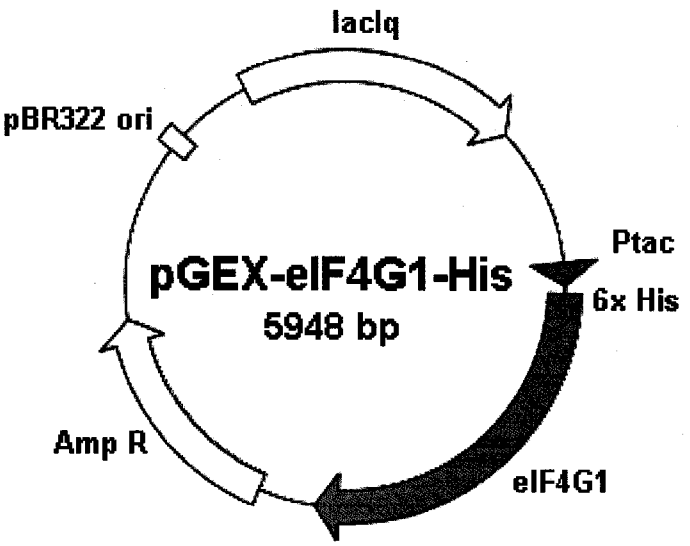

pGEX expressing a N-terminal His-tagged eIF4G1 protein from a Tac promoter/operator.

APPENDIX IV : eIF4G1 Progress

In addition to CPSF30 and PABP1, the effect of the MA NS1 mutations on the ability of the protein's ability to bind eIF4G1 is also of interest. This is because eIF4G1 is also an important component of the translation initiation complex that has been shown to bind to NS1, and also, many of the MA mutations map to the eIF4G1 binding domain. Although the eIF4G1-NS1 binding experiments have not yet been completed, the progress that I have made in these experiments is presented here for future follow-up.

Initial attempts to express eIF4G1 were made in BL21(DE3) and DH5α *E. coli* from both the pET-15G-Flag-eIF4G1 and the pGEX-His-eIF4G1 plasmids. Expression of eIF4G1 from the pET-15G-eIF4G1 construct failed in both *E. coli* strains. In contrast, the pGEX-His-eIF4G1 construct was able to express eIF4G1 in both strains, with a slightly better yield obtained in BL21(DE3) (Fig. 24a). Unfortunately, the eIF4G1 protein was not sufficiently stable and degradation products were already seen after separating the bacterial lysate into the soluble and insoluble fractions (Fig. 24b, column 1). Numerous induction conditions and protease inhibitors were tested to inhibit eIF4G1 degradation, but the only significant increase in soluble full-length eIF4G1 production was achieved by delaying induction with IPTG until the culture had reached an optical density of 1.00 at λ=600 nm (Fig 24b, column 2). Attempts were then made to column purify the expressed eIF4G1 with Ni-NTA agarose. Unfortunately none of these attempts were successful as eIF4G1 was not detectable by western blot in the purification eluant, nor was it in the column flow-through or washes.

Figure 24. Defining the optimal induction conditions for the expression of soluble eIF4G1 in *E. coli.* (A) His-eIF4G1 was successfully expressed from both DH5α and BL21 *E. coli* with greater protein expression obtained from BL21. Expression of Flag-eIF4G1 was not possible in the *E. coli* strains tested. **(B)** Expression of soluble His-eIF4G1 was possible from BL21, with the most efficient expression of soluble full length protein occurring when expression was induced with 1 mM IPTG once the culture had reached an optical density at λ=600nm of 1.00. However, breakdown products of the eIF4G1 protein are already visible in the western blot. "eIF4G1-His" denotes expression of His-tagged eIF4G1 from the pGEX-eIF4G1-His plasmid, while "eIF4G1-Flag" denotes expression of Flag-tagged eIF4G1 from the pET-15g-eIF4G1-Flag plasmid. The "T=0" samples were taken prior to induction, while the "T=3H" samples were taken at 3 post-induction. The "Soluble" and "Insol." samples were taken from the respective soluble and insoluble fractions of the bacterial cell lysate. "DH5α" and "BL21" denote the respective *E. coli* strains used for expression. Soluble fraction flow through, column washes, and elution fractions are labeled "F.T.", "Wash 1 & 2", and "Elution 1 – 6" respectively. "α-eIF4G1" denotes AP western blot performed with α-eIF4G1 as the primary antibody.

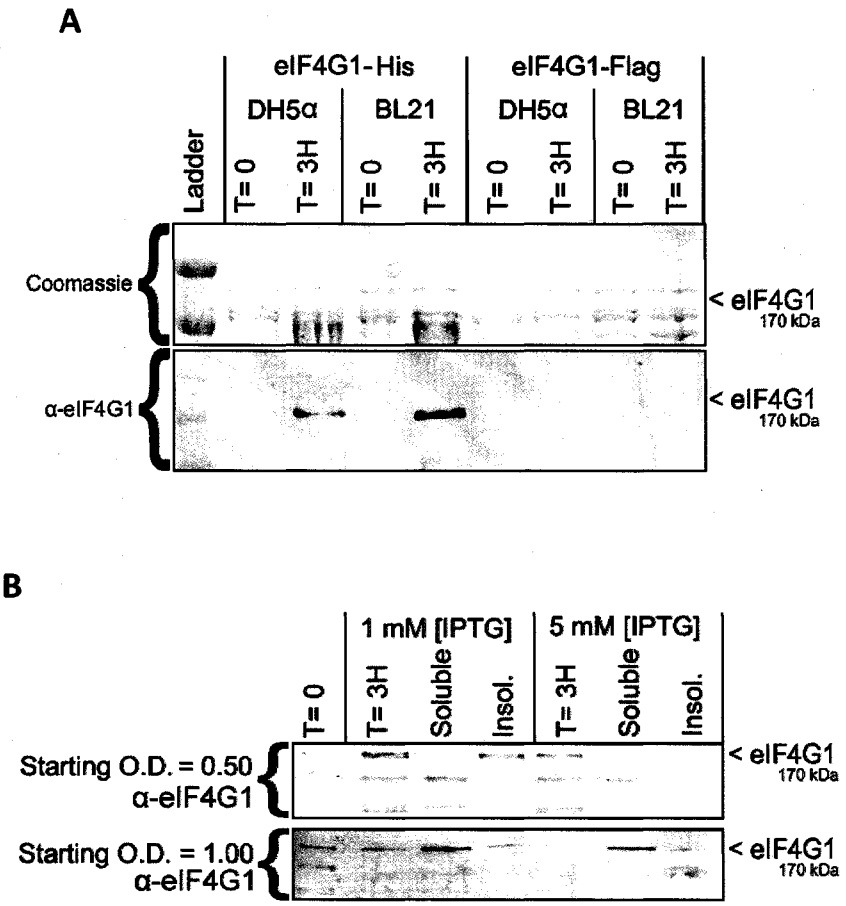

The disappearance of detectable eIF4G1 following purification suggests that the protein had degraded during the purification process, as reported by others (Derry, 2007, personal communication).

Expression of eIF4G1 in COS-1 and 293T cells was then attempted from the pcDNA3-HA-eIF4G1 and pET-15G-Flag-eIF4G1 constructs, but none of these expression attempts yielded any detectable eIF4G1 protein as assayed by western blot with α-eIF4G1 antibodies. Finally, the eIF4G1 protein was successfully expressed *in vitro* from the pcDNA3-HA-eIF4G1 construct using an *in vitro* transcription and translation strategy with rabbit reticulocyte lysate (Fig. 25, lane 5, column 2).

This eIF4G1 was then successfully pulled down by HK-wt NS1 in an α-NS1 CoIP (Fig. 25). Therefore, an α-NS1 CoIP was performed for each of the HK-MA NS1 variants. Unfortunately, the eIF4G1 that was pulled down in these experiments had already degraded into several bands and, therefore, could not be accurately quantified. Thus, it was necessary to CoIP NS1 from solution using eIF4G1 and rabbit α-eIF4G1 antibodies. However, the primary only α-NS1 antibody available for use in the western blots was rabbit in origin. Therefore, due to the overlap of the antibody light chain and NS1 band positions and the cross reactivity of the western blot secondary antibody with the antibody light chain used for the CoIP, it was impossible to quantify the amount of NS1 which was pulled down with a western blot (Fig. 25, lanes 1 and 2). I attempted to obtain α-eIF4G1 Ab of non-rabbit origin, but could not locate a supplier. Therefore, to circumvent this problem, NS1

Figure 25. Coimmunoprecipitation of eIF4G1-Flag with NS1, and of NS1 with HA-eIF4G1. The S^{35} autoradiogram clearly shows that eIF4G1 was successfully pulled down by NS1 in the α-NS1 CoIP (lanes 1 and 2). The presence or absence of NS1 is difficult to determine on the α-NS1 blot due to the masking effect of the α-NS1 or α-eIF4G1 antibodies that were used for the CoIP. However, it does appear that NS1 was successfully pulled down in the presence, but not in the absence, of eIF4G1 (lanes 3 and 4). "eIF4G1" and "HK-wt NS1" refer to the presence or absence of eIF4G1 and HK-wt NS1 protein input into the respective CoIP. "α-eIF4G1" and "α-NS1" refer to the presence or absence of the respective antibodies used to immunoprecipitate the corresponding protein. "1:20 eIF4G1 LC" and "1:20 NS1 LC" correspond to a 1:20 dilution loading control of the respective proteins used in the CoIP. "1:20 Luc TnT" corresponds to a 1:20 dilution of a Luciferase TnT reaction used as a positive TnT expression control. "α-NS1" denotes HRP western blot performed with α-NS1 as the primary antibody.

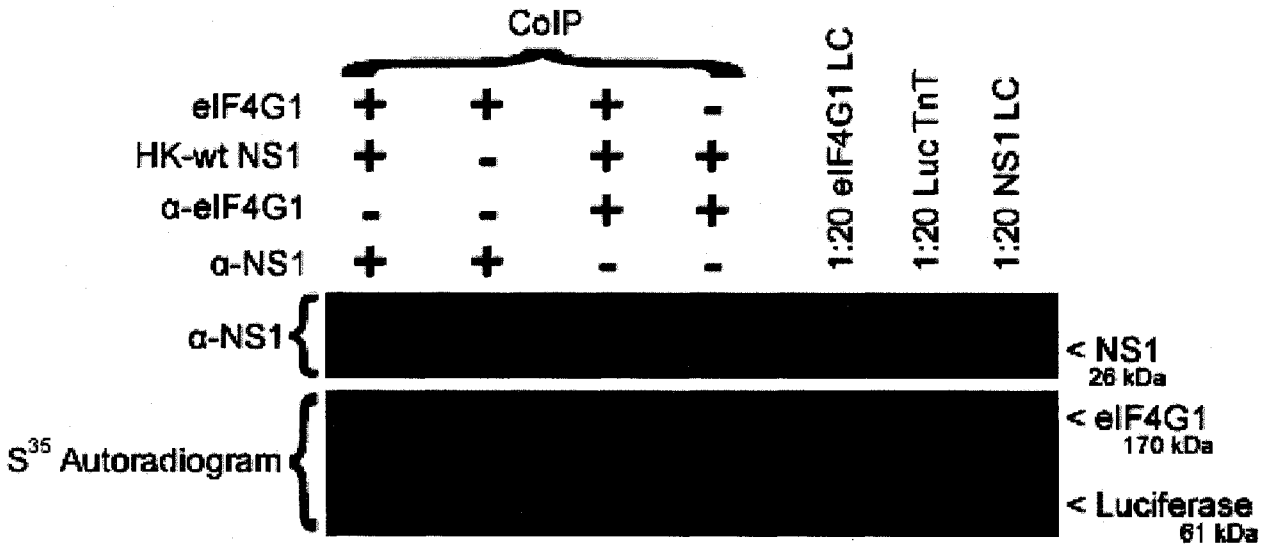

was expressed *in vitro* and radiolabelled using the *in vitro* transcription and translation strategy with rabbit reticulocyte lysate. Radiolabelled NS1 was then Coimmunprecipitated from solution with eIF4G1 and α-eIF4G1 antibody and then assayed by autoradiogram. Unfortunately, high levels of non-specific interaction between NS1 and the protein G bead/α-eIF4G1 complex in the absence of eIF4G1 made any interaction between NS1 and eIF4G1 indistinguishable from the background. Therefore, these CoIP experiments are promising, but the procedure must be further refined to yield reliable results.